Passive Afterload Working Mode in *Ex situ* Heart Perfusion

by

Bryan John Gellner

A thesis submitted in conformity with the requirements
for the degree of Doctor of Philosophy

Department of Mechanical and Industrial Engineering
University of Toronto

Passive Afterload Working Mode in *Ex situ* Heart Perfusion

Bryan John Gellner

Doctor of Philosophy

Department of Mechanical and Industrial Engineering

2019

Abstract

Ex situ heart perfusion (ESHP) is an emerging technique that aims to combat the shortage of organs suitable for transplantation through the augmentation of both donor heart preservation and evaluation. The oldest and most common modality for ESHP is Langendorff mode (LM), where oxygenated perfusate is provided retrograde to the aorta. While this technique is used clinically to extend donor heart preservation time, contractile evaluation of hearts is precluded. This evaluation has been made possible during ESHP, however, by recent research focused on the instillation of different working modes: Pump Supported Working mode (PSWM), where afterload is instilled by a pump providing retrograde support to the aortic root, and Passive Afterload Working Mode (PAWM), where passive Windkessel elements are used to instill physiological afterload.

In this thesis, the comparative effectiveness of these two working modes is examined. We first designed a novel ESHP system capable of perfusing hearts in all three main perfusion modes. While hearts remained in LM for the bulk of the perfusion period, contractile evaluation was successfully demonstrated in both PSWM and PAWM. An adjustable afterload module was then developed and tested in order to decouple aortic pressure from changes in ventricular contractility, enabling prolonged perfusion in PAWM. With our module, we were able to demonstrate perfusion in PAWM across 6 hours for 3 different hearts while maintaining physiological aortic pressures. With the functionality of our system thus confirmed, transplantation experiments were undertaken to

compare the predictive power of PSWM and PAWM. 5 porcine hearts donated after brain death (DBD) and 5 hearts donated after circulatory death (DCD) were perfused for 4 hours in LM, evaluated in both PSWM and PAWM, and transplanted into recipient pigs before being evaluated again. Correlating contractile parameters measured during ESHP and post-transplantation, measurements taken in PAWM showed greater predictive power than their PSWM counterparts. This augmentation of predictive power coupled with the ability to perfuse hearts in PAWM across extended perfusion periods serves to demonstrate our multimodal perfusion system as a promising step towards the optimization of donor heart preservation and evaluation during ESHP.

Acknowledgments

In the pursuit of my PhD over the last four years, there have been countless highs and lows, the navigation of which would never have been possible if not for the support of an extraordinary group of people that I have the privilege to have in my life. While there are countless people (too many indeed to mention all of them within these pages) who's contributions were invaluable in the completion of this work, I would first like to acknowledge the animals that were sacrificed in the name of scientific discovery in the completion of this research. Within these pages are described the discoveries enabled using hearts from not only the 30 pigs explicitly mentioned herein, but the numerous others utilized in the development and optimization of the perfusion system. It is my sincere hope that their sacrifice is justified by the lives that can one day be saved through the advancement of this technique.

First and foremost, I would like to thank the exceptional supervisors that I have been fortunate enough to work under: Professor Craig Simmons and Professor Jean Zu. Jean, thanks for believing in me and giving me the opportunity to work on something so incredible. Craig, thank you for your mentorship and for the example you set for what it means be to be a leader and a researcher. Thank you for taking me in and for your guidance in bringing this research through to completion. I couldn't have done it without you. Finally, to Dr. Mitesh Badiwala, the visionary behind this incredible project I have had the honor of working on, thank you for your guidance and drive to create something with the potential to help so many people.

To my labmates past and present, this journey wouldn't have been the same without you. From complex technical discussions about research directions to just kicking back and talking about life, thanks for making these last few years so invigorating and for helping me be the best I could be. In particular, thank you to Dr. Liming Xin and Dr. Roberto Vanin Pinto Ribeiro. It's been a crazy ride, and I'm so proud of what we were able to accomplish. It's hard to believe how far we've come since the days of using a thirty-year-old pump sitting on a rusty old table. Thank you for all your counsel and hard work, you are truly exceptional people and I'm grateful to have been able to work with you both. To everyone who has helped us with our experiments, thank you for all the time you've spent to make this work a success. Ved Bissoondath, David Banner, Mitchell Adamson, Frank Yu, Pengzhou Lu, Emanuela Paradiso, Giulia Maria Ruggeri, Arnaud Mbadjeu, and everyone

else who came in to help, your contributions have been invaluable, and I feel privileged to have been able to work with each of you.

Lastly, and most importantly, thank you to my family for all your love and support. To my parents who believed in me long before even I did, thank you for always being there and for everything you've done to give me the opportunity to strive for something as crazy as a PhD. I never could have done (or even dared to have tried) any of this without you. To the incomparable Snover Dhillon, thank you for being you. Your smile was a welcome sight regardless of whether things were going well or terribly. Thanks for sharing it :). To all of my family and friends who lent an ear for a rant about how great or badly things were going with my research (depending on the moment), thank you and I'm sorry. I can't promise it won't happen again.

And finally, to my Grandmother who passed away while I was writing this thesis and always wanted a doctor in the family; I miss you and I hope I did you proud.

Table of Contents

List of Tables

List of Figures

List of Acronyms

Bi-PAWM: Biventricular Passive Afterload Working Mode

Bi-PSWM: Biventricular Pump Supported Working Mode

CaO_2: Arterial Oxygen Concentration

CBF: Coronary Blood Flow

CI: Cardiac Index

CP: Centrifugal Pump

CPB: Cardio-Pulmonary Bypass

CS: Cold Storage

CT: Computed Tomography

CVR: Coronary Vascular Resistance

DBD: Donation after Brain Death

DCD: Donation after Circulatory Death

dP/dt Max: Maximum Rate of Developed Pressure

dP/dt Min: Minimum Rate of Developed Pressure

DPP: Direct Procurement Protocol

ECMO: Extracorporeal Membrane Oxygenation

EDPVR: End Diastolic Pressure Volume Relationship

EDV: End Diastolic Volume

EF: Ejection Fraction

EMax: Maximal Elastance

ESHP: *Ex Situ* Heart Perfusion

ESPVR: End Systolic Pressure Volume Relationship

FAC: Fractional Area Change

HBOC: Hemoglobin Based Oxygen Carrier

HTK: Histidine-Tryptophan-Ketoglutarate

LM: Langendorff Mode

LV: Left Ventricle

Max dP/dt/EDV: Maximum Rate of Developed Pressure Normalized to End Diastolic Volume

MOD: Method of Disks

MVO_2: Myocardial Oxygen Volume

NRP: Normothermic Regional Perfusion

OCS: Organ Care System

PAWM: Passive Afterload Working Mode

pCO_2: Partial Pressure of Carbon Dioxide

pO_2: Partial Pressure of Oxygen

PRSW: Preload Recruitable Stroke Work

PSWM: Pump Supported Working Mode

PV: Pressure-Volume

RV: Right Ventricle

SaO_2: Arterial Oxygen Saturation

SW: Stroke Work

Tau: Time Constant of Isovolumetric Relaxation

TEE: Transesophageal Echocardiography

ΔP: Developed Pressure

Chapter 1

1 Thesis Overview

1.1 Background

Ischemic heart disease is one of the leading causes of death in the world, accounting for over 300,000 deaths per year in the United States alone. [1] A multitude of treatment strategies have emerged to combat this problem, but for end stage heart failure patients, cardiac transplantation remains the standard of care. Here too there have been great strides made since Dr. Christian Barnard performed the first heart transplant in 1967.[2] These advancements have resulted in a drastic increase in the number of people qualified for heart transplantation, but a paucity of donor organs has precluded a corresponding increase in the number of transplants.[1] *Ex situ* Heart Perfusion (ESHP) has been proposed as a means to increase the number of hearts available for transplant by augmenting organ preservation to ensure more usable hearts can safely reach potential recipients, and organ evaluation to demonstrate the usability of some hearts that are currently discarded because their quality is unknown.[3] Specific protocols for ESHP are numerous and the optimal modalities for heart preservation and evaluation are not yet defined but all strategies do have similarities. Regardless of which modality is used, ESHP, by definition, constitutes the supply of oxygenated perfusate to the coronary vasculature as a means to facilitate aerobic heart metabolism *ex situ*. Of note however, with hearts being removed from the circulatory system they are also removed from the inherent homeostatic control systems associated with the *in vivo* environment. The re-institution of an *ex situ* form of this control is postulated to be necessary in creating a more physiological setting for ESHP, making perfusion more effective, and evaluation more relevant.

Control of aortic pressure in particular is of vital importance as it is the driving force of coronary perfusion. This pressure, while closely related to the contractile function of the heart, is very much dependent on supplied preload and afterload conditions during ESHP. Furthermore, with many evaluation parameters currently used to characterize cardiac contractile function being dependent on ventricular preload and afterload, the consistency of this aortic pressure setting is also closely related to our ability to evaluate hearts during ESHP. With this in mind, it is clear that a controllable

and physiological fluidic setting for *ex situ* hearts is necessary to evaluate the impact of ESHP in terms of augmenting the heart donor pool by improving cardiac preservation and evaluation.

1.2 Thesis Structure

This thesis contains 7 chapters that are organized as follows: **Chapter 1** introduces the principles that motivated this research work, defines the structure of this thesis and outlines the contributions of collaborators within the research. **Chapter 2** describes the existing literature related to the field of ESHP, and specifically the institution of a controllable afterload setting to *ex situ* hearts. **Chapter 3** outlines both the overarching and specific objectives of this thesis. **Chapter 4** describes published work about the creation of a multimodal ESHP system that enables the comparative evaluation of a multitude of ESHP techniques. **Chapter 5** describes work relating to the development and testing of an adjustable afterload module for use in prolonged ESHP. **Chapter 6** describes work centered around a porcine transplantation study to analyze the comparative relevance of evaluating hearts under consistent afterload conditions or with aortic pump support in terms of predicting post-transplant outcomes. Finally, **Chapter 7** concludes this work with a summary of the findings of this research and their impact, as well as a multitude of recommendations for future work.

1.3 Contributions

In terms of individual contributions, there are many people whose work in experimental design, experimental execution, and data analysis greatly aided in the completion of this research. Dr. Craig Simmons served in a supervisory role for all aspects of this research, aiding in experimental design and data analysis. Dr. Mitesh Badiwala served as the leader of the overall research project and also aided in the experimental design and data analysis of chapters 4 through 6. Additional supervisory support for chapter 4 and chapter 5 was provided by Dr. Jean Zu.

The work in chapter 4 was the result of a highly collaborative set of experiments in which I was responsible for the fluidic portion of the design of the novel ESHP system, the utilization of that system in executing the experiments, and large portions of the presented data analysis, especially pertaining to Passive Afterload Working Mode (PAWM). Experimental design was largely performed by Dr. Liming Xin, a postdoctoral fellow in Professor Jean Zu's lab. Dr. Xin also created the outline of the initial manuscript which we then wrote together. Dr. Roberto Vanin Pinto Ribeiro,

a PhD Candidate in the Faculty of Medicine in Dr. Badiwala's lab, served both to advise on clinical applicability in the design of the system and in carrying out the surgical portions of the experiments. Additional contributions in terms of carrying out the experiments were made by Giulia Maria Ruggeri, an anesthesiology fellow working at Toronto General Hospital, and David Banner, who was the manager of Dr. Badiwala's lab. This work was published in the Journal of Medical Systems in December of 2017.

The work in chapter 5 came out of collaboration from much of the same team as that of chapter 4. I was responsible for the experimental design, the design and fabrication of the device, conducting the experiments, data analysis and writing the manuscript. Assistance in carrying out the experiments and editing the manuscript was provided by Dr. Liming Xin, Roberto Vanin Pinto Ribeiro, Ved Bissoondath, the manager of Dr. Badiwala's lab, Pengzhou Lu, an MEng. student working under Dr. Badiwala, Mitchell B. Adamson a Master's student in medicine, Frank Yu, an undergraduate student at the University of Toronto, and Emanuela Paradiso, an anesthesiology fellow working at Toronto General Hospital.

I was responsible for the experimental design, data analysis and the completion of the manuscript for chapter 6. Roberto Ribeiro performed all of the surgical procedures and provided invaluable assistance in the interpretation of the results. Dr. Liming Xin assisted in carrying out the experiments and particularly in facilitating the non-invasive data collection. Additional assistance in carrying out the experiments was provided by Emanuela Paradiso, Arnaud Mbadjeu, an anesthesiology fellow working at Toronto General Hospital, Ved Vissoondath, Mitchell B. Adamson, and Frank Yu.

Chapter 2

2 Literature Review

In the following section, key findings from all relevant academic sources are reviewed and summarized. Specific topics include the motivation for research into ESHP, technical advancements that have occurred throughout the history of the technique, afterload specific considerations for isolated heart setups and a summary of necessary future research in the field.

2.1 Motivation for *Ex situ* Heart Perfusion

While techniques in cardiac transplantation have seen considerable development over the last number of years, a lack of available organs has precluded an increase in the number of transplants, leading instead to the growth of waitlists.[1, 4] Since the mid-1990s, there has been only limited growth in heart transplant numbers in spite of significant advancements in surgical technique, with yearly transplants in the United States falling just shy of 3200 in 2016 (Figure 2-1). With approximately 4000 people currently on the waiting list, and approximately 3300 new transplant candidates listed each year, significant growth in transplantation numbers is required in order to slow the growth of the waiting list, or better yet, begin to see it shorten. [5, 6]

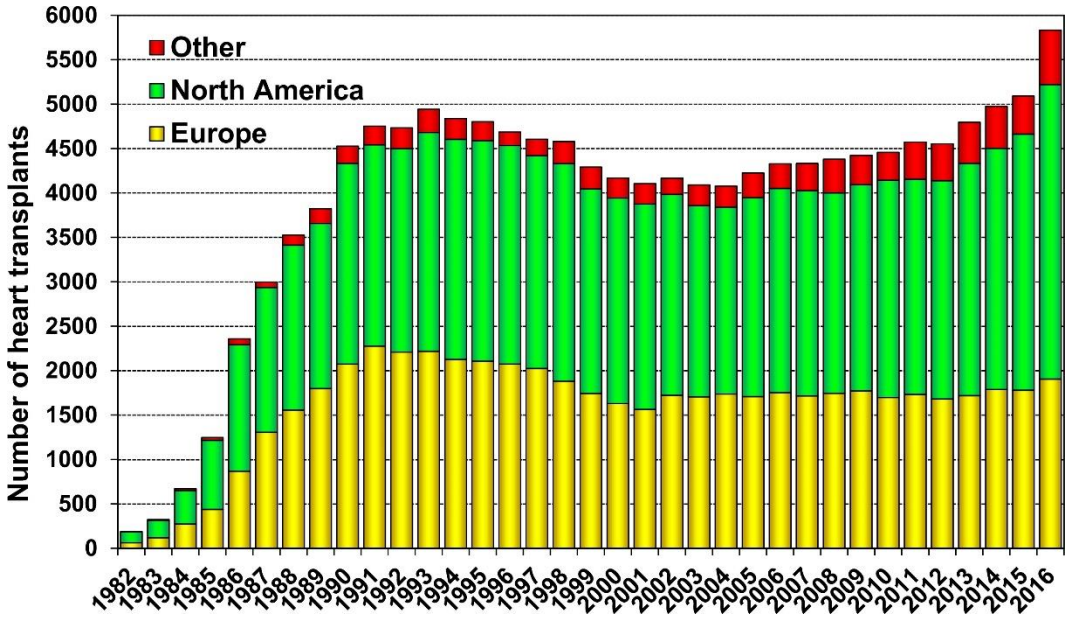

Figure 2-1, adapted with permission from [4]: Yearly heart transplants worldwide since 1982.

With this shortage of available and usable donor hearts in mind, a multitude of potential remedial strategies have been suggested. One commonly investigated solution is the augmentation of transportation strategies as a means to ensure that all currently usable donor hearts can reach a qualified and matching recipient. Using traditional cold storage, the typical allowable transport time for hearts is only four to six hours depending on the jurisdiction. This limited travel window is thought to result in the fact that many currently usable hearts are discarded for the lack of a suitable recipient within the allowable transportation distance.[7] By extending the allowable preservation time, many if not all of these unused organs could reach the patients that so desperately need them.

The efficient use of all currently available hearts could indeed result in a measurable increase in heart transplants, but in recent years, groups have begun to target a far more substantial organ source as a means to augment the donor pool. It has been suggested many times that institutional criteria for accepting hearts for transplantation is overly stringent and it is thought that many currently discarded hearts are in fact usable.[8] Chief among these marginal hearts are those donated after the declaration of circulatory death (DCD hearts) as, in most jurisdictions, only hearts donated after brain death (DBD hearts) are allowed for transplant. [9] As DCD hearts represent the vast majority of organs available for use, their safe use could represent an enormous step in alleviating the organ shortage, with estimates predicting an increase in transplant activity of up to 30% depending on the jurisdiction. [10]. Unfortunately, the use of these organs with current transplant approaches is dangerous. Invariably, DCD hearts are exposed to a period of warm ischemia prior to excision from the donor meaning that, for many of these potential donor hearts, significant myocardial injury is present. For many DCD hearts however, myocardial function remains acceptable after this ischemic period.[11] Due to the nature these organs, there is currently no widespread clinically accepted way to determine which specific DCD hearts are usable and which are not. For DBD hearts, contractile performance can be evaluated in the donor prior to heart excision but since asystole occurs before the heart excision process begins in DCD donors, for them, no such *in vivo* evaluation can be made. With such a large variance in contractile performance amongst DCD hearts, a means to quantitatively evaluate them is a necessity in allowing for their safe use.

Ex situ organ perfusion has been proposed as a means to both extend the allowable preservation period (and thus the allowable travel distance) and allow for quantitative assessment of donor organs between organ procurement and transplantation.[12] In some cases, the repair of damaged organs has even been suggested to be possible. [13] Compared to other organs however, the technical complexity of perfusing hearts *ex situ* has resulted in only limited clinical application of *Ex situ* Heart Perfusion (ESHP) (section 2.2). [14] To reach its potential, ESHP requires a great deal of additional research, much of which is currently underway in numerous labs around the world and will be detailed in subsequent sections. Recent clinical success with *ex situ* perfusion of donor lungs, livers and kidneys however offers both the motivation and blueprint for the advancement of ESHP.

By far the organ that has seen the most *ex situ* perfusion research is the lung. Lung transplantation dates to the early 1960s, though early success was quite limited.[15] In fact, over the 15 years immediately following the first successful lung transplant, only 38 additional procedures were even attempted with no patients surviving more than 11 months.[16] As is the case with hearts, advancements in surgical technique throughout the 1980s spurred exponential growth in lung transplants, only to lead to stagnation as donor organ availability became a limiting factor. [16] At the same time however, normothermic lung perfusion began to gain traction as an alternative preservation method to cold storage. [17] While these initial trials were eventually abandoned, they motivated the advent of new techniques throughout the 1990s, culminating in a system capable of evaluating lungs *ex situ*, and finally the first transplant of reperfused DCD lungs in humans. [18, 19] Intensive research into perfecting *ex situ* evaluation techniques in the following years in turn, pushed clinical research forward. [20-22] Motivated by their success, researchers proceeded to use the *ex situ* perfusion technique to transplant the first non-acceptable donor lungs, moving towards the aggressive expansion of the donor pool. [23] In its current state, lung transplantation stands on the precipice of a perfusion revolution with more and more centres accepting the use of *ex vivo* lung perfusion as a means to utilize DCD lungs and recent clinical work even suggesting that the safe use of hepatitis C positive lungs for transplantation could be possible using this technique, enabling further expansion of the lung donor pool.[24, 25]

This resounding clinical success extends beyond just lung perfusion to the perfusion of liver and kidneys as well. Following the example set forth by the lungs, liver and kidney perfusion really

came to the fore in the late 1990s.[26, 27] Since then, research has expanded to include the clinical use of DCD kidneys and livers and comparisons between hypothermic and normothermic perfusion.[28-31] With these successes in mind, the vast potential for ESHP is self-evident. ESHP itself is one of the oldest perfusion fields and offers every bit the same level of impact as has been seen for lungs, livers and kidneys. Research is currently underway to reinvigorate the field of cardiac transplantation through the use of ESHP enabling better preservation during transit and perhaps the evaluative capabilities necessary to facilitate the use of DCD hearts.

2.2 *Ex situ* Heart Perfusion

2.2.1 History and the Current State of Clinical Research

Compared to other organ groups, ESHP is quite old, though its initial purpose had very little to do with organ preservation and much more to do with studying heart physiology. In the late 1800s, Oscar Langendorff pioneered the isolated mammalian heart.[32, 33] Langendorff showed that by providing retrograde aortic flow of oxygenated perfusate, the aortic valve was forced closed, and the perfusate forced through the coronary system. The heart extracts the oxygen in the perfusate and can be preserved in an aerobic metabolic state. This original Langendorff Mode (LM) perfusion setup, was expanded on by scientists such as Otto Frank and Ernest Henry Starling in their isolated heart work, helping to enable the research that forms much of the backbone of our knowledge of cardiac function today.[34-36] While this perfusion mode is still commonly used today, *ex situ* heart perfusion saw a dramatic change in 1967 when Neely et al. developed what would become the first isolated working heart model.[37] In traditional LM, very little, if any blood enters the left ventricle, precluding the effective observation of ventricular ejection.[38] With the advent of the isolated working heart, as well as advancement in pressure and flow measurement techniques, more advanced aspects of hemodynamic cardiac function could now be evaluated.[39-41]

As with the lung, liver and kidney, ESHP experienced a swell in renewed interest in the 1990s as field wide transplant capability surpassed donor heart availability. As with these other organs, the main focus was on ESHP as a means to extend the allowable distance for organ transportation.[42] This is also the first ESHP work that has reached the clinical stage. The organ care system (OCS), developed by Transmedics and pictured in *Figure 2-2* has shown immense promise in the clinical setting, showing similar intermediate outcomes when used instead of cold storage during heart

procurement while substantially reducing cold ischemic time.[43, 44] While outcomes for these currently usable hearts were similar whether cold storage or ESHP was used during transport, early stage research has begun to show that extended criteria donors, and many hearts with longer transit times, show acceptable clinical outcomes after the use of the OCS.[45, 46] Recently, it has been shown that DCD hearts that were perfused on the OCS and then transplanted successfully. [47]

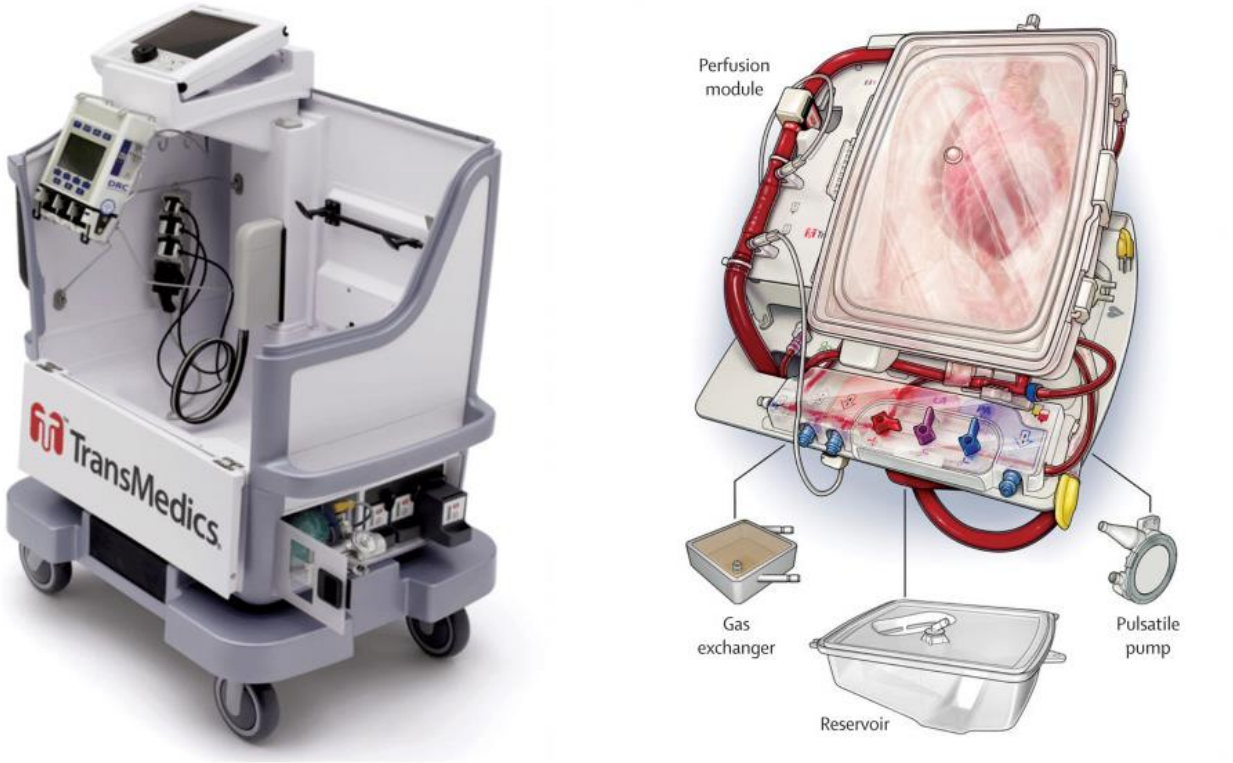

Figure 2-2, Adapted with permission from [44]: The Transmedics organ care system consisting of the portable console (left) and the heart perfusion set (right) which itself consists of a sterile housing, a venous reservoir, a gas exchanger, a sampling port and a flow probe.

While these clinical results are promising, there are a few limitations with the OCS that have been described in the literature. For starters, the OCS is quite costly, especially when compared to cold storage.[42] With medium term outcomes of currently usable hearts showing no appreciable difference when using the OCS as compared to cold storage, this can be seen to be problematic.[44] With post-transplant outcomes for DBD hearts being as good as they are, this is not an unexpected result, but the absence of more clinical studies confirming the OCS for use on extended criteria hearts has limited more widespread application.[48] Furthermore, many have questioned the

evaluation mechanism used on the OCS. Since this machine is only capable of perfusing hearts in LM, contractile assessment of donor hearts is impossible, with clinicians having to instead rely on lactate trends.[49] While these measurements have shown to be effective in the limited use of ESHP in the clinical setting, it is suggested that contractile evaluation is a more relevant predictor of post-transplant function, particularly for hearts with suboptimal function. [49-52] With these clinical limitations in mind, a thorough review of preclinical work is necessary in order to better understand the state of the field.

2.2.2 Hypothermic and Normothermic ESHP as Alternatives to Cold Storage

As in the clinical research, the area of preclinical ESHP study that has seen the most work done is in the comparative effectiveness of ESHP and Cold Static Storage (CS) as means of organ preservation during heart procurement.[53] Traditionally, hearts have been transported from the donation site to the recipient site in a hypothermic solution with the goal of keeping them between 4° and 8° C. [7] In this way, the heart can be kept arrested, metabolic function is slowed and the effects of ischemia reperfusion injury are minimized. [54] While this has proven to be a very effective technique, there are numerous concerns with the quality of heart preservation it provides. Groups have reported endothelial dysfunction as a result of cold static storage, that increases the longer the heart is kept stored. [55] Moreover, concerns about extracellular edema and ischemia reperfusion injury, especially over longer storage periods have limited the application of this technique.[7, 56] These drawbacks have manifested themselves in a hard limit on the allowable transportation time for donor hearts of only 6 hours. [57] With so many people on the waiting list, the use of every available organ is of paramount importance and as such, the extension of this transportation window is vital.

As the idea of augmented heart preservation began to gain traction, many groups sought to add LM perfusion to hearts in the same hypothermic setting as CS. As early as the late 1960s, experimentation with hypothermic LM perfusion showed that functional integrity could be maintained for periods as long as 72 hours, much longer than is possible using CS. [58-60] As measurable markers of contractile function began to become more sophisticated, these initial findings were replicated by Wicomb et al. who not only showed that contractile performance of hearts could be maintained across 48 hours of hypothermic perfusion, but successfully transplanted 4 baboon hearts after this perfusion period. [61] Since then, groups have demonstrated

that hearts preserved using hypothermic ESHP show better metabolic function, better hemodynamic recovery, better preservation of cellular structure and less DNA damage than those preserved using CS. [62-66] While these findings are promising, research has shifted away from hypothermic ESHP in recent years, with normothermic ESHP gaining popularity. Evidence suggesting that hypothermic ESHP provides any substantial preservation benefits compared to normothermic ESHP is notably absent from the literature. [67] In fact, working as a part of an Edmonton based team led by Dr. Darren Freed, White et al. show that at least in terms of initial reperfusion, warmer temperatures are beneficial for the preservation of DCD heart endothelial cell integrity. [68] Coupled with the fact that hypothermic perfusion precludes the use of working mode, in which physiologically relevant functional evaluation is possible, the shift in research focus towards normothermic perfusion is understandable. [67]

As evidenced by measurements of oxygen and lactate extraction by hearts during normothermic ESHP, aerobic metabolism can be maintained throughout the preservation period. [62, 69] To evaluate the impact of this phenomenon, as with hypothermic ESHP, much of the focus of normothermic ESHP research has been on its use as an alternative preservation strategy to CS. Aside from the aforementioned clinical studies involving the OCS, multiple groups have used preclinical studies to evaluate the feasibility of normothermic ESHP for transportation. Using DBD animal hearts preserved for clinically relevant 4-6-hour preservation periods, ESHP hearts have demonstrated superior ATP stores and improved contractile function compared to cold storage hearts, suggesting that at this timescale, ESHP offers a superior preservation setting. [70-72] Figure 2-3, adapted from Ozeki et al. shows the extent to which this difference is demonstrable.[72] In this work, with 9 canine hearts preserved for 6 hours using either CS or ESHP before evaluation, almost all measured contractile parameters presented better results in the ESHP group. At longer timescales, results have also been promising with successful preservation of up to 12 hours reported for porcine hearts. [73] At this timescale however, it has been shown that results of ESHP are not always consistent. Trahanas et al show that after 12 hours of perfusion, almost half of their tested porcine hearts either ceased electrical activity or showed unacceptable increases in coronary vascular resistance. [74] With these findings in mind, it is clear that in order to move forward with the clinical use of normothermic ESHP, work is needed to optimize the perfusion setting, particularly if the aim is the use of marginal donor hearts.

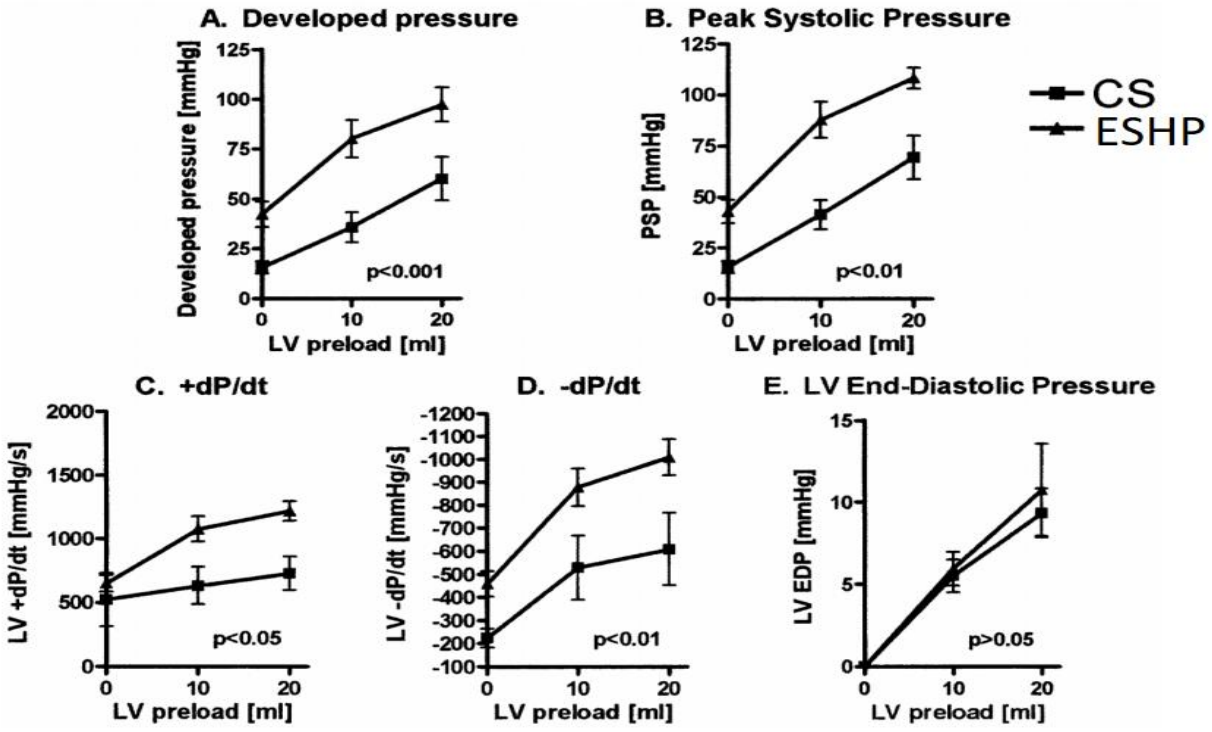

Figure 2-3, adapted with permission from [72]: The comparative left ventricular contractile performance of hearts perfused using CS and ESHP in terms of A, developed pressure, B, peak systolic pressure, C, maximum rate of developed pressure, D, minimum rate of developed pressure, and E end diastolic pressure.

2.2.3 ESHP Using DCD Hearts

The use of DCD hearts has long been an objective for cardiac transplant researchers. Estimated to represent an increase in transplant activity of up to 30% depending on the jurisdiction, the effective use of these hearts could prove revolutionary in the field. [10] Unfortunately, DCD hearts present numerous problems that are not present in their DBD counterparts. Due to the nature of the DCD donor, the process of circulatory arrest results in often extreme distention of the right ventricle, and a prolonged period of warm ischemia.[75, 76] In pigs, it has been shown that the exposure of hearts to more than 20 minutes of circulatory arrest is invariably associated with irreversible cardiac injury. [77] With this in mind, heart procurement strategy is a vital consideration. To date, two main strategies have emerged: the direct procurement protocol (DPP) and normothermic regional perfusion (NRP). [78] For DPP, upon extubation, a standoff period is observed, after which hearts are supplied a cardioplegic solution and a rapid cardiectomy is performed. [79] Upon

extraction, the heart is cannulated and normothermic ESHP is instituted. Conversely, using the NRP technique, after observing the post extubation standoff period, hearts are reanimated in the donor using a standard extracorporeal membrane oxygenation (ECMO) circuit. This approach allows for in situ reconditioning, and evaluation of DCD hearts, which can be followed by either CS or ESHP. To this point, both procurement approaches have demonstrated success. For additional information with respect to DCD heart transplantation itself, the reader is referred to the excellent review by White et al. [10]

In a similar manner to NRP, ESHP offers a unique platform for reconditioning, and perhaps more importantly, for functional evaluation of DCD hearts. Compared to DBD hearts, DCD hearts are particularly sensitive to ischemia.[77] With this in mind, over the last number of years, numerous groups have reported the successful reanimation of DCD hearts using ESHP. Using LM perfusion, Scheule et al. show that in terms of functional performance *ex situ*, ESHP with University of Wisconsin solution preserves DCD hearts more effectively than CS and enables evaluation of graft quality. [80] More specific and recent work has identified initial warm and cold ischemic conditions as paramount in importance for DCD hearts, as they are much more sensitive to ischemic injury than their DBD counterparts.[77, 81] With this in mind, it is unsurprising then that when Ilyer et al. extended their work to include porcine transplants that DCD hearts preserved using ESHP showed better post-transplant outcomes than those preserved using CS. [69] What the amalgamation of ESHP research in the area of DCD heart procurement suggests is that as improvements are made in limiting ischemia in reperfused hearts, the utility of this large group of potential donor organs could be realized. While it is promising that ESHP shows improvement over CS for DCD hearts, compared to DBD hearts, function is still generally thought to be worse using DCD organs. [82] As a means to allow for the use of DCD organs then, it is necessary to augment the quality of the ESHP technique itself, perhaps even to the point of cardiac repair *ex situ*.

2.2.4 The Differing Use of Perfusates and Additives in ESHP

With the aim of augmenting perfusion quality, investigation into the use of novel perfusate solutions in ESHP is a very important consideration in advancing the field. For lungs, the use of completely acellular solutions for *ex situ* perfusion is already a reality, with STEEN solution emerging as the most common for *ex situ* use for lungs, livers and kidneys. [83-85] As is the case

with the heart, tradition perfusion methods have utilized mostly whole donor blood for *ex situ* perfusion in all organs. [86-88] Clinically speaking, concerns about donor blood shortages preclude the widespread use of whole blood perfusates in *ex situ* practice. [89] For no organ is this more relevant than the heart. For lungs, livers and kidneys, typical perfusate flow rates are under 1 L/min. [90-92] For porcine hearts perfused or evaluated in a working heart mode, these flows are routinely higher than 2 L/min if only the left ventricle is loaded and closer to 4 L/min if both ventricles are loaded, necessitating the use of much more perfusate for the safe use of these systems. [93] To allow for clinical use of working mode, it is therefore of paramount importance that perfusates are optimized to limit the use of blood. Compared to other organs however, the investigation into these types of perfusates has been limited for ESHP.

While work in this aspect of the field is limited, there have been some important findings brought to light, perhaps most notably those from Dr. Freed's group in Edmonton. Research performed by White and colleagues came to two very important conclusions in terms of perfusate composition. Firstly, they found that the composition of initial reperfusion is very important and that a tepid adenosine-lidocaine cardioplegia performs better for minimizing myocardial injury than traditional cold hyperkalemic cardioplegia. [94] Perhaps more pertinently, they also showed that the use of a whole blood based perfusate (packed red blood cells and plasma) resulted in significantly better preservation of both systolic and diastolic function as compared to packed red blood cells alone, a hemoglobin based oxygen carrier (HBOC), or a perfusate consisting of HBOC and plasma. [95] Furthermore, they observe an increase in the development of myocardial edema in groups without plasma, an important consideration in the field.

Edema itself is a very prominent concern in the field as it is seen to result in diastolic dysfunction. [96] In an effort to reduce edema, in work currently under review, Ribeiro et al. perfused 24 porcine hearts with either a mixture of whole blood and saline, whole blood and STEEN solution, or whole blood and SOM-TRN-001, a novel solution specifically designed to enhance myocardial protection against reperfusion injury. [97] While the STEEN group did show improved preservation of LV systolic function during ESHP, all three groups showed substantial edema with no discernable difference observed between groups. To date, the most successful approach in reducing edema has been the use of methylprednisolone, which, in DCD hearts has been shown to reduce edema to a statistically significant degree.[98] This is a promising finding but the overall

impact this additive has on perfusion quality during ESHP remains unclear. In spite of recent progress, the optimal perfusate composition for successful ESHP has yet to be determined.

2.2.5 Working Mode as a Means for Cardiac Evaluation during ESHP

While research into the capability of ESHP as a preservation setting has been extensive, a substantial amount of recent work has focused on the use of ESHP as an evaluation setting for the prediction of post-transplant outcomes. Clinically, the OCS uses lactate measurements to assess heart function.[99] While in this specific setting these measurements have proven to be reasonably predictive of post-transplant outcomes, it has been suggested that the evaluation of contractile function is more relevant. [50] While it is possible to evaluate contractile function during LM perfusion, accurate observation requires ventricular loading along with a normothermic setting to allow for contraction. [100] With this in mind, groups have expanded on the pioneering work of Neely et al. to facilitate working heart perfusion in large animal models.[37] With these advancing systems, has also come a lack of consensus on the best methodologies for not only maintaining the working heart *ex situ,* but specifically measuring its function.

In terms of evaluation technique, numerous methodologies have been examined for use on working heart models over the last 20 years. Suehiro et al. described the use of a working mode perfusion to perform left ventricular (LV) contractile evaluation in a pre-transplant setting as early as 2001. [101] While their work only resulted in 4 of 13 canine hearts being successfully transplanted, they were able to show that post-transplant outcomes were closely correlated with measurements taken during ESHP. More recently, groups have begun to use working mode to keep hearts preserved as well as using it to evaluate them, with numerous reporting the capability of prolonged working mode perfusion. [80, 102, 103] What has been shown in abundance is that traditional methods for functional evaluation can be used *ex situ*. Pressure-volume catheterization has risen to prominence in the field, coming to be seen as the gold standard for *ex situ* evaluation. [104] In fact, it has even been shown that these contractile parameters obtained using pressure-volume catheterization are better markers of function than their metabolic counterparts. [50] As with any technique however, pressure-volume catheterization is not without its own drawbacks. The use of this technique consists of the insertion of a conductance catheter into the LV either through the aortic valve or a hole in the apex of the heart and while it allows for a very detailed analysis of LV function, many have suggested that it is too invasive to be clinically transferable. [105-107] Furthermore, and

perhaps more importantly, due to drastic differences in shape, the use of this evaluation technique in the accurate assessment of right ventricular (RV) contractile parameters is quite difficult. [108] With RV dysfunction post transplantation being of such large concern in the literature, this is a very important consideration. [109-111]

In an effort to circumvent some of the issues associated with pressure-volume catheterization, in recent years a few groups have sought alternative means to acquire these imperative contractile measurements. One such noninvasive technique that has been explored, following the example set by numerous *ex situ* lung perfusion groups, is the use computed tomography (CT) technology. [112] Pelgrim et al. were able to develop a protocol for the use of CT imaging on an *ex situ* circuit, and show that regional differences in myocardial perfusion parameters could be reliable determined. [113] While these results are promising, more research is needed for widespread adoption. Seeking an alternative solution that addresses concerns about both invasiveness and RV evaluative capability, Ruggeri et al. took the first steps in implementing an echocardiographic imaging setup for *ex situ* perfusion. [114] Initial results indicated that the assessment of LV function was eminently possible and additional pilot studies have suggested that this capability can be extended to the RV. [115] Characteristic images using their setup are pictured in Figure 2-4. As a clinically relevant technique, this approach offers considerable promise. Due to the nature of echocardiography however, quantitative results in terms of contractile parameters cannot be acquired in real time, instead requiring offline analysis. [116] Alternative means of evaluation such as machine learning based estimation have also been analyzed but both are only in nascent stages. [117]

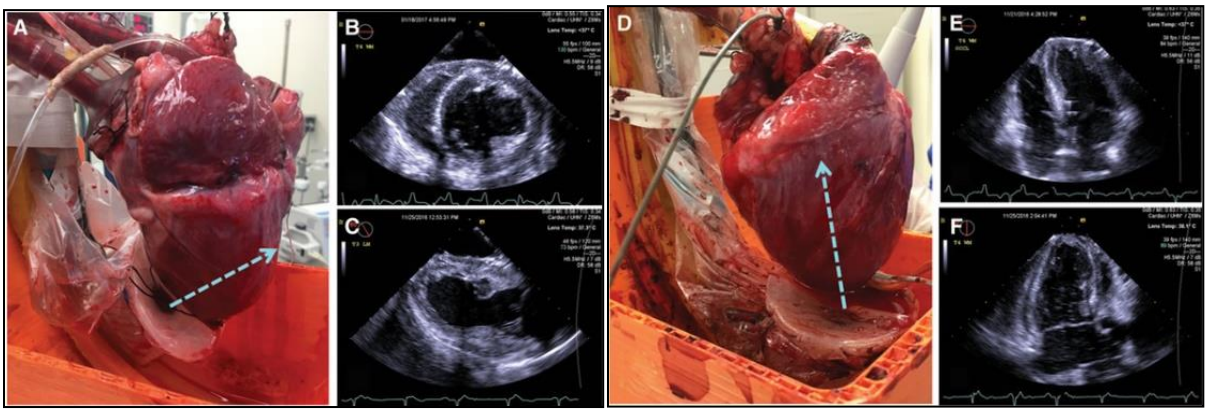

Figure 2-4 adapted with permission from [114]: TEE probe scanning positions and resultant images taken with the probe located behind the ventricles(A,B,C) and at the LV apex (D,E,F)

In addition to varying measurement techniques, it is important to consider that methodologies for employing working heart perfusion vary substantially across the literature. With physiological relevance important in providing a platform to predict post-transplant outcomes, and controllability important in terms of safety, different groups have made different tradeoffs to satisfy both goals. One of the main distinguishing features between working mode setups is the mechanism by which left ventricular afterload is instilled. During ESHP, aortic pressure is one of the most important parameters in terms of both heart preservation and ventricular evaluation. [118, 119] In LM, this pressure is set by the retrograde aortic flow from a pump or raised reservoir.[120] This directly controlled pressure (or more precisely the pressure difference between the aortic root and the coronary sinus), serves to drive the flow of oxygenated perfusate through the coronary system, with most perfusion occurring during diastole. [121]

For the working mode heart, where perfusate is pumped into the left atrium rather than retrograde to the aortic root, diastolic pressure is not always directly controlled. *In vivo*, diastolic pressure is instilled as a result of vascular compliance depending aortic pressure decay.[122] Absent this capability, diastolic pressure is either instilled using a second pump in a so-called pump supported working mode (PSWM) or using physical afterload elements in a passive afterload working mode (PAWM).[123] In PSWM, flow from the reservoir is split between two pumps with one pump providing perfusate for LV preload and the other serving to maintain diastolic pressure in the aorta. White et al. use this technique to great effect for both cardiac preservation and evaluation and a schematic of their system is pictured in Figure 2-5. [50] PAWM on the other hand, uses only the pump to provide preload while using passive elements to instill controllable afterload conditions. (section 2.3.3) Both of these modes have been used successfully implemented in large animal studies, but to this point, a comparative analysis of their effectiveness has yet to be undertaken. PAWM, while much less common offers a means to decouple the control of left atrial pressure, systolic aortic pressure, and diastolic aortic pressure through afterload manipulation. [103] However, an afterload solution capable of providing both safety and controllability in PAWM has yet to be proposed. PSWM is more common as it is seen to be safer due to the fact that, should contraction cease, aortic pressure is still maintained by the pump.

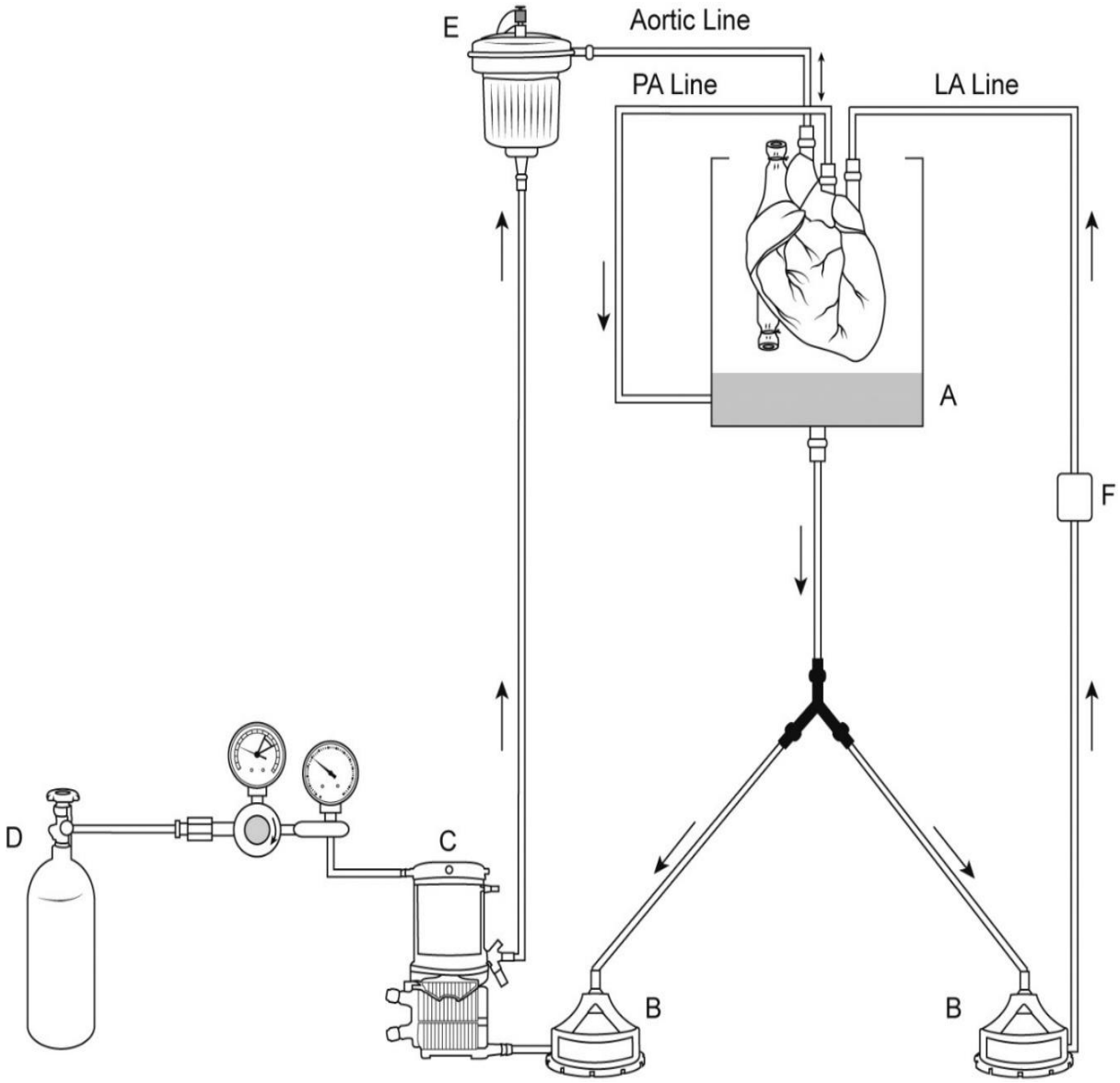

Figure 2-5, Adapted with permission from [50]: Simplified schematic of the ESHP circuit used by Dr. Darren Freed's research group consisting of A, a venous reservoir, B, 2 centrifugal pumps, C, a membrane oxygenator, D, an oxygen source, E, a Leukocyte filter and F, a flow probe

2.3 Artificial Afterload for the Isolated Heart

2.3.1 Windkessel Lumped Parameter Impedance Modelling

Very much separate from the goal of instilling physiological aortic pressures on the *ex situ* heart, the modelling of afterload phenomena is a very well-studied area that has been the subject of extensive research efforts for many years. Broadly speaking, the goal of this work has been to enable the analytical or, more recently, the numerical analysis of hemodynamic characteristics

throughout the body. One of the most analyzed areas in this respect has been in the relationship between aortic pressure and aortic flow. [124] The most commonly analyzed approaches in this type of modelling is the lumped parameter model. Models of this type use the electronic-hydraulic analogy whereby pressure is represented by a voltage drop, blood flow is represented by electric current, vascular resistance is represented by electrical resistance, vascular compliance is represented by capacitance, and fluid inertia represented by inductance. [125] In this way, systems can be solved as electric circuits and given measured pressure and flow conditions, afterload characteristics can be readily calculated from the associated model.

The coining of the term Windkessel as a means to describe the arterial system is generally attributed to Otto Frank.[126, 127] Otto Frank's Windkessel, now referred to as the two element Windkessel, consists of a restive element and a compliant element, and describes the entire arterial system. Frank proposed that the large arteries in the body functioned much like the air chambers (Windkessel in German) used by firefighters to dampen the pulsatile flow water. [128] Coupled with resistance, mainly characteristic of the smaller arteries within the periphery of the circulatory system, Frank postulated that the relationship between pressure and flow in the aorta could be characterized as follows, where P is blood pressure, Q is volumetric blood flow, C is total arterial compliance (defined as the change in volume across the heart beat divided by the change in pressure across the heart beat), and R_p is total arterial resistance[129]:

$$Q = C\frac{dP}{dt} + \frac{P}{R_P} \quad (2\text{-}1)$$

In spite of the fact that this model was developed over a century ago, it is still occasionally being used today. [130] That being said, as early as the 1940s, researchers such as Wetterer sought to expand the relevance of the Windkessel model. [131] With the advent of the electromagnetic flow meter in the mid-20th century, it became clear that while the 2 element Windkessel shows good fitting performance in diastole, the relationship between pressure and flow in systole is poorly described. [132] Through Fourier analysis, Westerhof et al. developed a three-element Windkessel model, sometimes referred to colloquially as a "Westkessel", that incorporated an additional impedance element to correct for this systolic disagreement. [133] In the two element Windkessel model, input impedance tends towards 0 at high frequencies. *In vivo* however, the input impedance decreases at high frequencies but reaches a non-zero plateau. [134] Westerhof et al found this input impedance to be equal to the characteristic impedance of the proximal aorta and added this element

to the model. [135] The revised characteristic equation is as follows, where Q is aortic blood flow, P is aortic pressure, R_c is the characteristic impedance of the proximal vasculature, C is total arterial compliance and R_p is total peripheral resistance [129]:

$$Q = C\,\frac{dP}{dt} - R_C C\,\frac{dQ}{dt} + \frac{P}{R_P} - \frac{R_C}{R_P}Q \quad (2\text{-}2)$$

This three element Windkessel model has been used to great success by numerous groups in modelling aortic pressure and flow relationships. [133, 136] Using Fourier analysis, these relationships have been analyzed extensively. [135, 137, 138] While the fitting performance of the three element Windkessel is quite robust in the time domain, these frequency domain analyses identified a mismatch between measured input impedances and those predicted using the three element Windkessel in the low frequency range, arising from the use of a resistive element to model characteristic impedance. [134] While this error is reasonably small and shows very little effect on the prediction of time domain pressures and flows, efforts have nonetheless been made to account for this low frequency mismatch. Inertance has been proposed as the fourth element in the Windkessel model, represented by an inductor and serving the purpose of increasing the low frequency accuracy of the model without impacting input impedance at higher frequencies. [139] Considerable disagreement has arisen however, in the positioning of this additional element within the model. Originally, Stergiopulous et al., following pioneering work by Burattini and Gnudi, proposed that this inductance element should be in parallel with characteristic impedance and showed very accurate modelling of aortic input impedance, especially when compared to the three element Windkessel. [139, 140] This work, however, differed from earlier work where the inertance element was placed in series with the characteristic impedance. [141] Mathematically speaking, the characteristic differential equation for the 4 element Windkessel with the inertance in parallel with the characteristic impedance, where Q is aortic blood flow, P is aortic pressure, R_c is the characteristic impedance of the proximal vasculature, C is total arterial compliance, R_p is total peripheral resistance, and L is total arterial inertance is as follows[129]:

$$LC\,\frac{d^2Q}{dt^2} + \left(R_C C + \frac{L}{R_P}\right)\frac{dQ}{dt} + \left(1 + \frac{R_C}{R_P}\right)Q = C\,\frac{dP}{dt} + \frac{P}{R_P} \quad (2\text{-}3)$$

Or with the inertance in series with the characteristic impedance [129]:

$$R_C R_P C L \frac{d^2Q}{dt^2} + L(R_C + R_P)\frac{dQ}{dt} + R_C R_P Q = R_P C L \frac{d^2P}{dt^2} + (L + R_P R_C C)\frac{dP}{dt} + R_C P \quad (2\text{-}4)$$

As is readily apparent, both versions of the 4 element Windkessel are much more mathematically complicated than their 3 element counterparts. Practically speaking, this results in an increase in the computational cost of fitting the model to measured data, and the degree to which there is a resultant improvement in fitting performance is still very much up for debate. [142] Segers et al. showed that in a large cohort of 2404 human subjects, in hearts with low blood pressure and low wave reflection magnitude, the 4 element Windkessel with the inertance in parallel with the characteristic impedance outperformed both its 3 element and 4 element counterparts. This group, however, only accounted for about 20% of the dataset. In the remainder of the dataset, where blood pressure and wave reflection magnitudes were not low, the three models behaved very similarly with the 4-element model with the inertance in series with the characteristic impedance presenting the best fitting performance. [142] Results from this study are shown in Figure 2-6. As can be readily observed, the fitting performance of the two different 4 element Windkessel models is very similar. Across the literature, there remain proponents of both approaches. [139, 143] Further, the demonstrable increase in required computation time for 4 element models, coupled with the difficulties associated with the calculation of inertance and thus the implementation of a physical manifestation of controllable inertance on isolated heart setups, has led some to conclude that in spite of slight decreases in accuracy, the 3 element Windkessel is still the most appropriate model. [124] As computational cost becomes less important however, owing to the augmentation of low frequency fitting, future study into the optimization of the 4 element Windkessel is still ongoing.

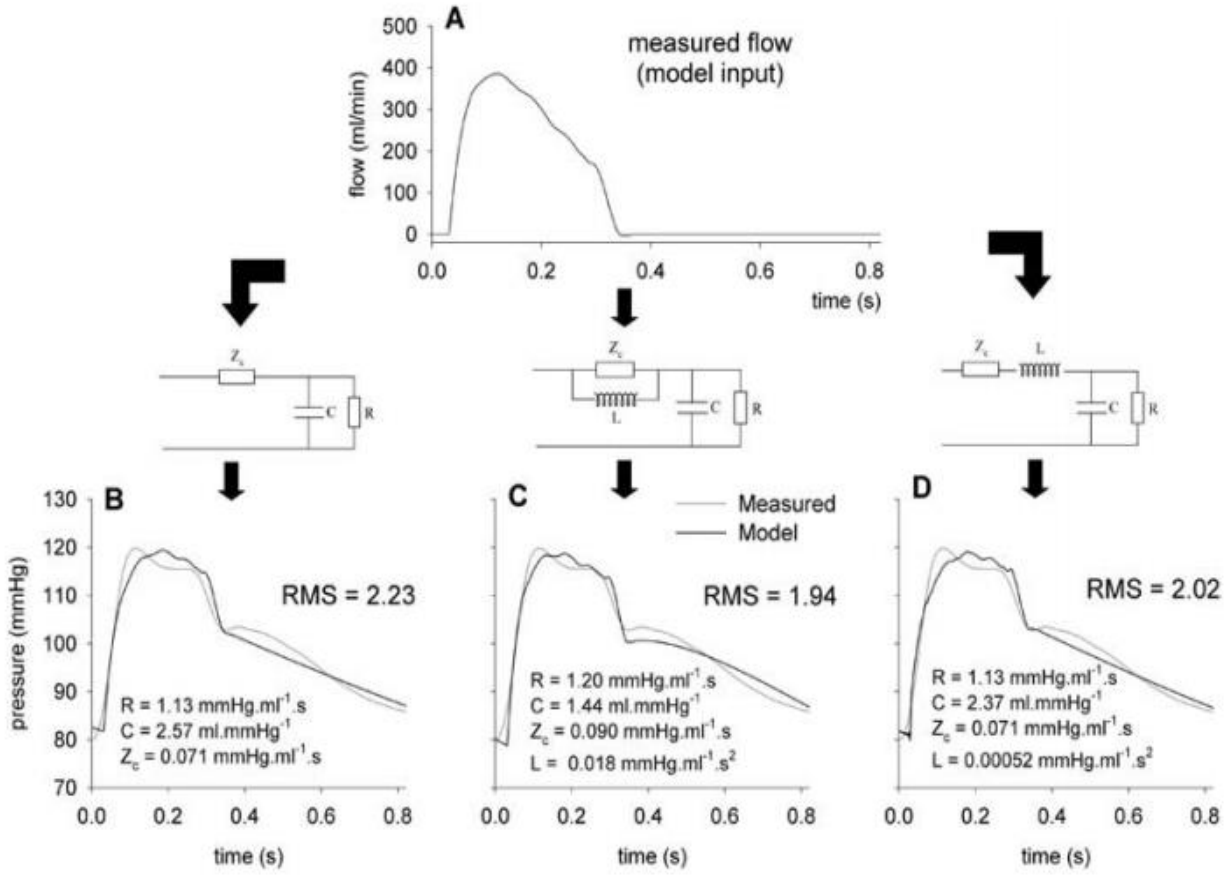

Figure 2-6, Adapted with permission from [142]: Measured aortic flow, A, used as the input to model aortic pressure as compared to measured aortic pressure using, B, the three element Windkessel model, C, the 4 element Windkessel model with the inductor in parallel with the characteristic impedance, and D, the four element Windkessel model with the inductor in series with the characteristic impedance.

2.3.2 Higher Order Modelling Techniques

Though lumped parameter, or 0D, modelling is the most studied approach for characterizing the relationship between aortic pressure and aortic flow, there have been research groups that have criticized their specificity.[144] While single compartment 0D models, such as the Windkessel, allow for very simple calculation of global pressure and flow relationships within the arterial system in terms of their temporal variance, they cannot be used to determine variation in these relationships in terms of position within the arterial system. [145] Since they treat the entirety of the systemic vasculature as a single block, the description of local pressure and flow distribution within the block is impossible. This has been in part addressed by splitting the entirety of the

arterial system into multiple so called “compartments”, such that each portion of interest within the broader system is represented by a separate lumped model, assumed to be homogenous.[146] These individual compartments are connected together to form larger and more accurate vascular models without drastically increasing computational cost. In essence, this multi-compartment approach discretizes the totality of the arterial system allowing for calculation of local phenomena within each individual compartment.[147] That being said, multi-compartmental 0D modelling is still just an approximation of true spatial-temporal or 1D models and, while computationally simple, are not seen to be comparatively accurate.[144]

Without sacrificing computational simplicity, groups have begun to use the so-called tube-load model as a replacement for 0D models. This model represents the arterial system as a system of parallel, uniform, lossless cylindrical tubes with parametric loads.[148] In terms of aortic hemodynamics, the tubes represent the various wave propagation paths throughout the arterial system while the loads represent the wave reflections distal to those specific paths. This ability to account for both wave reflection and propagation represents important progress compared to both mono-compartmental and multi-compartmental 0D models. These models have been used in many clinically relevant applications. Hahn et al., for example, used femoral and radial arterial pressure measurements to derive central aortic pressure.[149] In addition to monitoring central aortic pressure, tube-load models have been used to monitor arterial compliance, wave reflection, and pulse transit time. [150-152] That being said, while more accurate than the 0D models, tube-load models still offer room for improvement in terms of accuracy.[144]

In recent years, much of the research in the field of cardiovascular modelling has shifted from 0D models to 1D models. It is generally believed that throughout the body, the relationship between pressure and flow waveforms can be indicative of pathophysiological conditions of numerous organs, precipitating the rise of pulse wave studies in cardiovascular research. [153] Using modified versions of the axisymmetric form of the Navier-Stokes equations, 1D models allow for accurate and detailed prediction of pressure and flow waveforms over time and across the entirety of a vessel length of interest. [154] In this way, not only can flow and pressure waveforms be calculated, but the way that they propagate throughout the arterial system can be better understood. In terms of the estimation of central aortic pressure however, the sheer number and complexity of vascular parameters have limited the use of 1D modelling.[144] By limiting the number of parameters, clinically relevant aortic pressure estimations can however, be obtained. [155] Even

these simplified models have some drawbacks however in terms of their feasibility. The estimation of aortic pressure requires accurate measurement of aortic flow and artery geometry, which can both be challenging and expensive. [144, 153]

In this same respect, higher order 2D and 3D models of arterial circulation have been studied, and while they come with even greater drawbacks in terms of computational complexity, they offer exceptional accuracy for modelling smaller portions of the arterial system. Broadly speaking, these higher order models differ substantially in that 2D models are generally analyzed analytically while the complexity of 3D models generally precludes the discovery any analytical solutions.[153] Within 2D analytical models, common assumptions made on the 3D Navier-Stokes equations include: the flow is axisymmetric, the radius of the artery in question is much smaller than its characteristic length, and that the artery itself is a thin walled homogenous elastic cylinder.[156, 157] With these assumptions, groups have successfully used 2D analytical modelling to describe radial variations in blood pressure and flow, as well as to accurately characterize boundary conditions for both 2D and 3D computational models.[153, 156, 157] Often utilizing these computed boundary conditions, 3D models seek to combine the radial accuracy of 2D models with the ability to analyze changes in pressure and flow along the axial direction of the arteries in question.[158] By breaking complex geometries into multiple smaller segments, computational fluid dynamic (CFD) software can yield very accurate descriptions of many fluid phenomena of interest.[159] The successful implementation of this technique has far reaching implications, but to date, substantial challenges remain. Early research in terms of CFD used idealized geometries, hurting the accuracy of the computed results. More recently, medical imaging data has been successfully used to provide subject specific results.[160] These systems however are expensive and as utilized geometry becomes less idealized, the computational cost of solving these models only increases. As computational power continues to increase, we will no doubt see the rise of 2D and 3D models in the field of arterial modeling. Until then however, and particularly in terms of physical experimentation, lower order models remain the most effective option.

2.3.3 Physical Afterload Modules

In addition to extensive work in modelling, research has proceeded apace in the creation of physical manifestations of these afterload models. Owing to their simplicity, these physical afterload modules are almost entirely based on lumped parameter Windkessel models. Owing to the electronic-hydraulic analogy, simply creating physical versions of individual model elements and assembling them can result in a robust module that is suitable for use in a multitude of different research areas.[124] At their outset, these physical models were mainly created as a means to validate the applicability of the theoretical models themselves, or to study the impact of impedance phenomena on cardiac function. In more recent years however, while primarily still used for model validation, their use has expanded substantially.

One of the first physical modules was created by Westerhof et al. in 1971 during the course of their research into the applicability of the three element Windkessel model (pictured in Figure 2-7). [133] Within this module were physical manifestations of each of the three modeled elements. Compliance was instilled using a precisely measured volume of air that served to dampen the pressure pulsatility. Characteristic impedance and peripheral resistance, meanwhile, were instilled by forcing flow through capillary tubes and thus instilling fluid resistance with peripheral resistance being adjustable using a movable screen. They showed that the use of this physical lumped parameter model allowed for the creation of physiological aortic pressure and flow, just as shown in their model. While the demonstration of this model agreement was important, Westerhof's research also showed that hearts could be perfused *ex situ* in a physiologically relevant working mode. In fact, Elzinga and Westerhof used this same system to study the impact of resistance and compliance changes on aortic flow. [161] Throughout the 1980s, multiple groups expanded on this work, laying the foundation for much of our understanding of the relationships between aortic impedance and stroke work and ventricular ejection.[162-164] While this work on this front has slowed down in recently years, Kung et al. have shown that it is still a relevant research direction as they utilize physical Windkessel modules to validate computational fluid dynamic models. [165, 166]

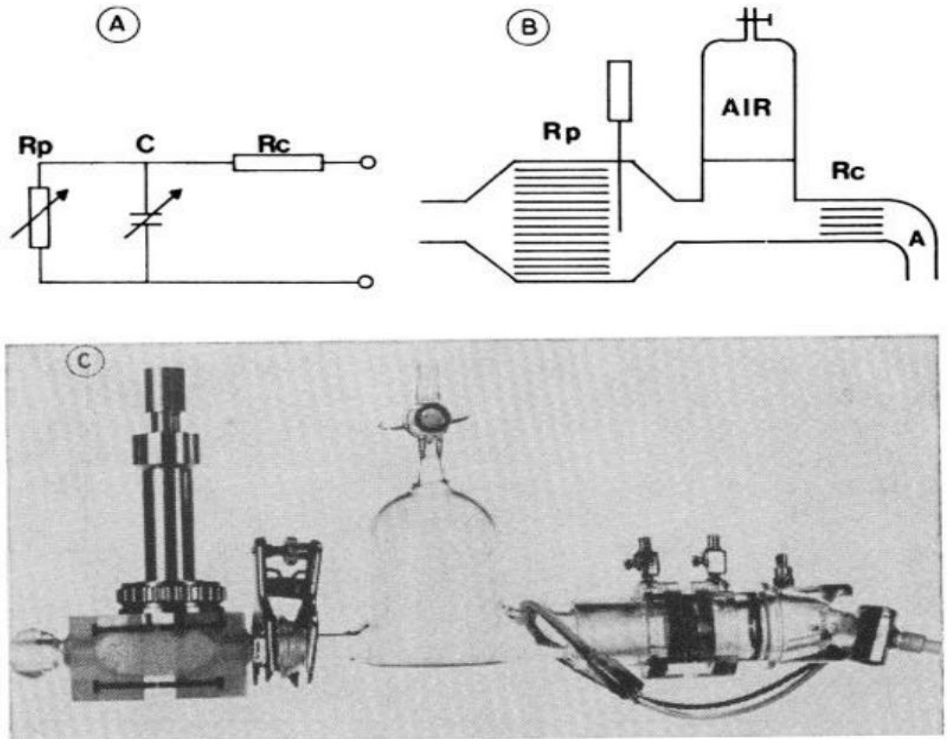

Figure 2-7, adapted with permission from [133]: A, the electrical representation of the three element Windkessel, B, the hydraulic schematic of the physical design proposed by Westerhof et al. including a peripheral resistance Rp, a characteristic impedance element Rc and an air based compliance chamber, C, a photograph of the physical system.

In more recent years, the explosion of research into engineered heart valves has offered an additional avenue for the application of the physical Windkessel. Warnock et al., Hildebrand et al. and Dumont et al. proposed two different bioreactors for tissue engineered heart valves that included a two element Windkessel in conjunction with a pulsatile mock circulatory loop in an effort to introduce physiological pressure and shear stress conditions to the in vitro environment. [167, 168] Similar Windkessel based work has also been performed with mock circulatory loops in the field of LVAD design. By creating mock circulatory loops, these devices can be validated without the need for *in vivo* analysis.[169-172] Konduri et al. took this work further showing that porcine hearts cultured in this type of bioreactor showed better maintenance of biological characteristics as well as less apoptosis than seen in valves under static incubation. [173] In spite of these efforts, the specific impact of the use of Windkessel modules in engineered heart valves remains unclear, with optimal conditioning protocols being heavily dependent on cell type. [174]

All told, as part of the cardiomimetic approach to valve culture, this technique shows great promise as an avenue for future research. [175]

In spite of their ability to produce physiological afterload conditions, adoption of Windkessel based afterload modules in ESHP has been much slower than in these other areas. The depressed pace of development in this specific area can be directly attributed to the inherent complexity of ESHP. While research using isolated hearts to study the relationships between hemodynamic phenomena seeks mostly to expose organs to a physiological setting in order to better understand the mechanics involved in cardiac function, ESHP has the actual preservation of these hearts as its top priority. With this in mind, issues of sterility and safety become much more important. The traditional Windkessel modules described above, while adept for the purposes they were designed for, have demonstrable drawbacks for ESHP. Firstly, the use of air driven compliance introduces multiple factors that limit its clinical applicability. Firstly, the risk for coronary air embolism in the event that a heart in PAWM momentarily ceases contraction is a very real concern. Additionally, the mandated interface between the air and the perfusate within the compliance chamber introduces concerns about both sterility and hemolysis should the perfusate be blood based. [176] Coupled with concerns around the ease of adjustability of afterload parameters and the mandate for sterility and reusability of resistive components, these considerations have limited excitement in the field. [177]

Nevertheless, a few groups have utilized PAWM in ESHP. Rosenstrauch et al. used a compliance chamber and a combination of hydrostatic pressure and tube clamps for resistance in order to instill afterload in adult porcine hearts. Across their 30 minutes of perfusion, they were able to successfully reanimate hearts and instill physiological hemodynamic parameters. This short perfusion period however precluded the capability of identifying the impact of prolonged PAWM, an important consideration as the changing contractile performance of the hearts necessitates corresponding changes in afterload. [129] More recently, work by Abicht et al., using the afterload module developed by Kung and Taylor, have confirmed PAWM as a usable mode for *ex situ* perfusion periods of up to 3 hours. [103, 166] Hemodynamic parameters were successfully maintained within physiological ranges and all tested porcine hearts showed favourable contractile function throughout the perfusion period. While no specific conclusions can yet be drawn about the impact of PAWM, this capability opens up an exciting new avenue for research into the

comparative effectiveness of this new mode and the more traditional modes of ESHP in terms of both their evaluative and preservative capabilities.

2.4 Summary and Future Perspectives

In summary, a vast amount of work has been completed and published in the combined fields of ESHP, circulatory system modelling, and the instillation of artificial afterload modules. While progress has been encouraging, research gaps remain in each respective area and in particular the integration of research within the three fields.

ESHP has seen incredible development over the last 3 decades, evolving from a nascent technology for the study of cardiac physiology to a clinically used platform for organ preservation. Preclinical work has shown demonstrable improvement over classic cold storage methods, and both clinically and preclinically, the use of DCD hearts has begun to be realized. [11, 77] Even with these great achievements taken into account, there is still much work to be done. Myocardial edema brought about by ischemia reperfusion injury remains a concern in ESHP, though the impact of *ex situ* edema on post-transplant outcomes is not yet fully understood.[98] It is postulated that changes in perfusate composition can limit this edema and augment cardiac preservation, but to this point, the optimal perfusate for ESHP remains unclear. [97] In terms of evaluation, preclinical studies show that contractile function measured during ESHP is more indicative of cardiac function than metabolic parameters used in current clinical studies.[50] The measurement of these parameters mandates the use of working heart models during ESHP but the impact this has on cardiac preservation is heretofore unknown. Furthermore, the optimal methodology for the instillation of working mode during ESHP is unclear with groups using either passive elements or pumps to instill afterload on the *ex situ* working heart. It is clear that an analysis must be undertaken to determine the optimal perfusion setting in terms of both cardiac preservation and evaluation and that a system capable of perfusing hearts in Langendorff mode and both separate working modes needs to be developed to move forward in the optimization of ESHP.

With the use of the cardio-mimetic approaches showing exceptional results in numerous fields, it has been postulated it’s application in ESHP could be an important consideration.[178] In strides taken towards the validation of lumped parameter Windkessel models, groups have shown that physiological aortic pressure and flow waveforms can be achieved using isolated hearts in working mode.[103] While higher order models show better accuracy in terms of predicting wider ranging

circulatory system phenomena, the fact that physical lumped parameter modules can be used to create a physiologic aortic setting is an important step. These modules have allowed for groundbreaking work in the analysis of the impact of changing pressure and flow conditions not only on circulatory system model accuracy, but on the development of tissue engineered cardiac structures as well.[168] Moving forward, however, important design consideration must be taken into account. Generally speaking, many physical Windkessel modules consist of resistive elements using valves or capillary tubes and compliance elements that use air chambers or compliant tubing to dampen pressure decay. These systems, while quite adept in their own applications, are limited in their larger scale applicability due to concerns around the sterility and reusability of the capillary tubes as well the direct interface between the air and perfusate within the compliance chambers. The resolution of these concerns could lead to much more widespread use of Windkessel modules in isolated heart setups.

In terms of this work, the most relevant area for the expansion of physical afterload modules is in ESHP itself. A few groups have begun to explore their use in this setting and have shown that physiological aortic flows and pressures are achievable in the ESHP setting. [103] ESHP itself however offers unique challenges in terms of changing cardiac contractility across longer perfusion periods. These changes mandate the adjustability of any afterload module used for ESHP which introduces the additional necessity of accurate modelling and controllability of the individual physical elements themselves. To this point, no physical afterload module with both adjustable parameter settings for the optimization of heart preservation and predictable parameter values to enable a consistent evaluation setting across different hearts has been described for ESHP. The implementation of such an afterload system would represent a progressive step in the field, especially if adapted to a system capable of use for comparing the applicability of all three ESHP perfusion modes.

Chapter 3

3 Research Objectives

3.1 Overall Aim

The overarching goal of this research was to develop a platform with an adjustable, passive afterload module and characterize its impact on *ex situ* heart preservation and the predictive relevance of *ex situ* heart evaluation.

3.2 Specific Aims

1) To develop an *ex situ* perfusion system capable of perfusing hearts in all three primary perfusion modes: Langendorff mode, Pump Supported Working mode, and Passive Afterload Working Mode. The execution of this aim is described in chapter 4.

2) To design and construct an afterload module with continuously adjustable parameter settings and validate its capability in maintaining physiological aortic pressure during ESHP. The execution of this aim is described in chapter 5.

3) To analyze the comparative relevance of a contractile parameters measured in PSWM and PAWM as they pertain to predicting post-transplant outcomes. The execution of this aim is described in chapter 6.

4) To develop and analyze an early stage non-invasive alternative to pressure volume catheterization for measuring contractile performance *ex situ*. The execution of this aim is described in chapter 6.

Chapter 4

4 The Development of a Multimodal *Ex situ* Perfusion System[1]

4.1 Introduction

Heart Failure affects over 7.5 million people and it is the primary cause of death in over 300,000 people per year in North America. [94, 179] While numerous treatment strategies have been developed to alleviate symptoms or decrease mortality, cardiac transplantation remains the gold-standard treatment for eligible patients.[50, 74] Recent medical advances have resulted in a steady increase in patients qualified for this procedure, but a shortage of usable donor hearts has limited growth in transplant numbers. *Ex situ* heart perfusion (ESHP) is a promising technology that has been proposed to expand the donor pool.[94] This technique offers the potential to both enhance our ability to preserve organs, potentially increasing the number of hearts capable of transplant, and reduce the number of hearts that are discarded without quantitative functional evaluation.

The first isolated heart perfusion experiment was conducted by Langendorff in the late 1800s[33, 50, 180]. Groups have since attempted to improve on Langendorff's technology for metabolic investigation and more recently, studying organ preservation.[60, 102] The only ESHP system currently approved for clinical trials is the Transmedics Organ Care System (Transmedics, Andover, MA) designed for heart transportation.[44] This system employs the traditional Langendorff technique, precluding the assessment of contractile function. In order to determine organ transplantability, the Transmedics system relies on the assessment of lactate metabolism. [44]While these measurements are important, left ventricular contractile parameters have proven more effective in predicting cardiac performance post transplantation.[50]

1 Work Presented in this chapter was published as:

Xin L, **Gellner B**, Ribeiro RVP, Ruggeri GM, Banner D, Meineri M, et al. A New Multi-Mode Perfusion System for Ex Vivo Heart Perfusion Study. Journal of Medical Systems. 2017 2017/12/23;42(2):25.

Some recent ESHP research has focused on the use of working modes (where blood is provided to the left heart) to enable graft evaluation during perfusion. [50, 67, 95, 102, 105, 181] Most systems use a two-chamber working mode [50, 102, 103] in which blood is provided to the left atrium and ejected from the left ventricle. Abicht et al. successfully developed a biventricular (four chamber) working heart platform using a pump to load the left atrium, and a reservoir to load the right atrium by gravity.[103] The coupled design of the loading system, however, makes it difficult to independently manipulate the preload of the left and right atria. In terms of afterload, this system uses passive elements for working mode while others have used a pump to support diastolic pressure in the aorta. [50] While left ventricular functional assessment has been successfully demonstrated in each working mode, the optimal afterload strategy remains unclear. No existing ESHP system can facilitate the comparison of pump supported afterload and passive afterload or evaluating right ventricular contractile parameters.

In this paper, a novel, modular *ex situ* perfusion platform is described. The system can produce physiological hemodynamic characteristics and evaluating contractile parameters in both the left and right ventricles of adult-sized porcine hearts in three different modes: Langendorff Mode (LM), Pump-Supported Working-Mode (PSWM) and Passive Afterload Working-Mode (PAWM). In each perfusion mode, performance is evaluated across six experiments in terms of how well the goals of multimodal perfusion control and system stability were demonstrated. It is shown that the system is capable of both preserving and evaluating hearts and thus provides a flexible platform for *ex situ* cardiac research.

4.2 Materials and Methods

The animals used for this study received humane care in accordance to the Canadian Council on Animal Care guidelines. The protocol was approved by the Institutional Animal Care Committee of University Health Network.

4.2.1 Heart Preparation

Six male Yorkshire pigs (55±5kg) were anesthetized with an intramuscular injection of Ketamine (30 mg/kg) and Atropine (0.04 mg/kg). Orotracheal intubation was established, and general anesthesia maintained with 2% isoflurane. A 20g peripheral intravenous catheter was inserted into

an ear vein, and a 1000 ml bolus of 0.9% Sodium Chloride was administered. Magnesium Sulfate (2 g) was also given intravenously to prevent arrhythmia.

A median sternotomy was performed and heparin (30,000 units) was given intravenously. After dissection of the cardiac structures, a baseline left ventricular contractility assessment with a pressure-volume (PV) catheter was performed. A cannula was introduced into the inferior vena cava (IVC) for blood collection, and a cardioplegia cannula was secured to the ascending aorta. A baseline blood gas analysis was performed on a blood sample taken prior to cardioplegia. Two litres of whole blood were collected by gravity, the aorta was cross clamped, and the hearts were arrested with 1000 mL of Celsior cardioplegic solution at 4ºC. The organ was excised and placed in ice cold Celsior solution for 1 hour, during which the aorta, pulmonary artery, superior vena cava, and left atrium were cannulated. The IVC was ligated for ESHP.

4.2.2 Perfusion System Preparation

An overview of the custom-made platform is depicted in Figure 4-1. In brief, this ESHP system consisted of a venous reservoir (Affinity Fusion®, Medtronic, Minneapolis, MN), an oxygenator with heat exchanger (Affinity Fusion®, Medtronic, Minneapolis, MN), a heater (Sarns Dual Heater Cooler Model 11160) and 2 centrifugal pumps (560A and 540T, Medtronic, Minneapolis, MN) mounted on to a Medtronic Performer CPB machine (Medtronic, Minneapolis, MN) and a Bio-console 560 (Medtronic, Minneapolis, MN).

The system was primed with 1.5 L of autologous whole blood along with 1g of Cefazolin and 2g Magnesium Sulfate to prevent arrhythmias. Normal saline (0.9% NaCl) was added to adjust hematocrit to 25% per standard practice [182, 183]. The fraction of inspired oxygen (FiO2) and oxygen flow through the oxygenator (sweep) were manipulated to maintain a pH between 7.35 and 7.45, a P_{O2} between 100 and 300 mmHg and a P_{CO2} between 35 and 45 mmHg.

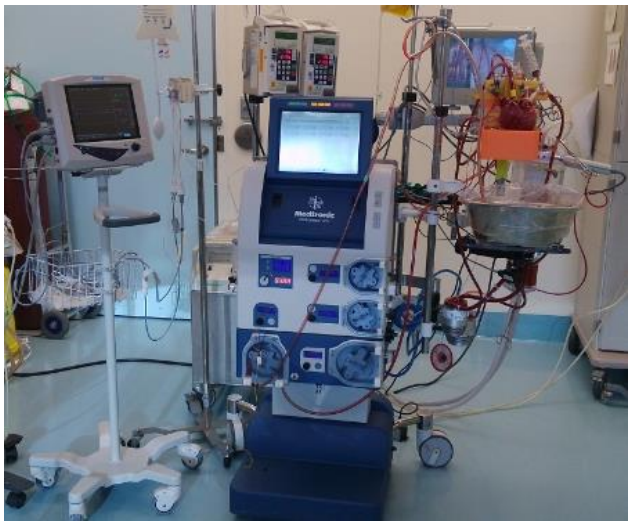

Figure 4-1 Ex situ Heart Perfusion System

4.2.3 Reperfusion Procedure

After 1 hour of cold ischemic storage, the heart was connected to the ESHP system via the cannulas. The left heart was de-aired by forward perfusion and the left atrial line was clamped. Retrograde aortic perfusion was commenced at a pressure of 50 mmHg (in Langendorff Mode). The organ was rewarmed to 37ºC over 30 minutes by increasing the temperature of the perfusate. Hearts that fibrillated during this period were defibrillated. If necessary, ventricular pacing was implemented at 100 bpm until stabilization. Continuous infusions of Dobutamine (5 mcg/min) and Insulin (5 units/h) were maintained throughout the experiment.

Once the heart was rewarmed, arterial and venous samples were taken from the aorta and pulmonary artery, respectively, for electrolyte analysis. Calcium chloride 10%, sodium bicarbonate 8.4%, and dextrose 50% was added to correct calcium (1.1-1.3mmol/L), glucose(5-10 mmol/L), and bicarbonate(24-30 mmol/L) concentrations as needed. Samples were taken and corrections made every hour for the remainder of the experiment.

All hearts were transitioned from Langendorff mode to 2 chamber Pump-Supported Working-Mode at 1(T1) and 4 hours (T4) for functional assessment. This transition was achieved by opening the clamp on the left atrial inflow line, and gradually opening the left atrial resistor until a left atrial pressure of 10 mmHg was achieved. The pump was then set to maintain a diastolic pressure of 30 mmHg in the aorta. Each functional assessment lasted approximately 30 minutes; hearts were perfused in Langendorff Mode (LM) throughout the remainder of the experiment. After the four-

hour functional evaluation, hearts were randomly transitioned into either biventricular Pump Supported Working Mode (Bi-PSWM) or biventricular Passive Working Mode (Bi-PAWM) to evaluate system capability (n=3 per group). Switching from PSWM to bi-PSWM consisted simply of introducing flow into the right atrium. Switching from PSWM to bi-PAWM meanwhile consisted of engaging the Windkessel afterload module and clamping the line connecting the pump to the aortic outflow and adjusting it to provide a pressure of 10 mmHg to the left atrium. Once stabilized, flow was introduced to the right atrium. A summary of the experimental protocol can be viewed in Figure 4-2.

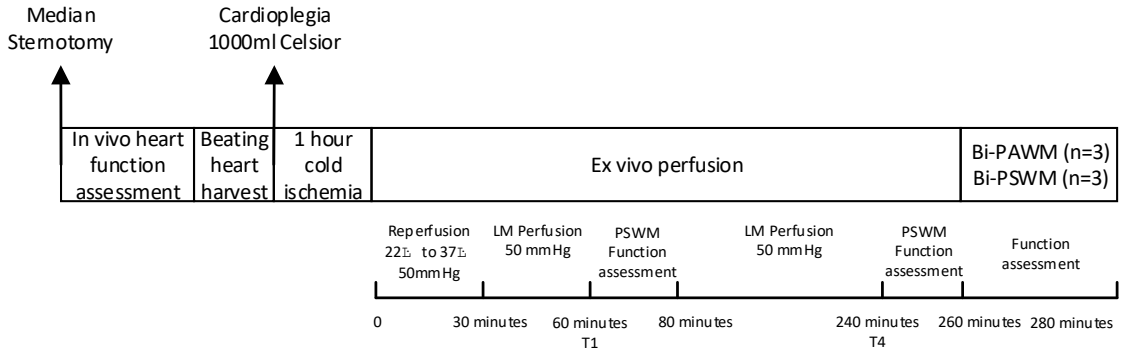

Figure 4-2: The Experimental Protocol: The following hemodynamic parameters and metabolic variables were measured in Langendorff Mode (LM) hourly (T1 to T4): aortic flow, aortic pressure, perfusate temperature, pH, lactate, pO2, pCO2, hemoglobin, hematocrit, oxygen saturation, and electrolytes. Functional parameters were measured at T1 and T4 in Pump-Supported Working Mode (PSWM).

4.2.4 Perfusion Modes

4.2.4.1 Langendorff Mode

During Langendorff Mode (Figure 4-3 a), oxygenated perfusate was pumped retrograde into the aorta at a constant pressure of 50 mmHg with centrifugal pump 1 (CP1). This pressure forced the aortic valve closed and the perfusate into coronary vessels, oxygenating and supplying substrate to the myocardium. The perfusate emptied into the coronary sinus and, ultimately, into the right ventricle where it was ejected back to the reservoir through the pulmonary artery. No perfusate was supplied to the left and right atria during Langendorff Mode.

4.2.4.2 Pump-Supported Working Mode

In Pump-Supported Working Mode, a portion of the blood pumped through CP1 to the aorta was redirected into the left atrium (Figure 4-3 b) by manipulating the resistance in the left atrial line. Initially, CP1 was adjusted to maintain a diastolic pressure of 30 mmHg in the aortic root while the left atrial line was slowly opened using an adjustable clamp (VWR® Talon® Regular Hosecock Clamp), loading the left atrium with a pressure between 5 and 10 mmHg. During diastole, the aortic pressure was sustained by the retrograde support provided by CP1. In systole, with the left ventricle ejecting, this retrograde support acted as a resistance to aortic flow giving rise to systolic pressure. Optionally, centrifugal pump 2 (CP2) could be used to load the right atrium at a pressure between 5 and 10 mmHg instituting biventricular Pump-Supported Working Mode.

4.2.4.3 Passive Afterload Working Mode

In this mode, all the flow from CP1 is directed to the left atrium. The line connecting CP1 to the aortic line was clamped and pump speed kept very low to maintain a left atrial pressure between 5 and 10 mmHg. The aortic pressure waveform in this mode can be manipulated using an adjustable two-element Windkessel module placed on the line connecting the aorta to the reservoir. [166] Increasing resistance results in an increase in both systolic and diastolic pressure. Increasing compliance results in a decrease in systolic pressure and an increase in diastolic pressure. Through manipulation of resistance and compliance, systolic and diastolic pressures could be varied independently. In this mode, measured *in vivo* aortic pressures were targeted. Optionally, CP2 could be used to load the right atrium at a pressure between 5 and 10 mmHg instituting biventricular Passive Afterload-Working Mode.

(a)

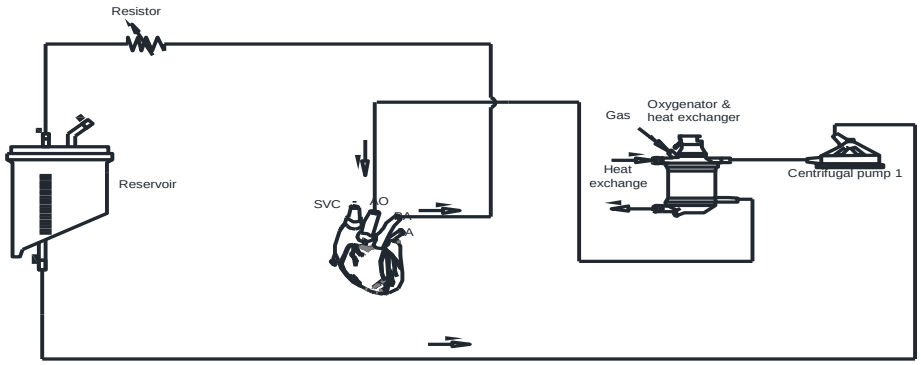

(b)

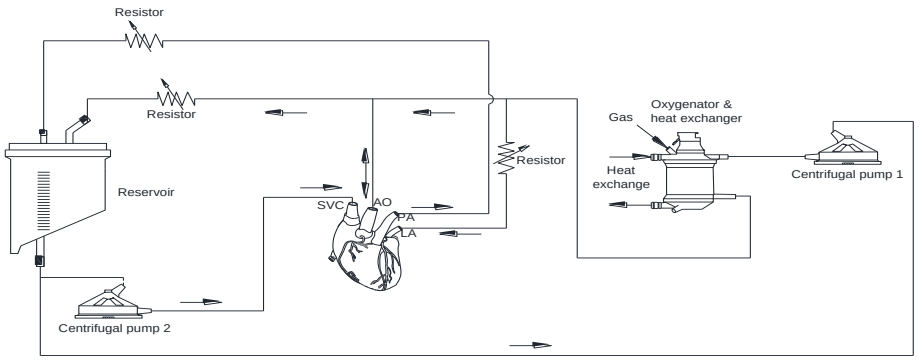

(c)

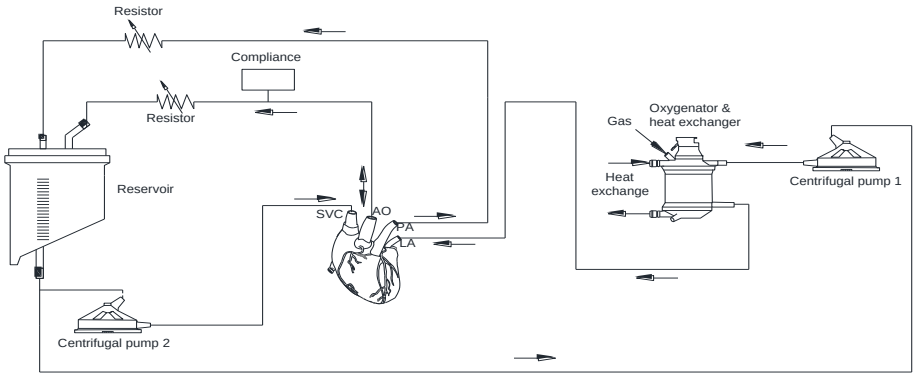

Figure 4-3:(a) Langendorff Mode, (b) Pump-Supported Working Mode, (c) Passive Afterload Working Mode.

4.2.5 Hemodynamic Parameters

In order to validate system stability, perfusate flows and pressures were measured throughout the perfusion circuit and recorded. Pressure was measured (TruWave disposable pressure transducer, Edwards, Irvine, California, USA) at the inflow of the right and left atria and the outflow of the aorta and pulmonary artery. Flow was measured in the aortic line with the flow probe (H9XL, Transonic Systems Inc.) placed as close to the aortic root as possible. This flow was recorded hourly. Perfusate temperature and blood gases were monitored (Terumo Blood Parameter Monitoring System CDI500) at the oxygenator's outlet.

4.2.6 Metabolic Assessment

All metabolic parameters were assessed with hearts perfused in Langendorff Mode. Hourly samples of arterial and venous perfusate from the aorta and pulmonary artery, respectively, were collected for blood gas analysis. Parameters such as pH, lactate level, pO_2, pCO2, hemoglobin, hematocrit, oxygen saturation, and electrolytes (RAPIDPoint® 500 Blood Gas Systems, Siemens)

were measured and recorded. Myocardial lactate metabolism, coronary vascular resistance and myocardial oxygen consumption were derived as detailed below.

Myocardial lactate metabolism was determined as follows:

$$Myocardial\ Lactate\ Metabolism = Pulmonary\ Artery\ Lactate - Aortic\ Lactate$$

Indexed Coronary vascular resistance (CVR) was calculated as follows:

$$CVR = \frac{(Mean\ Aortic\ Pressure - Mean\ Right\ Atrial\ Pressure)}{CBF \cdot 100g\ Heart\ Weight}$$

Where CBF is the coronary blood flow, assumed to be equivalent to the aortic blood flow. Indexed myocardial Oxygen consumption (MVO_2) was as follows:

$$MVO_2 = \frac{CBF\ \times (C_aO_2 - C_VO_2)}{100\ Heart\ Weight}$$

Where C_aO_2 is the arterial oxygen concentration (aorta) and C_vO_2 is the venous oxygen concentration.

CaO_2 and CvO_2 can be calculated as follows:

$$C_aO_2 = (1.34\ \times Hemoglobin\ Concentration\ \times SaO_2) + (0.0031\ \times\ PaO_2)$$

Where SaO_2 is the arterial oxyhemoglobin saturation and PaO_2 is the arterial oxygen tension.

Left Ventricular Functional Parameters

In Pump-Supported Working Mode and Passive Afterload Working Mode, left ventricular functional parameters were measured using a conductance catheter (SPC-571, Millar Inc, Houston, TX) inserted transapically. Prior to each evaluation period, the catheter system was calibrated using both a pressure calibration module (PCU 2000, Millar Inc, Houston, TX) and a volume calibration module (Sigma 5 DF, CD Leycom, Hengelo, Netherlands). Volume-dependent measurements were collected under steady loading conditions while volume-independent measurements were collected by intermittent clamping of the LA line. Maximum rate of ventricular pressure change (dP/dt_{max}), end-systolic elastance (ESPVR) and pre-load recruitable stroke work (PRSW) were used to assess systolic function. Diastolic function was assessed using minimum rate of ventricular pressure change (dP/dt_{min}), isovolumetric relaxation constant (Tau), and end-diastolic pressure volume relationship (EDPVR) [184].

4.2.7 Echocardiography

Surface echocardiography was performed using a standard 3D transesophageal echocardiographic (TEE) probe (Z6Ms, Siemens, ACUSON SC2000) during each functional assessment period. The scan protocol included 3 views: left ventricular short axis, apical four and two chamber. Systolic function was evaluated in terms of ejection fraction (EF) computed using the biplane method of disks (MOD). Analysis of fractional area change (FAC) was completed on left ventricular short axis at the level of papillary muscles.

Statistical Analysis

Normally distributed continuous variables are compared using repeated-measures analysis of variance or paired t-test were appropriate (Minitab 15) and reported as mean ± standard error. A p-value < 0.05 was considered statistically significant.

4.3 Results

4.3.1 Langendorff Mode System Parameters

4.3.1.1 Aortic Root Pressure and Flow

During Langendorff-mode, the aortic root pressure was precisely controlled by changing the speed of CP1. Despite changes in coronary vascular resistance, the target aortic pressure was maintained throughout the *ex situ* perfusion period (Figure 4-4 a and 4b).

4.3.1.2 pH

pH was regulated by manipulating the oxygenator sweep and FiO_2. Perfusate analysis indicated that the pH was stable and within physiological limits (7.35-7.45) during perfusion (Figure 4-4 c).

4.3.1.3 Temperature

Hearts were rewarmed slowly in Langendorff Mode to 37°C after which the temperature remained stable for the final 3 hours of perfusion (Figure 4-4 d).

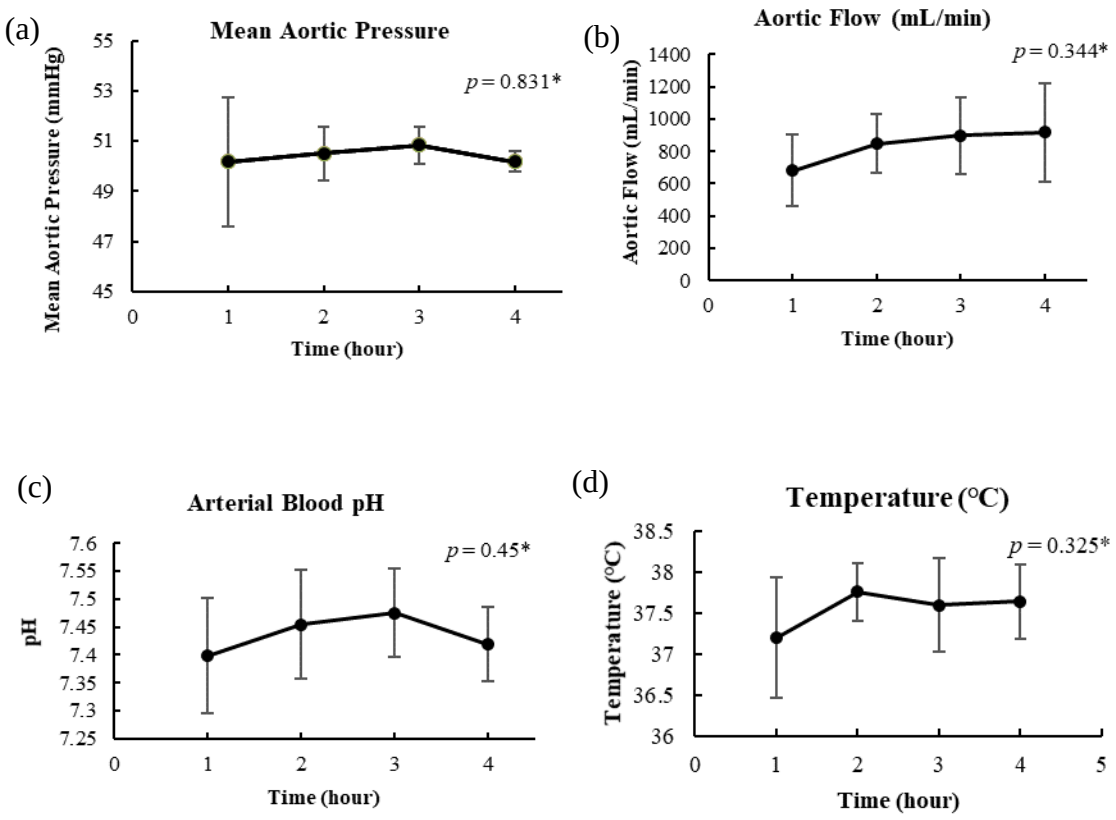

*Figure 4-4: (a) Mean Aortic Pressure, (b) Mean Aortic Flow, (c) Perfusate pH, (d) Perfusate Temperature. *Indicates p values for comparison at T1, T2, T3 and T4 using repeated measures ANOVA. The range bars show the standard error of the mean.*

4.3.2 Metabolic Assessment

Myocardial Lactate Metabolism

As seen in Figure 4-5 a, hearts demonstrated a relatively neutral lactate metabolism throughout the perfusion period. No statistically significant changes occurred during the 4-hour perfusion period (p=0.943).

4.3.2.1 Coronary Vascular Resistance

The change in CVR over the preservation interval is shown in Figure 4-5 c. Hearts showed a non-significant decrease in CVR over the first two hours of the perfusion period and then stabilized for the remaining period (p=0.489).

4.3.2.2 Myocardial Oxygen Consumption

A linear increase in oxygen consumption was seen over the first 3 hours of perfusion (Figure 4-5 d), however this increase was not statistically significant (p = 0.178)

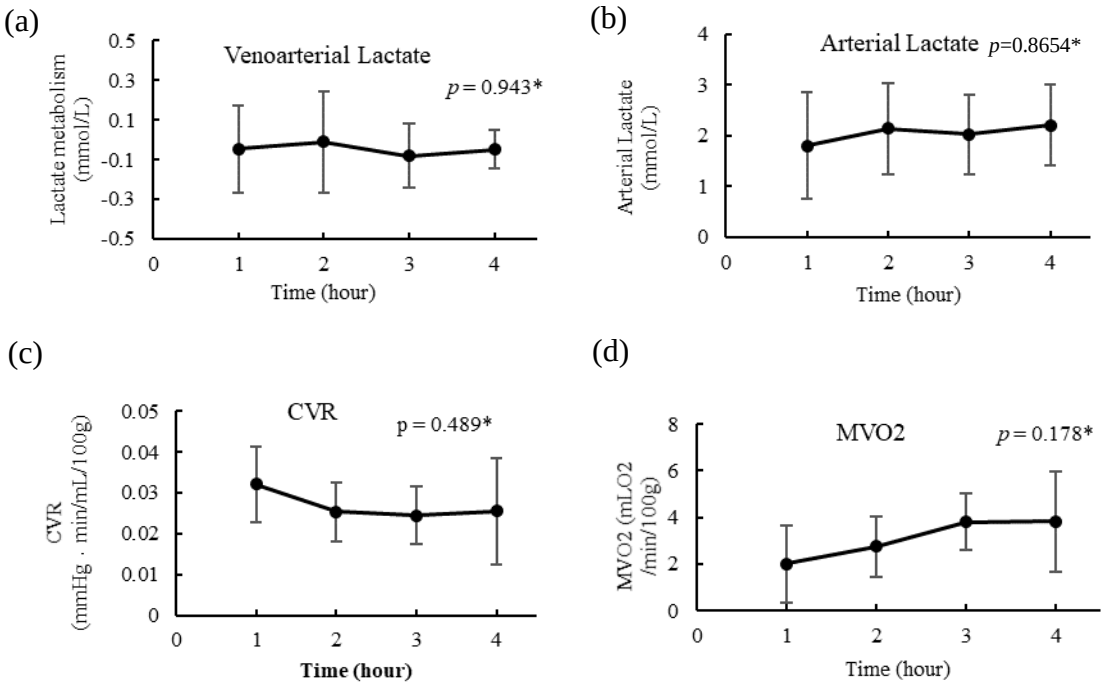

*Figure 4-5: (a) Lactate Metabolism during Perfusion, (b) Arterial Lactate during Perfusion, (c) Coronary vascular resistance during Perfusion, (d) Myocardial Oxygen Consumption during Perfusion. *Indicates p values for comparison at T1, T2, T3 and T4 using repeated-measures ANOVA. The range bars show the standard error of the mean.*

4.3.3 Working Mode Aortic Pressure Control

Figure 4-6 a, b and c illustrate representative examples of the aortic pressure curves measured *in vivo*, during Pump-Supported Working Mode, and during bi-ventricular passive afterload working mode respectively. Waveforms in passive working mode were closer to the physiological waveform than their Pump-Supported Working Mode equivalents. Figure 4-6 d shows a waveform in Passive Afterload Working Mode in which systolic pressure was intentionally elevated while diastolic pressure was maintained at a physiological level.

(a) (b)

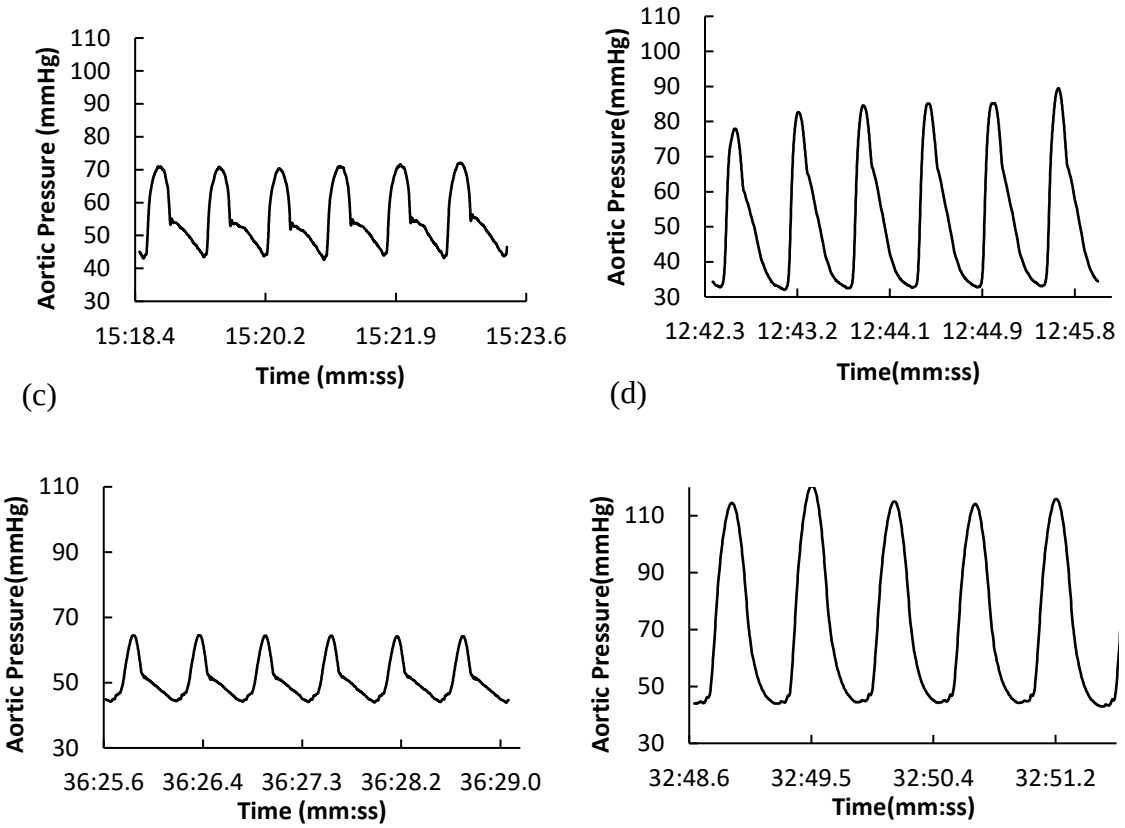

Figure 4-6: (a) In vivo Aortic Pressure, (b) Aortic Pressure during Pump-Supported Working Mode, (c) Physiological Aortic Pressure in Passive Afterload Working Mode, (d) High Systolic Pressure in Passive Afterload Working Mode

4.3.4 Left Ventricular Functional Assessment

4.3.4.1 Pressure Volume Relationships

Cardiac function was assessed in Pump-Supported Working Mode (T1 and T4) and Left ventricular function remained stable after four hours of perfusion. As shown in Table 4-1 there are no statistically significant changes in any of the parameters between the 1 and 4-hour marks.

Table 4-1: Functional Parameters Measured Using Pressure-Volume Catheterization

	Parameter	Unit	T1 PSWM	T4 PSWM	p-value*
Diastolic Function	LV dP/dtmin	mm Hg/s	-1010±584	-857±435	0.740
	Tau	ms	49±41	62±31	0.487
	EDPVR		0.27±0.09	0.35±0.16	0.390
Systolic Function	LV dP/dtmax	mm Hg/s	1045±322	1101±277	0.526
	PRSW		50.7±20.33	41.29±7.47	0.339
	ESPVR		6.83±1.60	8.14±3.72	0.122
	Cardiac output	mL/min	1478±685	1599±549	0.542

*indicates p value for comparison of T1 and T4 using paired student's t-test

Representative PV loops taken during transient inflow occlusion are shown in *Figure 4-7* below. These occlusions were done at each evaluation time point. An *in vivo* occlusion image is included for comparison.

(a) (b) (c)

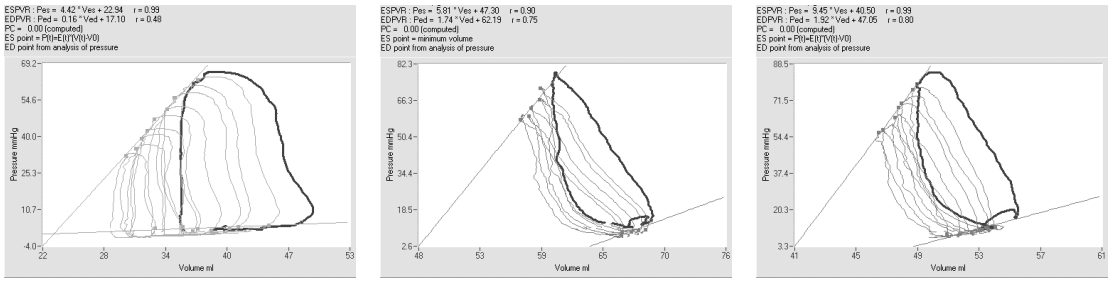

Figure 4-7: Left Ventricular Pressure-volume Loops during Transient Inflow Occlusion, (a) In vivo Occlusion, (b) 1 Hour Pump-Supported Working Mode Occlusion, (c) 4 Hour Pump-Supported Working Mode Occlusion.

Additional PV measurements were taken on hearts that were switched to Bi-Ventricular passive working mode after four hours and representative loops can be seen in *Figure 4-8*.

(a) (b)

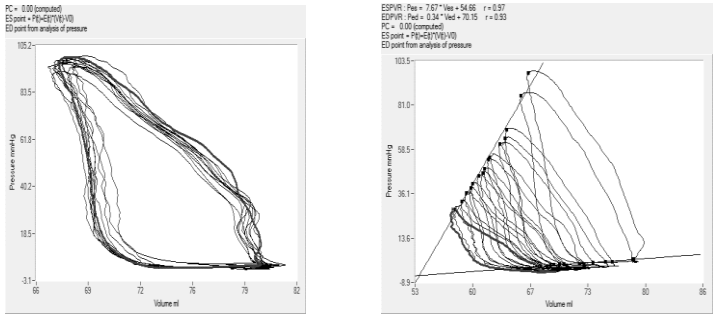

Figure 4-8: Bi-Ventricular Passive Afterload Left Ventricle Pressure-Volume Loops after 4 Hours of Perfusion, (a) Passive Afterload Steady, (b) Passive Afterload Occlusion

4.3.5 Echocardiography

Epicardial views were successfully obtained by two different operators in all pigs and resemble standard transthoracic equivalents[185] (Figure 4-9).

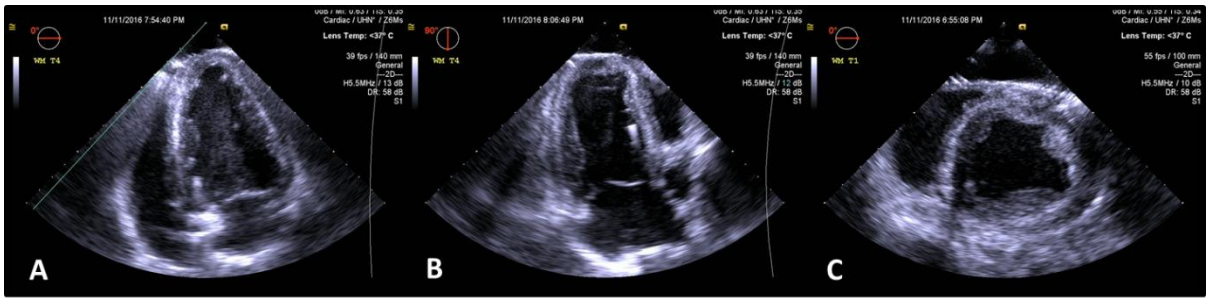

Figure 4-9: Echocardiographic evaluation. (a) Equivalent of Apical 4 chamber, (b) Apical 2 chamber, and (c) LV short axis

Additional images were obtained in biventricular Pump-Supported working mode as seen in Figure 4-10 below:

(a) (b)

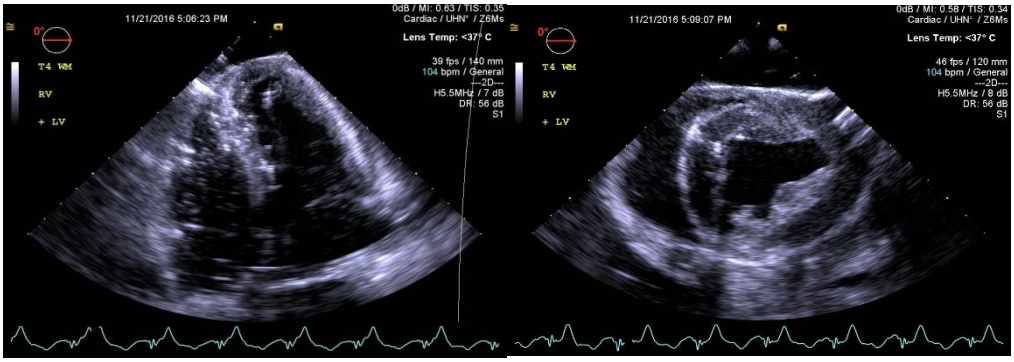

Figure 4-10: Representative examples of echocardiographic images in Biventricular Pump Supported Working Mode (a) Apical 4 Chamber View, (b) Left Ventricular Short Axis View.

Throughout the perfusion period there was no significant change in EF and FAC.

Table 4-2: Parameters of Systolic Function Measured with Echocardiography

	T1 PSWM	**T4 PSWM**	p-value
FAC, %	34±8	23±5	0.080
EF 4 Chamber, %	29±11	29±9	0.937
EF 2 Chamber, %	32±20	31±6	1.000
EF BiPlane, %	32±16	30±7	0.859

Parameters of systolic function measured with echocardiography (TEE) during functional timing of ex situ heart perfusion. FAC, Fractional Area Change; EF, Ejection Fraction; WM, Working Mode. Student T-test; P<0.05 as significant.

4.4 Discussion

In this study, a novel, modular *ex situ* heart perfusion system has been described. The experimental results demonstrate the functionality of our design across 3 different perfusion modes: Langendorff Mode, Pump-Supported Working Mode and Passive Afterload Working Mode. In both Pump-Supported Working Mode and Passive Afterload Working Mode, the system facilitated left sided and biventricular loading, with independent control of right and left atrial pressures. In each of the six experiments, the system demonstrated stability across the 4-hour perfusion period. System parameters including; aortic pressure, aortic flow, perfusate temperature and pH were controllable and within a physiological range in both Langendorff Mode and Pump Supported Working Mode (Figure 4-4). The functionality of Passive Afterload Working Mode was also demonstrated on our system (Figure 4-6 and Figure 4-8) with further experimentation needed to validate its stability

over longer perfusion periods. To our knowledge, this is the first description of a platform capable of perfusing the heart in both Pump-Supported Working Mode and Passive Afterload Working Mode.

Hearts demonstrated predominantly aerobic metabolism throughout each experiment as evidenced by the neutral lactate metabolism (Figure 4-5 5a) and the stable lactate levels across the perfusion period (Figure 4-5 b). This conclusion is corroborated by the myocardial oxygen consumption results. As expected, MVO_2 increased as the heart was rewarmed and regained function. We notice further rise in this parameter following the initial working-mode functional assessment at 1 hour, presumably due to the increase in energy demand during that period (Figure 4-5 d). A similar pattern is seen with coronary vascular resistance (Figure 4-5 c). Following the first hour functional assessment, we see a drop in CVR, likely enabling increased oxygen delivery to the myocardium during the period of higher energy demand. Both the increase in MVO_2 and decrease in CVR suggest the recovery of myocardial metabolic function during reperfusion and demonstrate the regulatory capacity of the organ to respond to rises in energy demand during the functional assessment.

We have successfully demonstrated the capability of transitioning from non-working (Langendorff) perfusion mode to two different working modes by loading the left (and optionally the right) atrium, an important step in facilitating functional assessment *ex situ*. There is currently no validated method to assess cardiac function during ESHP. In this study, we chose to assess left ventricular function using pressure volume relationships (Table 4-1 and Figure 4-7). The capability of performing this type of functional assessment on our system in each working mode has been demonstrated. We note that hearts regained contractile function following reperfusion and the platform was capable of preserving contractility throughout the perfusion period. This evaluation technique is not perfect, however. Clinical use is very limited due to its invasiveness and evaluation of equivalent parameters in the right ventricle is quite difficult. Evaluation of the right heart during ESHP has not yet been demonstrated by any group.

As a less invasive functional assessment technique, and one that can also be used to evaluate the right heart, we also measured function using echocardiography. We have shown that on our platform, echocardiographic evaluation is a feasible method to assess and monitor cardiac function during ESHP. Our pilot scan protocol is a good starting point although a tailored study to further

evaluate echocardiography in this setting is necessary to strengthen these preliminary results. The views acquired during this study were comparable with the conventional transthoracic exams [185] and the image quality allowed for functional cardiac assessment. Future studies are being prepared by our group to develop a comprehensive biventricular echocardiographic assessment strategy and to correlate these results with the analysis of the pressure volume loops with the goal of replacing catheterization with a non-invasive, flexible evaluation methodology. As seen in Table 4-2, there was no significant change in left ventricular contractility over the perfusion period.

Cold storage remains the standard preservation technique for organ transplantation; however, it invariably leads to a progressive decline in viability and function. It also precludes organ assessment to determine adequacy for transplantation. *Ex situ* Organ Perfusion systems, including cardiac platforms, enable organ resuscitation and preservation in and oxygenated and normothermic environment, providing substrate to meet energy requirements. This technique has already demonstrated capability of extending preservation periods and metabolic evaluation [9] and has allowed the use of marginal donor organs, such as hearts donated after circulatory death.[94]

Distinct from other perfusion circuits, the modular design of the system provides a means of assessing a multitude of different perfusion strategies on the same platform. Owing to the independent control of the two pumps, the system can operate in Langendorff Mode, left- and right-sided two-chamber Working Mode, Biventricular Working Mode, and with a passive or pump-supported afterload. Having shown the capability of the system, this modularity provides a means for future study of very specific characteristics of *ex situ* recovery without interfering with the organ's reperfusion process. Of particular interest is the potential for evaluating right ventricular contractile function.

This modularity also permits analysis of the comparative efficiency of the different modes. While Langendorff Mode perfusion remains the standard technique for ESHP, working modes offer a means to study many cardiac states that are impossible to achieve in Langendorff Mode. In pump-supported Working Mode, a physiological diastolic pressure can be maintained. In our case, since the speed of the pump changes both the diastolic pressure and the resistance against which the left ventricle ejects however, independent control of the systolic and diastolic pressure was not possible. The coupling of these pressures could potentially be mitigated with more rigorous

optimization, though the impact of this strategy requires additional research. Using a passive afterload module, such as a two-element Windkessel module, both systolic and diastolic aortic pressure along with waveform shape can be controlled by changing resistance and compliance values.[166] This control could offer an avenue to evaluate the effect of different clinically relevant scenarios (such as post-operative vasoplegia) on the *ex situ* heart, however more investigation is needed to determine the impact this phenomenon has on heart preservation and evaluation.

In summary, the novel *ex situ* heart perfusion system has successfully enabled preservation of large animal donor hearts for up to 4 hours. The system also has also demonstrated the capability of independently loading the left and right chambers in each perfusion mode. We present our findings with a limited sample size; however, the primary goal of the investigation was to determine system functionality, which has been demonstrated across the experiments. Moving forward, this system offers an ideal platform for further experimental studies in the field of cardiovascular science. To validate the clinical relevance of the system, porcine transplant studies must be performed. Additional future research could include; the optimization of perfusate composition and perfusion modes for cardiac preservation, the effect of prolonged perfusion, and the effectiveness of different *ex situ* organ assessment strategies that combined could potentially increase the number of hearts available for transplantation.

Chapter 5

5 The Development and Testing of a Novel and Adjustable Afterload Module for *Ex situ* Heart Perfusion

5.1 Introduction

Ex situ heart perfusion is a novel and effective means of facilitating the preservation and functional evaluation of donor hearts. [44, 53, 72, 186] Using this technique, hearts that have brain-death induced transient dysfunction could be proven usable with *ex situ* evaluation, while poor quality hearts could potentially be treated using reparatory therapies to improve their performance, thus expanding the donor pool.

Isolated heart perfusion was first described by Oscar Langendorff in the late 1800s.[32]96 In traditional Langendorff Mode perfusion, oxygenated perfusate is provided via retrograde flow to the aorta, forcing the aortic valve closed and perfusate through the coronary arteries. By providing the heart with oxygen and an energy substrate, an aerobic metabolism can be maintained in the organ. This is an effective technique for metabolic investigation; however, with *ex situ* contractile parameters proving more useful than metabolic parameters in organ evaluation,[50] groups have sought to load the left and right atria to facilitate ventricular ejection. In the majority of these Working Mode models, a secondary pump is used to facilitate ventricular afterload in a so-called Pump Supported Working Mode.[187] Blood is pumped into the left atrium to load the heart and retrograde down the aorta to maintain aortic pressure through diastole. With only two controllable parameters (the speeds of the two pumps), the control of left atrial pressure, aortic systolic pressure and aortic diastolic pressure is functionally coupled in PSWM, precluding their completely independent control without considerable heart specific optimization. This deficiency in controllability can result in a substantial difference between measurable contractile parameters and aortic pressure waveforms measured during ESHP as compared to those seen *in vivo*. [187]

As originally popularized by Otto Frank with his Windkessel model,[126, 127] lumped parameter impedance analysis is the most common way to model afterload phenomena. In this way, the relationship between pressure and flow can be described as a function of passive electrical circuit

elements that represent systemic resistance, characteristic aortic impedance, arterial compliance, and inertance. A few groups have expanded on these models to create physical manifestations of these systems,[166, 175] with early investigations into the usefulness of this technique in *ex situ* heart perfusion.[103] Attaching an afterload module upstream of the aortic root can result in *ex situ* aortic pressure waveforms that are quite similar to their *in vivo* equivalents, and precludes the need for retrograde aortic support in diastole (as is the case in Pump Supported Working Mode).[103, 187] In this so called Passive Afterload Working mode, as a heart recovers function or deteriorates across prolonged perfusion periods, changes in left ventricular contractility can result in dramatic changes in the *ex situ* flow waveform.[188] Without corresponding changes in afterload parameters, the aortic pressure waveform will also change dramatically, adversely impacting perfusion quality.[53] With most physical afterload modules having fixed parameter values, however, their use in prolonged perfusion has been understandably limited.

In more recent years, a few groups have improved parameter adjustability within the classic Windkessel setup. The overwhelming majority of these adjustable afterload modules have been developed for mock circulation loops with applications including tissue engineered heart valves,[167, 168, 174] ventricular assist device validation,[170, 171] and the validation of computational models on isolated hearts.[165, 166] In terms of prolonged *ex situ* perfusion, de Hart et al successfully created a system in which an adjustable afterload module was attached to the aorta in order to produce accurate aortic pressure waveforms.[102] Within this system, coronary perfusion is decoupled from aortic pressure as a pump directing perfusate to the isolated coronary arteries is utilized, while aortic pressure is varied by adjusting both preload and afterload. Expanding on these developments, in our own previous work, we utilized a simple 2 element Windkessel module consisting of an adjustable clamp and air based compliance chamber to successfully implement a Passive Afterload Working mode.[187] In this perfusion mode, the afterload module serves as both a means to set aortic pressure, and to institute specific afterload settings across different hearts to allow for evaluative consistency. In terms of afterload module development therefore, the ability to adjust parameter settings based on changing contractile function and to set parameters to known values for evaluation are of paramount importance. Despite recent advances in the field, no single system has been validated in terms of the simultaneous achievement of both of these aims during *ex situ* heart perfusion.

In this paper, a novel and adjustable afterload module, expanding on our previous module, is developed and tested in terms of its capability in decoupling the control of left atrial pressure, systolic aortic pressure and diastolic aortic pressure. Each element within the module was tested individually to evaluate element setting predictability. The complete afterload module maintained consistent aortic pressure waveforms across a six-hour perfusion period when tested with three porcine hearts. These data confirm the apparatus' applicability as a load for the isolated perfused heart.

5.2 Methods

5.2.1 The Four Element Windkessel Model

The four element Windkessel (Figure 5-1), previously demonstrated to be an effective load on isolated heart setups, [133] was chosen as the basis for the physical afterload module. This model consists of 3 design elements: a proximal resistance (R_p) representing the characteristic impedance of the proximal aorta in series with a systemic resistance (R_s) representing the fluid resistance associated with the periphery of the circulatory system, and a capacitance (C) representing arterial compliance in parallel. While physically speaking, only these three components were created (in effect making the physical afterload module a three element Windkessel), the system has inherent inertance associated with perfusate flow. This inertance, modelled as an inductor (L) in series with the other elements, has been described as the final element in the four element Windkessel. Inclusion of this inertance element, either in parallel or series with the proximal resistance, has resulted in better fit between theoretical and measured impedance values than the three element model. [139] The theoretical inertance for our system is 0.0557 $mmHgs^2/cm^3$ calculated as the density of the perfusate multiplied by the length of tubing between the heart and reservoir and divided by its cross-sectional area. [166] In our analysis, the four element Windkessel with the inductor in series with the proximal resistor was used. As theoretical inertance is very low compared to *in vivo* values, the difference between the series and parallel representations of the four element Windkessel should be minimal. The characteristic frequency domain equation for the model that relates pressure (P) and flow (Q) as a function of frequency (ω) [142] is as follows, where j is the square root of -1:

$$P(\omega) = Q(\omega)(R_P + j\omega L + \frac{R_S}{1+j\omega CR_S}) \quad (5\text{-}1)$$

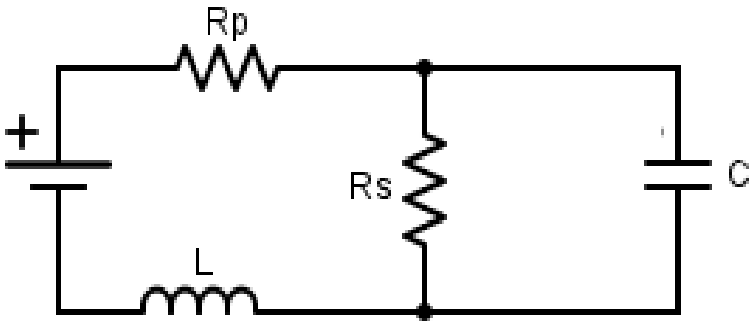

Figure 5-1:The electrical representation of the four element Windkessel model. In our case, design elements include the proximal resistor (Rp) representing the characteristic impedance of the proximal aorta, the systemic resistor (Rs) representing the fluid resistance in the periphery of the circulator system and the capacitor (C) representing the total arterial compliance. The inductor(L) represents the inertia of the fluid flow and while present in the model, is simply inherent to our physical system.

5.2.2 Afterload Module Component Development and Validation

5.2.2.1 Systemic and Proximal Resistor

The systemic resistor in the afterload module was designed to mimic the entirety of the physiological range of total vascular resistance (shown in pigs to have a maximum value of 2.122 mmHgs/cm^3,[189] and in humans to have a maximum value of 2.28 mmHgs/cm^3 [190]) and be reusable. The systemic resistor (Figure 5-2 a) consists of a rectangular aluminum channel with a steel bar inside. The bar compresses the tubing within the resistor into an ellipse, never coming into contact with the perfusate, and instituting a wide range of resistances (R). The instituted resistance (R) is defined as follows, where μ is the fluid's dynamic viscosity, L the conduit length, and a and b, the semi-major and semi-minor axes of the ellipse respectively.[191]

$$R = \frac{Pressure}{Flow\ Rate} = \frac{4\mu L(a^2+b^2)}{\pi(ab)^3} \quad (5\text{-}2)$$

It is important to note that at low radii, the risk of turbulent flow is introduced, potentially impacting the accuracy of equation (5-2) and interfering with resistance control. Considered with concerns around increased hemolysis when the working fluid is blood,[192] avoiding turbulence is imperative. Reynolds number is the key parameter for evaluating turbulence [193] and is defined as follows:

$$Re = \frac{\rho v d}{\mu} \quad (5\text{-}3)$$

where ρ is the fluid's density, μ its dynamic viscosity, v its velocity, and d the diameter of the conduit. In designing the systemic resistor, it is necessary to ensure a sufficient length of tubing is compressed such that at high flows, diametral compression can be minimized enough to keep Reynold's number below 4000 and thus, keep flow from being turbulent. At physiological left atrial pressures, *ex situ* hearts, as a result of ischemic injury, have a left atrial inflow below 2.5 L/min[187]. A considerable portion of this flow travels down the coronaries rather than proceeding through the aorta. Taking 2.5 L/min to be the maximum flow, using the hemodynamic properties of blood for our calculations, and using a maximum operating resistance of 4 mmHgs/cm^3 (considerably higher than the maximum seen *in vivo)*, the resistor length required to keep flow from being turbulent is 19 cm.

In order to determine the predictive accuracy of equation (5-2) for the systemic resistor, resistance was measured at numerous flow and compression conditions. Using a magnetic levitation centrifugal pump (Bio-console 560, Medtronic, Minneapolis, MN), a mixture of heparinized porcine blood and saline solution (0.9% NaCl), titrated to a hematocrit of 25%, was pumped from a reservoir (Affinity Fusion®, Medtronic, Minneapolis, MN) through the resistor. Diametral compression was increased in intervals from 0% to 85% compression (corresponding to the designed resistance range) and flow varied between 0.25 L/min and 4 L/min in 0.25 L/min intervals at each compression level. In each scenario, the pressure drop across the resistor was measured (TruWave disposable pressure transducer, Edwards, Irvine, California, USA) and resistance calculated. These measured values were compared to theoretical values found using equation (5-2).

The proximal resistor was designed on a similar principle to the systemic resistor using an adjustable tubing clamp (Pinch Valve PV-4, Flow-Rite, Byron Center, Michigan, USA). Proximal physiological resistance values are low (0.06-0.08 mmHgs/cm^3) [194], so turbulence was not a concern.

5.2.2.2 Compliance Chamber

The compliance chamber design followed a similar process. The compliance element in the 4 element Windkessel (Figure 5-1) is responsible for dampening the pulsatility of the aortic pressure wave under pulsatile flow. *In vivo*, the maximum arterial compliance in pigs is 3.44 cm^3/mmHg [194] (very similar to the 3.90 cm^3/mmHg maximum compliance observed in humans [195]) but to facilitate supraphysiological conditions, the compliance chamber was designed to impose compliances between 0 and 6 cm^3/mmHg. Compliance itself can be described as the quotient of a volume change ($\triangle V$) and the pressure change that brought it about($\triangle P$) [196]:

$$C = \frac{\triangle V}{\triangle P} \quad (5\text{-}4)$$

Traditionally, compliance is instituted using trapped air however, changing and measuring the air volume that drives compliance in this case can be difficult resulting in problems in compliance adjustability. [166, 175] Rather than air, the compliance chamber design (Figure 5-2 b) utilizes a spring-loaded piston. In systole, when pressure in the chamber is high, the spring is compressed, storing energy. In diastole, as pressure drops, the piston pushes against the blood, dampening pressure decay. The compliance chamber consists of 5 components: a bag (General Purpose Probe Cover, PC1290, Ecolab, Saint Paul, Minnesota, USA) to ensure perfusate sterility, a funnel which connects the chamber to the system tubing, a cylinder with an inner diameter of 7 cm, the piston which presses against the bag, the spring(Compression Spring PC072-1000-28.800-HD-12.000-C-Z-IN, Acxess Spring, Colton, California, USA), and the cylinder cap that the spring pushes against and through which the spring can be wound, changing coil engagement. Applying Hooke's law, where k is the spring constant, equation (5-4) can be reduced to:

$$C = \frac{\pi^2 r^4}{k} \quad (5\text{-}5)$$

To vary compliance, the spring constant is varied by winding the spring through the cylinder cap according to equation (5-6); where *D* is the spring's coil diameter, d, its wire diameter, *G*, its modulus of rigidity and *n*, the number of engaged coils.

$$k = \frac{G d^4}{8 n D^3} \quad (5\text{-}6)$$

In order to verify the adjustability of the compliance chamber, perfusate was pumped from a reservoir using a centrifugal pump into the chamber at 30 mmHg and then 80 mmHg. These specific pressures, while not a determining factor in the value of instilled artificial compliance, were chosen as they correspond to *in vivo* porcine diastolic and systolic pressures. At each coil

engagement (from 1 to 24), the height change of the piston across these two pressures was measured and used to calculate a measured compliance from equation (5-4). Measured compliance was compared to theoretical compliance values attained using equations (5-5) and (5-6) to evaluate the chamber's ability to accurately prescribe compliance values. This test was run three times using three different perfusates: a mixture of blood and saline solution (0.9% NaCl) titrated to a hematocrit of 25%,[187] saline solution alone (0.9% NaCl), and water.

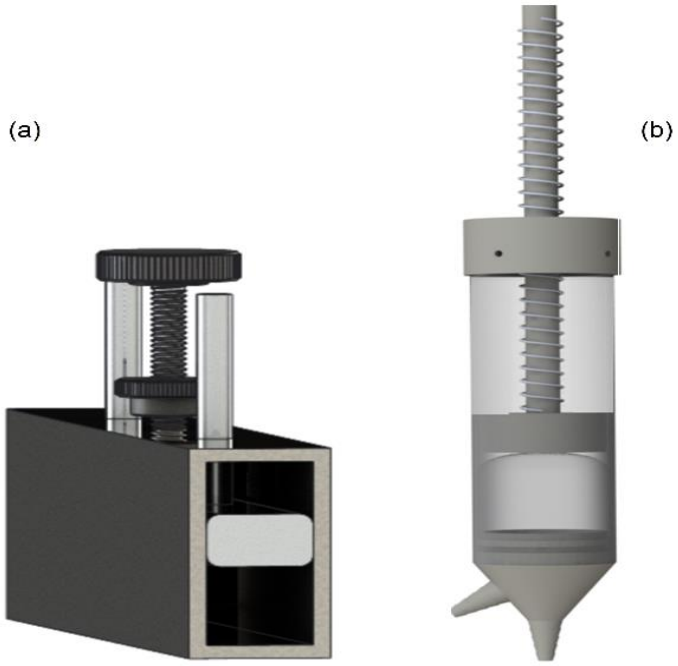

Figure 5-2: a) The systemic resistor consists of an aluminum channel through which the tubing runs and a steel bar which, held in position by guide posts, can be forced downwards by the thumb screw, evenly compressing the entire length of tubing. b) The compliance chamber consists of a spring loaded piston within a cylinder. The piston pushes against a bag connected to the aortic outflow line via a reducing funnel.

5.2.3 Afterload Module Assembly and Passive Afterload *Ex situ* Heart Perfusion

Hearts were excised from three 50±5 kg male Yorkshire pigs and attached to a custom made *ex situ* heart perfusion circuit as described previously.[187] The system was primed with 2 L of autologous blood mixed with STEEN solution (XVIVO Perfusion, Goteborg, Sweden), such that

a hematocrit of 20% was achieved. Additives including 1 g of Cefazolin, 2 g of magnesium sulfate, and 10,000 units of heparin were also present in the solution. Dobutamine (5 mcg/min) and Insulin (5 units/h) were infused continuously throughout the experiment.

Once attached to the system, Langendorff Mode perfusion was initiated at a target aortic pressure of 50 mmHg. Over the course of 30 minutes, hearts were rewarmed to 37°C, at which time they were immediately transitioned to Passive Afterload Working Mode by loading the left atrium with a pressure of 5 mmHg.[187] The full afterload module was assembled with flow from the aorta passing through the proximal resistor, into the compliance chamber, through the systemic resistor and then back to a reservoir (Figure 5-3). The afterload inflow line was connected as close to the aortic root as possible with approximately 15 cm of tubing between the aortic root and the proximal resistor.

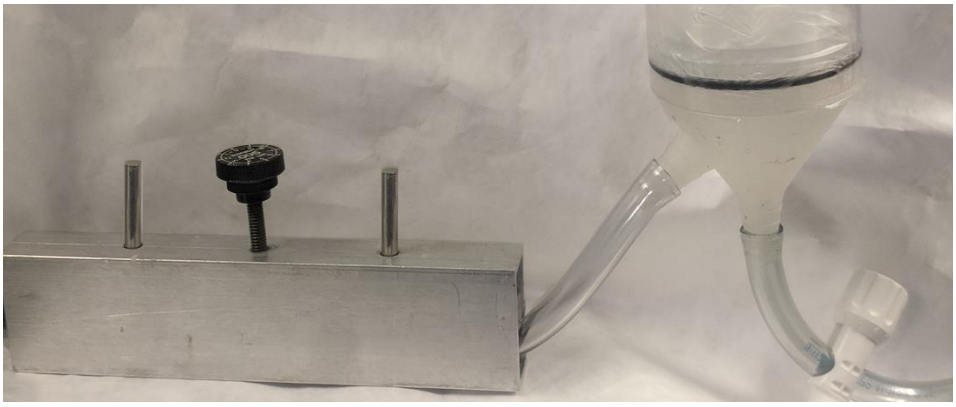

Figure 5-3: The Physical Windkessel setup. The aortic outflow from the ex situ heart flows through the proximal resistor, into the bottom of the compliance chamber, out the side of the compliance chamber, through the systemic resistor and back to the reservoir. By manipulating these parameter values, the pressure waveform, and thus the character of the perfusion can be changed

Hearts remained in this mode for 5.5 hours. Physiological diastolic pressures between 25-35 mmHg and systolic pressure between 80-100 mmHg were targeted in the aorta. Systemic resistance and compliance values were continuously adjusted to maintain pressures in this range. If systolic pressure was too high, systemic resistance was decreased and if systolic pressure was too low, systemic resistance was increased. If diastolic pressure was too low, compliance was increased and if diastolic pressure was too high, it was decreased. To maximize aortic pressure stability, adjustments were halted the moment that both systolic and diastolic pressures were within

their target ranges. In the event that systolic and diastolic pressures simultaneously fell out of their target ranges, the systemic resistance was adjusted first, followed by the compliance. The proximal resistor was set to the middle of the physiological range at 0.07 mmHgs/cm^3 across all experiments. Aortic pressure (TruWave disposable pressure transducer, Edwards, Irvine, California, USA) and flow (SONOFLOW CO.55/120 V2.0, Sonotec USA, Islandia, New York, USA) measurements, measured on the aortic tubing line as close to the aortic root as possible, along with afterload component settings were recorded each hour.

Finally, to evaluate the contractile performance of the three hearts against one another and those evaluated in previous studies, at the end of the perfusion period a conductance catheter (SPC-571, Millar Inc, Houston, TX) was inserted into the left ventricle trans-apically for pressure volume loop analysis. Volume dependent parameters were collected under steady loading conditions. Volume independent parameters were collected by gradually decreasing left atrial inflow in a stepwise fashion. Measured parameters were: end systolic elastance (ESPVR), the maximum rate of left ventricular pressure change (LV dP/dt_{max}) and preload recruitable stroke work (PRSW) to evaluate systolic function as well as the isovolumetric relaxation constant (Tau), the minimum rate of left ventricular pressure change (LV dP/dt_{min}) and the end-diastolic pressure volume relationship (EDPVR) to evaluate diastolic function.

5.2.4 Impedance Analysis

At the 6-hour time point, simultaneously measured aortic flow and pressure waveforms (averaged over 100 beats [138, 166]) were discretized using Fourier analysis, enabling the calculation of input impedance. Input impedance moduli and phase angles were calculated for each of the first 8 harmonics by dividing the pressure modulus by the flow modulus and by subtracting the flow phase angle from the pressure phase angle, respectively. The results were plotted as functions of frequency and compared to four element Windkessel estimations from equation (5-1).

5.3 Results

5.3.1 Resistor Validation

Figure 5-4a shows the comparison between measured resistance values at each level of compression (averaged across all flows) and the resistances predicted by equation (5-2). Measured resistance values matched theoretical values (R^2=0.99, p<0.000001), with deviations of no more than 0.1 mmHgs/cm^3 and as little as 0.0042 mmHgs/cm^3 across all levels of compression. Figure 5-4b shows the plot of resistance versus flow rate at the maximum operating compression (85%). Across all flows, resistances were constant at 4.32 ± 0.32 mmHgs/cm^3 (mean ± SD). Of note, in the operating range of the resistor (flows under 2.5 L/min), mean resistance was 4.10 ± 0.09 mmHgs/cm^3.

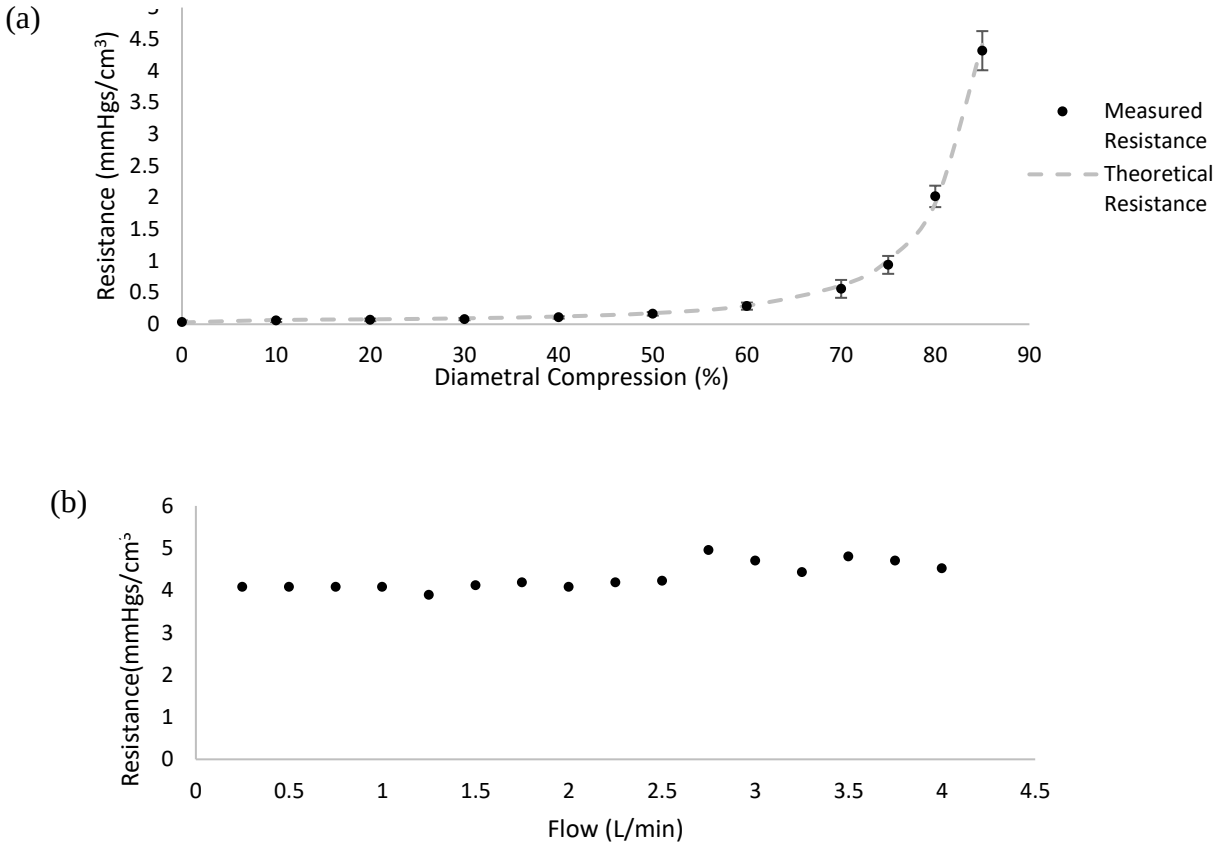

Figure 5-4: a) Resistance as a function of tube compression for the systemic resistor. Measured resistance values were averaged across all flows at each compression. The error bars represent

the standard error of the mean. b) Resistance as a function of flow rate at maximum diametral compression.

5.3.2 Compliance Validation

The measured zero-frequency compliance values closely matched the theoretical valves calculated from equations (5-5) and (5-6) (Figure 5-4; R^2=0.97, p<0.000001). For each spring engagement, mean compliance varied from theoretical compliance by no more than 0.64 cm^3/mmHgs and as little as 0.034 cm^3/mmHgs.

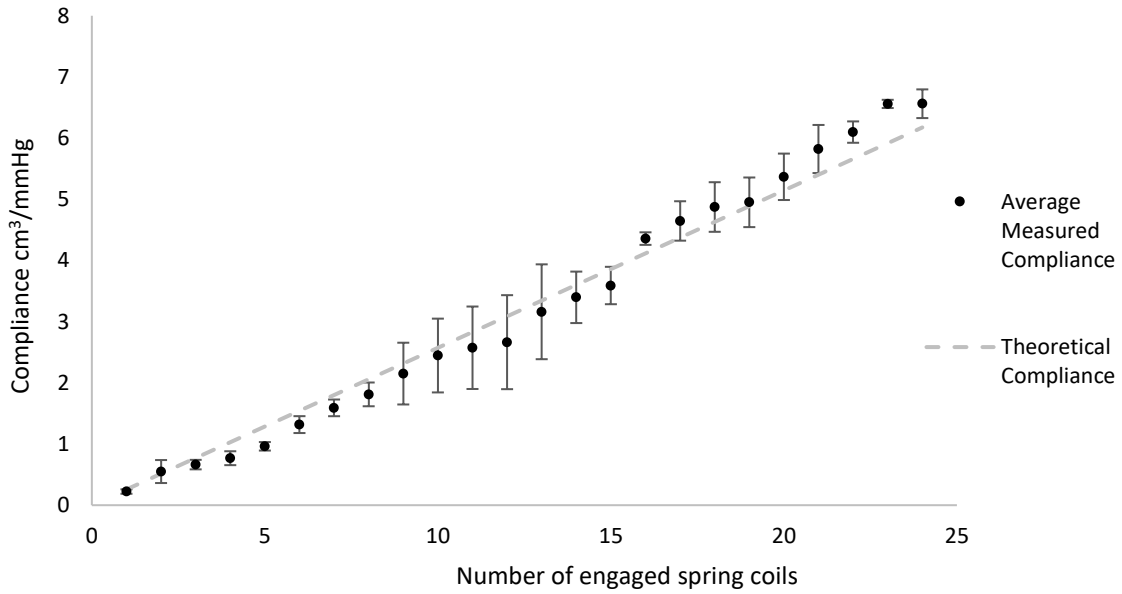

Figure 5-5: Compliance Testing. Spring engagement was varied from 1 to 25 coils and at each engagement level measured compliance values were averaged across the three perfusates. The error bars represent the standard error of the mean.

5.3.3 Passive Afterload *Ex situ* Heart Perfusion

Shown in Figure 5-6 are representative pressure and flow waveforms (measured simultaneously) taken from the three tested hearts. Both systolic flow and diastolic flow were different across the three hearts. Despite these differences, the pressure waveforms take similar forms with systolic pressures between 94 and 98 mmHg and diastolic pressures between 28 and 32 mmHg across the three hearts.

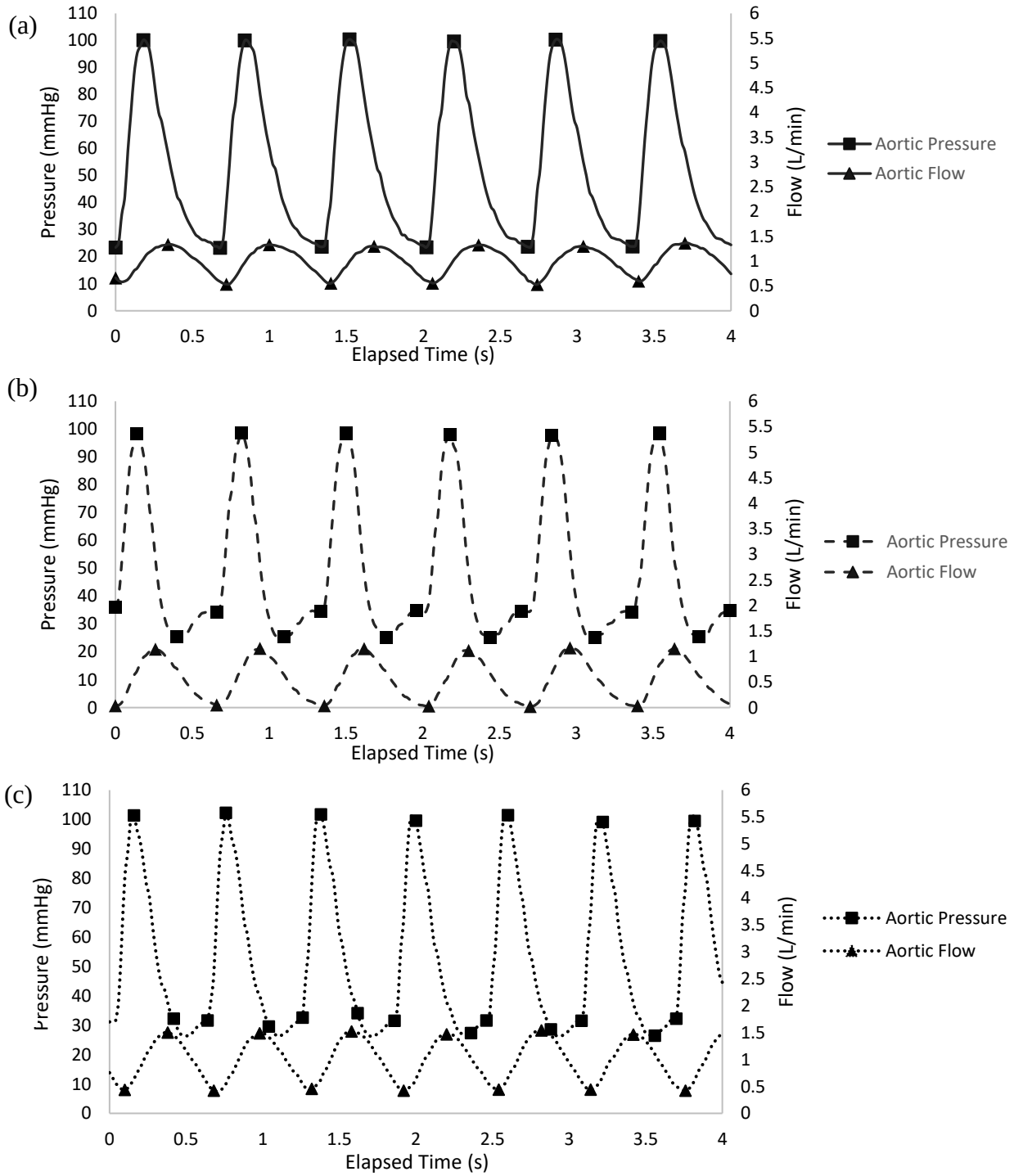

Figure 5-6: Representative Pressure and flow waveforms measured just prior to the 5-hour time point a) Representative waveforms for heart 1. Systolic and diastolic aortic flow rates were 1.4 and 0.5 L/min, respectively. Systolic and diastolic aortic flow rates were 1.2 and 0 L/min, respectively. Systolic and diastolic aortic pressures were 99 and 25 mmHg respectively. respectively c) Representative waveforms for heart 3. Systolic and diastolic aortic flow rates were

1.5 and 0.4 L/min, respectively. Systolic and diastolic aortic pressures were 98 and 29 mmHg respectively.

Figure 5-7 shows hourly systolic and diastolic pressures, mean aortic flow rates, and measured afterload parameter values for all three hearts. Despite aortic flow rate changes across the perfusion period brought on by changes in myocardial contractility, systolic and diastolic pressures were maintained within the target ranges for all three hearts by adjusting afterload parameters. Also included in Figure 5-7 are 95% confidence intervals for both the hourly and combined systolic and diastolic aortic pressures. For systolic aortic pressure (Figure 5-7 a), the overall 95% confidence interval was between 95 mmHg and 96.2 mmHg while the lowest and highest hourly limits measured 91.9 mmHg and 99.5 mmHg respectively. For diastolic aortic pressure (Figure 5-7 b), the overall 95% confidence interval was between 26.8 mmHg and 28.8 mmHg while the lowest and highest hourly limits measured 22.9 mmHg and 33.0 mmHg respectively.

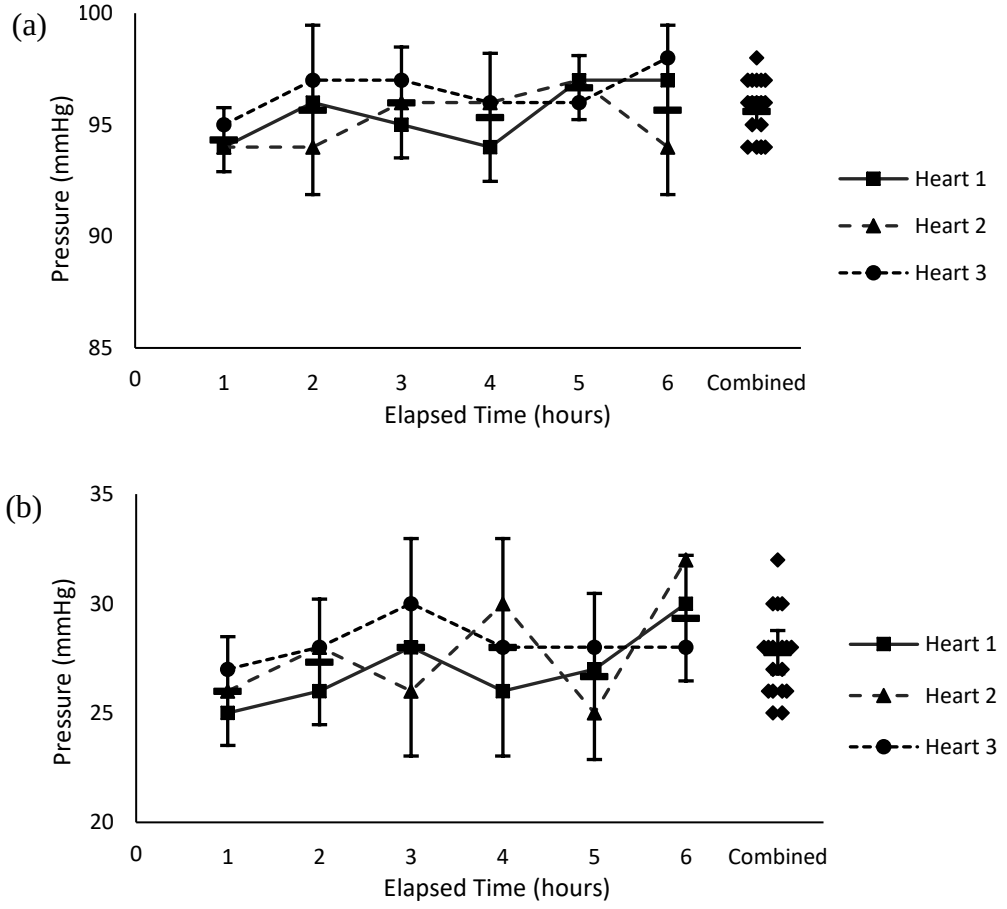

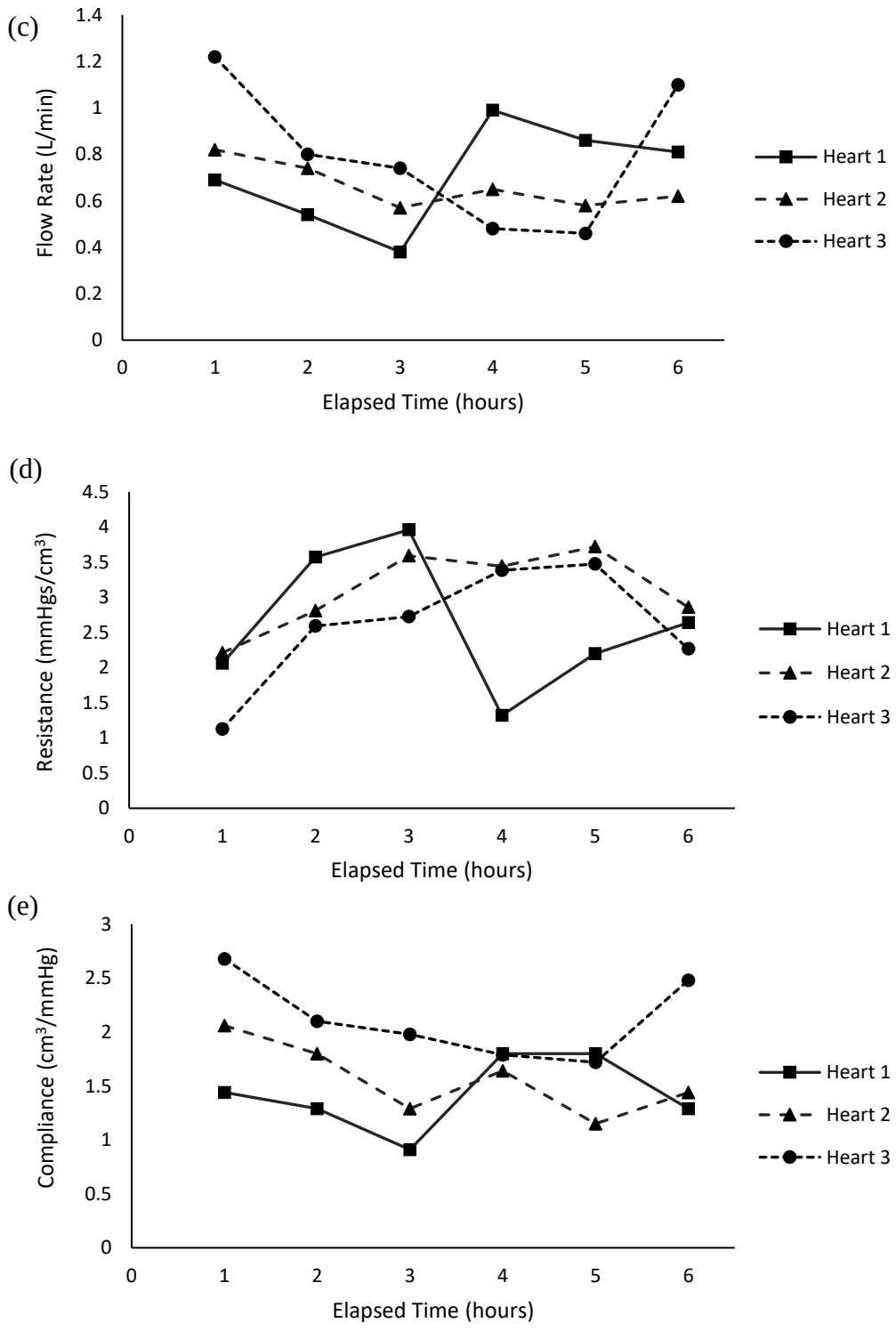

Figure 5-7: Ex situ experimental data measured hourly over the 6-hour perfusion period. a) Hourly systolic pressures plotted with means and 95% confidence intervals. All measured values were within the target range for all 3 hearts. b) Hourly dystolic pressures plotted with means and 95% confidence intervals. All measured values were within the target range for all 3 hearts. c) Mean aortic flow rate measured directly upstream of the aorta. d) Hourly systemic resistance

values. Tube compression was adjusted using the systemic resistor to maintain suitable aortic pressure. Resistance values plotted here were calculated from compression using equation (5-2). e) Hourly compliance values. Spring engagement was adjusted using the compliance chamber to maintain suitable aortic pressure. Compliance values plotted here were calculated from equations (5-5) and (5-6).

5.3.4 Functional Evaluation

Shown in Figure 5-8 are representative steady state pressure volume loops obtained from heart 1 at the 6-hour time point of our experiment. Loop geometry was consistent across all three hearts as well as with those previously obtained.[187]

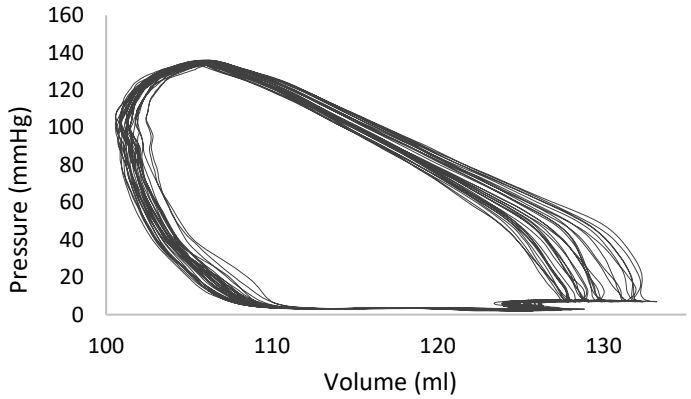

Figure 5-8: Representative Pressure volume loops at the six-hour time point for heart 1. Pressure volume loops presented similarly across all 3 hearts.

Similarly, left ventricular functional parameters were within ranges previously described for *ex situ* experimentation and are presented for all 3 hearts in Table 5-1.

Table 5-1: Functional parameters

Parameter	Heart 1	Heart 2	Heart 3
LV dP/dtmax (mmHg/s)	863	1849	973
LV dP/dtmin (mmHg/s)	-1319	-1631	-800
Tau (ms)	45	24	51
PRSW (mmHg)	30.23	139.24	52.29
ESPVR (mmHg/ml)	2.48	5.09	3.74
EDPVR (mmHg/ml)	0.36	0.50	1.87

5.3.5 Impedance Analysis

Shown in Figure 5-9 are the 6-hour frequency domain plots for input impedance modulus and phase angle for all three tested hearts. The four element Windkessel model (calculated at prescribed parameter conditions) fits the experimental model well with R^2 values above 0.865 for the impedance modulus and above 0.778 for impedance phase. Additional theoretical Windkessel models are included in a supplemental figure (Appendix A)

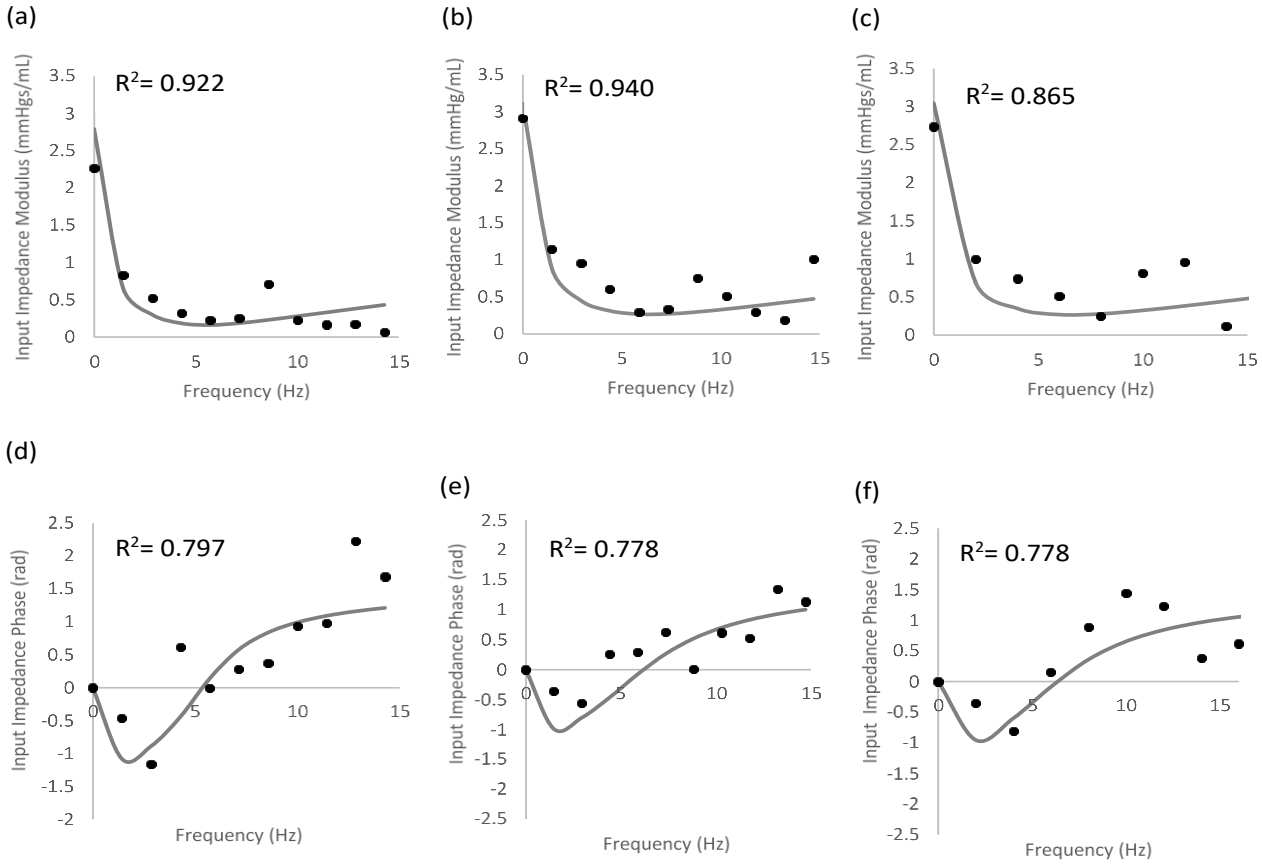

Figure 5-9: a), b), c) The comparison, at the 6-hour time point, of measured and theoretical input impedance moduli for the three tested ex situ hearts. d), e), f) the comparison, at the 6-hour time point, of measured and theoretical input impedance for the three tested ex situ hearts. Theoretical input impedances were calculated using the 6-hour Resistance and compliance values as well as the inertance value calculated in the methods section.

5.4 Discussion

In this study, the design and testing of a novel adjustable afterload module for *ex situ* perfused hearts is described. The model, based on the traditional four element Windkessel, facilitated the

creation of physiological *ex situ* pressure waveforms on three porcine hearts across differing contractile conditions. While the application of windkessel afterload modules in *ex situ* perfusion has been described previously, the demonstrated adjustability and controllability of our module is an important distinction from both existing passive afterload solutions, and all systems that utilize retrograde pump support to support working heart perfusion.[50, 187]. In this way, we have functionally decoupled the contractile function of the heart from perfusion pressure, offering the capability to provide physiological perfusion pressure to even poorly contracting hearts without an increase in left atrial pressure. Additionally, this capability allows us to subject hearts to a variety of prescribed afterload conditions and, using traditional methods such as pressure-volume loop relationships or echocardiography,[187] evaluate their performance in the consistent settings across different hearts. With further research, this could provide a means of enabling the *ex situ* evaluation of donor hearts in recipient specific settings meaning a heart could not only be evaluated in terms of its absolute quality, but also its performance in its intended end environment. Conversely, for the functional comparison of different hearts (particularly important in research pertaining to the correlation of *ex situ* functional parameters to post transplant outcomes), standardized afterload parameter values can be used. As such, in order to ensure consistency across multiple hearts, the ability to control and predict these values is of paramount importance.

Single element testing results, undertaken for both the systemic resistor and the compliance chamber, support our ability to both measure and implement specific afterload settings using this new afterload module. Measured systemic resistance values were accurately predicted by equation (5-2) across the entire range of operating flows and compressions (Figure 5-4a). In verifying the applicability of this model, this result also suggests that turbulence across the resistor is not substantial enough to warrant concern. Indeed, observing Figure 5-4b, at the maximum compression condition where flow is theoretically most turbulent, resistance remains relatively constant across the operable flow range. Similarly, observing Figure 5-5, measured compliance values matched their theoretical counterparts quite closely, indicating that across its intended operating range compliance is controllable and measurable.

In addition to single element results, impedance analysis on the assembled afterload module during *ex situ* perfusion, supports the conclusion that afterload parameter values can be accurately predicted and controlled. As can be seen in Figure 5-9, for all three hearts and across the first 8

harmonics, experimental input impedances matched those calculated using the four element Windkessel model closely, confirming the accuracy with which resistance and compliance values can be predicted. It is also important to note that the impedance modulus and phase curves represented in Figure 5-9 are quite comparable with those seen in previous studies both *in vivo*[138] and *ex situ*. [133] At higher frequencies, as has been previously observed, there is some scatter leading to a few outlying points, particularly in the phase diagram. ,[134, 197] Even taking this into account, impedance results support the findings from single element testing that our system's resistance and compliance values can be accurately predicted and characterized by equations (5-2) and (5-4), respectively.

Referring back to equation (5-1), in the context of *ex situ* perfusion, the ability to manually and controllably adjust afterload parameter settings is imperative in the decoupling of aortic pressure and aortic flow. At higher mean aortic flow rates, higher compliance values were generally required with systemic resistance following an inverse trend (Figure 5-7). Observing equation (5-1), these results are intuitive given our control strategy. Increasing systemic resistance results in an increase in aortic pressure relative to aortic flow while increasing compliance leads to a decrease in the pulsatility of the pressure wave as compared to the flow wave.(24) Higher aortic flow rates tended to be indicative of more pulsatility in the aortic flow and thus, necessitated higher compliances and lower resistances.

Across the perfusion period, and indeed across different hearts, changes in contractile function led to drastic changes in mean aortic flow (this is particularly evident between the third and fourth hour of perfusion for heart 1). Observing Figure 5-6, we were able to maintain relatively consistent aortic pressure waveforms at varying aortic flows. It is important to note that for each of our hearts, aortic flow remains positive throughout the cardiac cycle. *In vivo*, aortic root flow would be expected to reverse in diastole to allow for coronary perfusion. Since our tube mounted flow probes necessitate that we measure flow slightly upstream of the aortic root, this is likely a biproduct of the negative diastolic portion of the aortic flow wave not having enough time to propagate to our measurement point prior to the subsequent systole. Also of note, the dicrotic notch is noticeably absent from all of our pressure recordings. With *ex situ* perfusion pressure targets being necessarily lower than their *in vivo* counterparts, and dicrotic notch amplitude dependent on mean aortic pressure, this is perhaps an intuitive result. [198] Finally, we observe that for each of the three

hearts, it seems as though aortic pressure begins to rise before aortic flow rather than simultaniously as expected. This is likely due to latency in our pressure and flow measurement techniques that will be adressed as part of our future work.

As our protocol required a constant left atrial pressure of 5 mmHg, increases in left ventricular contractility necessitated increases in left atrial inflow while decreases in left ventricular contractility required the opposite. Aortic outflow changed correspondingly and since aortic pressure and flow are linearly related, aortic pressure changed as well. If systolic or diastolic pressures fell outside of the target range, systemic resistance and compliance were adjusted. It is important to note that this adjustment was an iterative process as aortic outflow itself is not completely independent of afterload. Often adjusting resistance and compliance resulted in a change in left atrial pressure (and ultimately aortic flow), necessitating finer readjustments until stability was reached.

As shown in Figure 5-7, across the entire perfusion period, for all three hearts, by adjusting systemic resistance and compliance within their operating ranges, systolic and diastolic pressures were successfully maintained within their target ranges. Overall 95% confidence intervals for systolic and diastolic pressures also fall within their respective target ranges (80-100 mmHg for systolic pressure and 25-35 mmHg for diastolic pressure) at 95-96.21 mmHg and 26.8-28.8 mmHg, respectively. It is worth noting that due to our pressure control strategy, specifically the fact that adjustment was stopped as soon as systolic and diastolic pressures fell within their target ranges, some individual pressure measurements approached the limits of the target range. This was particularly true for diastolic pressure as it was adjusted after systolic pressure was set. While all hourly 95% confidence intervals for systolic pressure were within the target range, this led to the lower limit of the 95% confidence interval for diastolic pressure falling below the lower limit of our target range at the 1, 3, 4 and 5-hour marks, with a minimum value of 22.9 mmHg. Moving forward, a change in adjustment strategy to target the center of the desired range would preclude this result. Even so, with other groups demonstrating successful *ex situ* perfusion at mean aortic pressures as low as 20 mmHg [199], diastolic pressures temporarily falling this low would be considered acceptable.

In addition to maintaining a constant aortic pressure setting, results from pressure volume loop analysis (presented in Table 5-1, with representative pressure volume loops shown in Figure 5-8) confirm our ability to analyze contractile function in Passive Afterload Working Mode. Of note, Heart 1 came from an animal with an incidental finding of chronic pericarditis and, thus, presented poor left ventricular function. We chose to include this heart to test the module's capability in a setting with left ventricular dysfunction but also note the discriminatory ability of this evaluation technique with hearts supported in a Passive Afterload Working Mode. In spite of functional differences between the three hearts, all parameters were within the functional ranges we have previously reported for *ex situ* hearts.[187] While it can be concluded that the evaluation of hearts perfused in this mode is possible, the impact remains unclear and requires further research. Moving forward, the comparative effectiveness of functional evaluation in Passive Afterload Working Mode and Pump Supported Working Mode, as well as how these measures compare to their metabolic counterparts must be tested and analyzed in detail.

We do present our work in a limited sample. While the trial size presented herein is not sufficient for drawing conclusions about the impact that perfusing hearts in this adjustable Passive Afterload Working Mode, we assert it sufficient in demonstrating the capability of our afterload module in its implementation. The stability in pressure across 18 combined hours of *ex situ* perfusion is demonstrated by the fact that overall 95% confidence intervals fall well within our target ranges, serving to validate the results of single element testing (Figure 5-4, 5-5) and impedance analysis (Figure 5-9). We therefore confirm our ability to independently vary and control afterload parameter settings and thus decouple aortic pressure and aortic flow in the *ex situ* working heart. As aortic pressure is an imperative parameter in *ex situ* heart perfusion,[53] and many have postulated that the working heart offers distinct advantages over the Langendorff heart,[93] this capability is an important step.

In clinical studies, only Langendorff Mode perfusion has been used, with metabolic parameters utilized for evaluation. [44] The functional impact of prolonged perfusion in Passive Afterload Working Mode on *ex situ* hearts remains unclear and requires future research. In particular, the impact of Passive Afterload Working Mode on gradually failing hearts needs to be better understood. As contractility decreases, the necessary corresponding increase in systemic resistance could result in further functional degradation. That being said, the potential of this strategy for

evaluating multiple *ex situ* hearts under constant afterload conditions is readily apparent. The future preclinical validation of this perfusion mode as a preservation and evaluation setting could lead to the implementation of a clinical working mode system, expanding the clinical capability of *ex situ* heart perfusion. Future research will focus on the development of an evaluation protocol and the correlation of evaluation parameters at different afterload settings to post transplant outcomes. Coupled with further research into unique afterload centred preservation strategies, this technology offers the potential to augment *ex situ* heart preservation and evaluation and increase the number of hearts available for transplantation.

Chapter 6

6 Passive Afterload Working Mode as a Physiological Setting for Post-Transplant Prediction

6.1 Introduction

Heart failure is one of the leading causes of death in the world, affecting 6.5 million people and accounting for over 300,000 deaths per year in the United States alone. [1] Though numerous treatment options have emerged to alleviate symptoms and improve mortality, cardiac transplantation remains the gold standard for eligible patients with advanced refractory heart failure. [200] Unfortunately, while the number of patients on the waiting list has grown steadily, a paucity of donor organs has precluded a corresponding increase in the number of yearly transplants. [201] To combat this organ shortage, *ex situ* heart perfusion (ESHP) has been developed and proposed as an alternative organ preservation method. Through the reinstallation of coronary perfusion, hearts can be reanimated and kept in an aerobic metabolic state, augmenting preservation. Within this reanimated state, the functional evaluation of donor hearts is also possible prior to transplantation. [50] Coupling the augmentation in cardiac preservation and evaluation, it is proposed that ESHP could facilitate the use of currently unused marginal donor hearts, expanding the donor pool. [93, 94, 187]

The majority of ESHP research has been focused on improving cardiac preservation in a transportation setting, especially as compared to traditional cold storage. [43, 44] Typically, these systems operate in a very similar fashion to what was described in the pioneering work of Oscar Langendorff in the late 1800s. [32] In Langendorff Mode (LM) perfusion, oxygenated perfusate is pumped retrograde to the aortic root, forcing the aortic valve closed and perfusate into the coronary circulation, facilitating aerobic function. The perfusate either drains passively or is ejected by the right ventricle (RV) into a collection reservoir. [93, 94, 187] In a strictly preservation setting, LM is effective, but since the left ventricle (LV) remains unloaded, the reliable evaluation of contractile function is not possible.

When considering the impact of predicting post-transplant outcomes of marginal donor hearts, the inability to evaluate contractile function in LM is an important consideration.

It has been postulated that many donor hearts that are currently discarded, could be usable, but with the use of extended criteria donors comes an inherent increase in patient risk. [202] In particular, as hearts donated after circulatory death (DCD) are invariably submitted to a period of unprotected warm ischemia, most institutions worldwide use exclusively hearts donated after brain death (DBD). It has been estimated that the use of these DCD organs could increase the number of heart transplants by 30%. [9] With this in mind, despite concerns about functional degradation associated with warm ischemia, in the past few years, a few groups have successfully utilized ESHP in clinical studies to show that the transplantation of some of these DCD hearts is possible. [11, 49] In each case, ESHP was instilled using the Transmedics Organ Care System with hearts preserved only in LM and functional evaluation limited to the observation of lactate profiles. [99] While the trials themselves have shown success, the validity of using lactate profiles as evaluative markers has been called into question by multiple groups and presents an enormous barrier to the widespread adoption of DCD transplantation.[51, 203, 204] Until a more robust and quantitative assessment method is adopted and validated to quell concerns about unnecessary patient risk, the widespread use of DCD hearts in clinical practice is limited.

In preclinical settings, it has been suggested that left ventricular contractile parameters are more indicative of *ex situ* cardiac function than metabolic parameters, including lactate trends. [50, 205] With *ex situ* function, shown to be directly related to post-transplant function, this is a very important assertion. [101] With this in mind, groups have sought to load the left and right atria, facilitating ventricular ejection in a so-called working heart mode. The most common working mode is Pump Supported Working Mode (PSWM), in which perfusate is pumped both antegrade to the left atrium and retrograde to the aorta. [50, 187] In systole, the LV overcomes the aortic backpressure ejecting perfusate to the reservoir. In diastole meanwhile, the aortic backpressure facilitates coronary perfusion. In PSWM, the resistance brought about by the pump support provided to the aortic root is difficult to calculate. While increasing or decreasing pump RPM has the same effect on resistance, the actual value of resistance is also dependent on coronary vascular resistance as compared to resistance in the reservoir return line. With this in mind, some groups have attempted implementation of a more controllable preservation and evaluation setting. [103] Passive Afterload Working Mode (PAWM) has been proposed as an alternative to PSWM that

seeks to improve the physiological relevance of left ventricular afterload *ex situ*. [166, 187] Instead of using retrograde flow to maintain coronary perfusion during diastole, a Windkessel based afterload module is used in PAWM, meant to facilitate a physiological aortic pressure curve. [166] While it is postulated that the physiological setting provided in PAWM could improve the predictive relevance of contractile evaluation during ESHP, to this point no comparison has been made between PAWM and PSWM as it pertains to the prediction of post-transplant LV function. Furthermore, with contractile evaluation requiring invasive pressure-volume catheterization, the clinical applicability of *ex situ* evaluation has been called into question. [107]

We have previously developed and validated an ESHP system capable of perfusing hearts in LM, PSWM and a fully adjustable version of PAWM over prolonged perfusion periods.[187] Using this system, in a porcine transplant model, we compared PSWM and PAWM as settings for *ex situ* functional measurement in terms of how well LV contractile parameters measured in each mode correlated with post-transplant function using both the standard pressure-volume loop analysis and a newly developed noninvasive control volume technique. It was hypothesized that the stability of afterload parameters across multiple hearts in PAWM would allow for a more effective setting for post-transplant functional prediction.

6.2 Methods

Experimental protocols were approved by the institutional animal care committee, and animals were treated following the “Guide for the Care and Use of Laboratory Animals” prepared by the Institute of Laboratory Animal Resources, National Research Council, 1996.

6.2.1 Experimental Design

A total of 10 hearts were procured from 40±5 kg male Yorkshire pigs. Donor animals were randomly assigned to standard beating-heart donation (DBD, n=5) or donation after circulatory death (DCD, n=5) in order to achieve a range of post-transplant outcomes with hearts from both groups analyzed together for the purposes of this study. Hearts were preserved on our custom ESHP system, undergoing biventricular functional assessment during the final hour in both PSWM and PAWM. Donor hearts were then transplanted into recipient pigs and evaluated again following 3 hours of reperfusion. An experimental timeline can be seen in Figure 6-1.

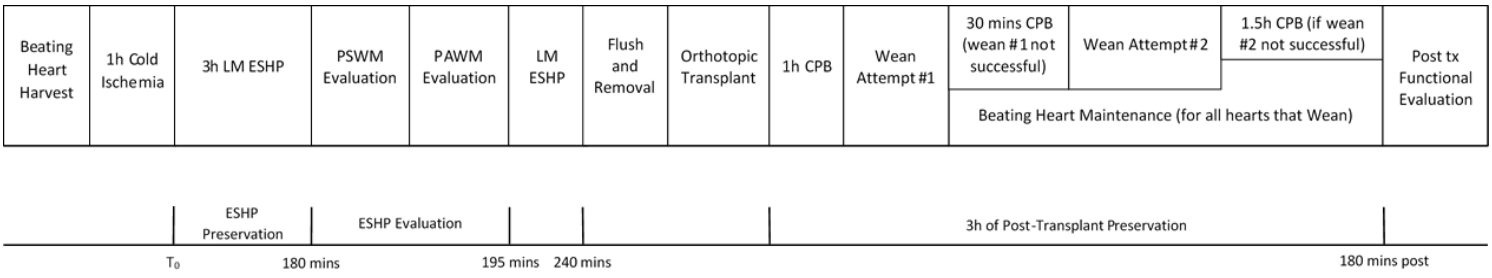

Figure 6-1: Timeline of ESHP and Transplantation Procedure

6.2.2 DBD Heart Procurement

Animals were sedated with an intramuscular injection of midazolam (0.3 mg/kg) and ketamine (20 mg/kg) and anesthesia induced and maintained using inhaled isoflurane (end tidal volume of 4-5% for induction, and 2-3% for maintenance). Following a median sternotomy and exposure of the heart and great vessels, 30,000 units of heparin were injected intravenously. Animals were then exsanguinated into an autotransfusion system (Frensenius Kabi C.A.T.S., Terumo, USA) for red blood cell isolation via an 18F venous canula inserted into the inferior vena cava. A cross clamp was placed on the aorta and hearts were arrested using 1 L of histidine-ketoglutarate-tryptophan (HTK). Hearts were then excised and cannulated for ESHP.

6.2.3 DCD Heart Procurement

Anesthesia was conducted as described in the DBD group. A median sternotomy was performed followed by exposure of the heart and great vessels and administration of intravenous heparin. Infusions of propofol (1 mg/kg/min) and remifentanil (1 µg/kg/min) were started to ensure adequate anesthesia during DCD induction. Mechanical ventilation was then withdrawn, and circulatory arrest observed. Upon the onset of mechanical asystole, defined as the absence of pulse pressure in the aortic pressure waveform, a 15-minute warm ischemic stand-off period was observed. At the end of this stand-off period, the animals were exsanguinated into the autotransfusion system, and hearts were flushed and excised as described for DBD hearts.

6.2.4 Heart Cannulation and *Ex situ* Circuit Preparation

Upon excision, all hearts were placed in ice-cold HTK solution for 1 hour. The left atrium, right atrium, aorta and pulmonary artery were cannulated, and vents were placed in both the left and right ventricles for pressure measurement during ESHP.

Simultaneously, the ESHP system was primed with 750 mL of STEEN solution (XVIVO Perfusion, USA), 750 mL of SOM-TRN-001 (Somahlution, USA), and isolated red blood cells to a final perfusate hematocrit of 15%. Also included in the solution were: mannitol (1mg/kg), Cefazolin (1g), Methylprednisolone (500mg), lidocaine (1mg/kg) magnesium sulfate (2g), and heparin (10,000 units). Dobutamine (5 mcg/min), insulin (5 units/h), and nitroglycerine (1mcg/kg/min) were infused continuously throughout the experiment. Calcium chloride 10%, sodium bicarbonate 8.4%, and dextrose 50% were added as necessary to correct calcium (1.1-1.3 mmol/L), glucose (5-10 mmol/L), and bicarbonate (24-30 mmol/L) concentrations, respectively. The perfusion circuit itself was as previously described.[187]

6.2.5 *Ex situ* Heart Perfusion

After a standardized 1-hour cold ischemic period for cannulation, hearts were attached to the ESHP system and de-aired by way of forward perfusion through the left atrium. Once hearts were de-aired, LM perfusion was initiated at a target aortic pressure of 40 mmHg. Over the course of 30 minutes, hearts were rewarmed to 37 ℃. Hearts that fibrillated were defibrillated as required. Perfusion was kept steady at these settings until the 3-hour timepoint when functional evaluation commenced.

6.2.6 *Ex situ* Evaluation

For functional evaluation, hearts were transitioned to PSWM as described previously, and the left atrium loaded with an inflow corresponding to a cardiac index of 1.8 L/m/m^2 based on donor weight. [187] With only the left atrium loaded, coronary flow was calculated as the mean left atrial inflow less the mean aortic outflow. The right atrium was then loaded with an inflow of 1.8 L/m/m^2 less the coronary flow. The centrifugal pump and left atrial resistance were adjusted such that diastolic pressure was 25 mmHg. Systolic aortic pressure was not controlled. At this baseline loading, data from a pressure-volume catheter (Ventri-Cath-507S, Millar Inc, Houston, TX) was recorded, as was left ventricular pressure (TruWave disposable pressure transducer, Edwards, Irvine, California, USA) and all flows (SONOFLOW CO.55/120 V2.0, Sonotec USA, Islandia, New York, USA) into and out of the heart. Flow probes were placed on the tubing immediately adjacent to the heart cannulas. All measurements were taken again with the speed of each pump decreased by 10% and then one final time with the speed of the pumps decreased by 20% in order to characterize load independent pressure-volume parameters (denoted by † throughout this paper).

Finally, hearts were switched into PAWM and the entire evaluation process was repeated with a standardized systemic resistance of 2 mmHgs/cm^3 and a standardized arterial compliance of 2 cm^3/mmHg. To assess global LV function, measured contractile parameters were Preload Recruitable Stroke Work (PRSW†) and Stroke Work (SW). For assessment of LV systolic function, measured contractile parameters were: End Systolic Pressure Volume Relationship (ESPVR†); the Maximum rate of Developed Pressure (Max dP/dt); Max dP/dt normalized to End Diastolic Volume (Max dP/dt/EDV†); Maximal Elastance (EMax†); and developed Pressure (ΔP). Finally, for assessment of LV diastolic function, measured contractile parameters were the End Diastolic Pressure Volume Relationship (EDPVR†); the Minimum rate of Developed Pressure (Min dP/dt); and the time constant of left ventricular relaxation (Tau). The entire evaluation procedure in both modes took a total of approximately 15 minutes, after which hearts were transitioned back to LM for the remainder of the perfusion period.

In conjunction with collection of pressure-volume catheter data, measured flows were used in control volume analysis to estimate real time volume change in the LV. In combination with measured LV pressures, these estimated volume waveforms were used to perform a non-invasive pressure-volume analysis. Each parameter measured using the catheter was calculated using the non-invasive methodology and the results compared. As control volume analysis calculates volume change rather than absolute volumes, in order to calculate the slopes of load independent pressure volume relationships (PRSW, ESPVR, Max dP/dt/EDV, EMax, and EDPVR), SV was used rather than end diastolic volume (EDV). For these load independent parameters, a partially invasive measurement protocol, utilizing the end diastolic volumes measured by the catheter, was used in conjunction with the non-invasive measurements.

6.2.7 Transplantation Procedure and Post Transplantation Evaluation

At the 4-hour time point of ESHP, hearts were removed from the *ex situ* perfusion machine, flushed with cold blood cardioplegia and placed in ice cold HTK. Orthotopic transplantations were performed as previously described. [206, 207] Size matched recipient animals were sedated identically to donor animals. A median sternotomy was performed, and systemic anticoagulation induced with an intravenous injection of heparin (30,000 units). Bicaval and ascending aortic cannulas were put in place and used to institute normothermic cardiopulmonary bypass (CPB)

targeting a mean arterial pressure greater than 50 mmHg. The aorta was then cross clamped, and the recipient heart excised.

Donor hearts were implanted using the biatrial anastomotic technique.[207] Every 15 minutes, 300 mL of a 2:1 mixture of blood/crystalloid cardioplegia was delivered at 10 °C. Immediately prior to the removal of the aortic cross clamp, an additional 500 mLof warm blood cardioplegia was administered to the donor heart while 500 mg of methylprednisolone was administered to the recipient. The aortic cross clamp was then removed and hearts reperfused for 60 minutes. After 60 minutes of reperfusion, calcium chloride was administered (1 g) and hearts weaned off CPB. If an arterial systolic pressure above 60 mmHg was maintained for 30 minutes after the cessation of CPB, the wean was considered successful and hearts were maintained in this state for 2 hours. For hearts that did not wean successfully, CPB was reinstituted for an additional 30 minutes and weaning was once again attempted. If the second wean was not successful, support was kept until 3 hours of reperfusion at which point, CPB was halted. At this 3-hour time point, all hearts were evaluated using both a pressure-volume catheter and a pulmonary artery catheter to evaluate cardiac output using the thermodilution technique. A vasoactive infusion of Dobutamine (5-10 mcg/kg/min) and Epinephrine (0.1-0.2 mcg/kg/min) was used at the investigators' discretion to assist in weaning from CPB, simulating the clinical scenario.

6.2.8 Statistical Analysis

Statistical analysis was performed using Prism 8 (GraphPad, USA). Comparisons between measured parameters in PSWM and PAWM were done using paired, non-parametric Wilcoxon matched pairs signed rank tests. Correlations between measurements in both ESHP modes with post-transplant measurements were done using Spearman correlation analysis; any correlation coefficients with an absolute value above 0.7 were considered indicative of strong correlation. Correlation between invasive and non-invasive measurements during *ex situ* perfusion was performed using Pearson correlation analysis with measurements in both PSWM and PAWM evaluated as one group. Significance was set at $\alpha = 0.05$ for all statistical tests. P values were calculated using two-tailed tests for all correlations except for selfsame correlations where only positive correlations were considered relevant and thus a one-tailed test was used

6.3 Results

6.3.1 Contractile Performance

Ten hearts were perfused *ex situ* with contractile parameters evaluated in both PSWM and PAWM at the 4-hour timepoint. Comparisons of these contractile parameters were made between working modes and post-transplant measurements. Significant differences between parameters measured in PSWM and PAWM were observed for PRSW, SW, Emax, ΔP, Max dP/dt, and Min dP/dt (Figure 6-2). Additionally, significant differences between measurements in PSWM and post-transplant were seen for PRSW, ESPVR, EMax, ΔP, Max dP/dt and EDPVR. EMax represented the only significant difference between PAWM and post-transplant measurements.

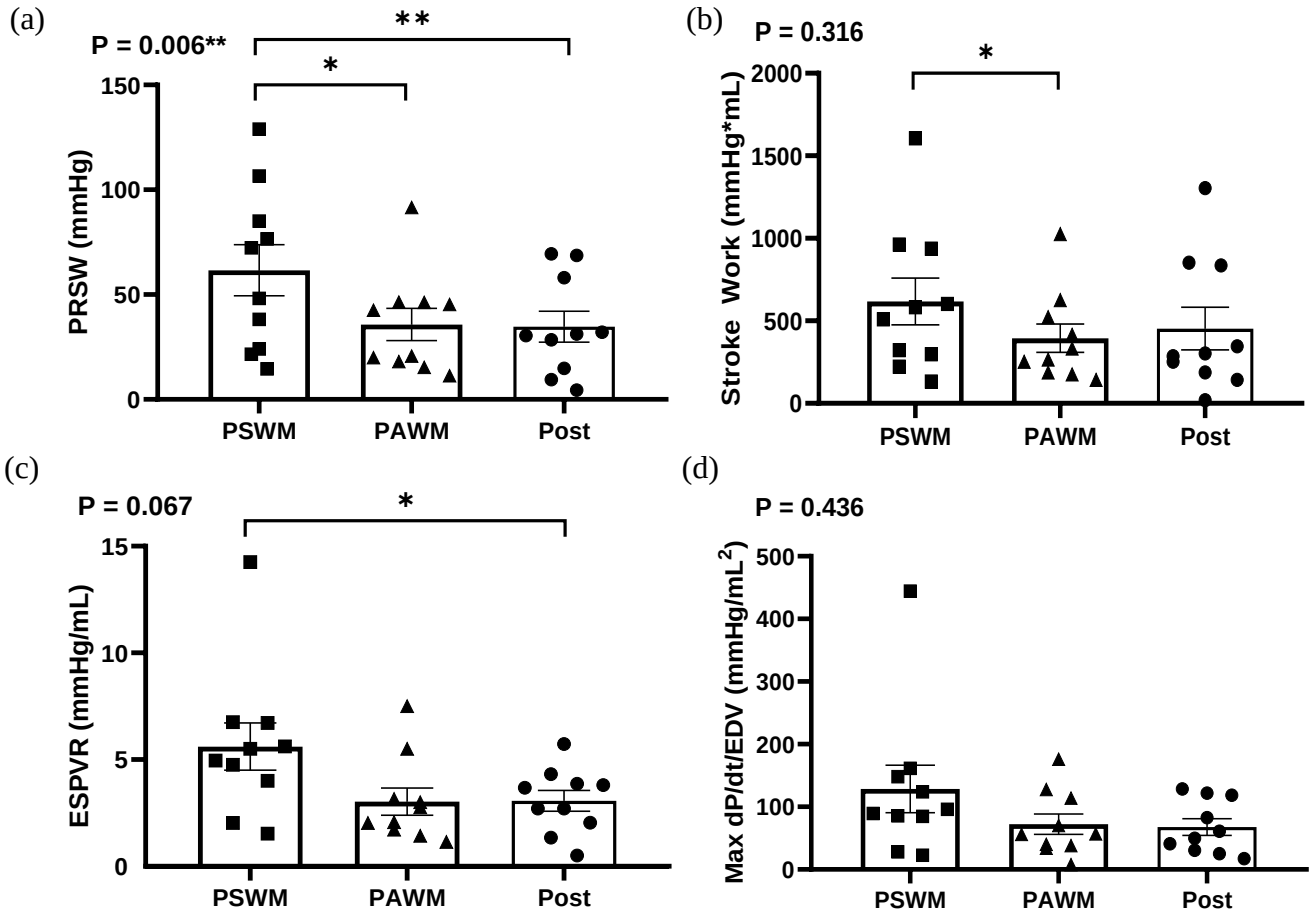

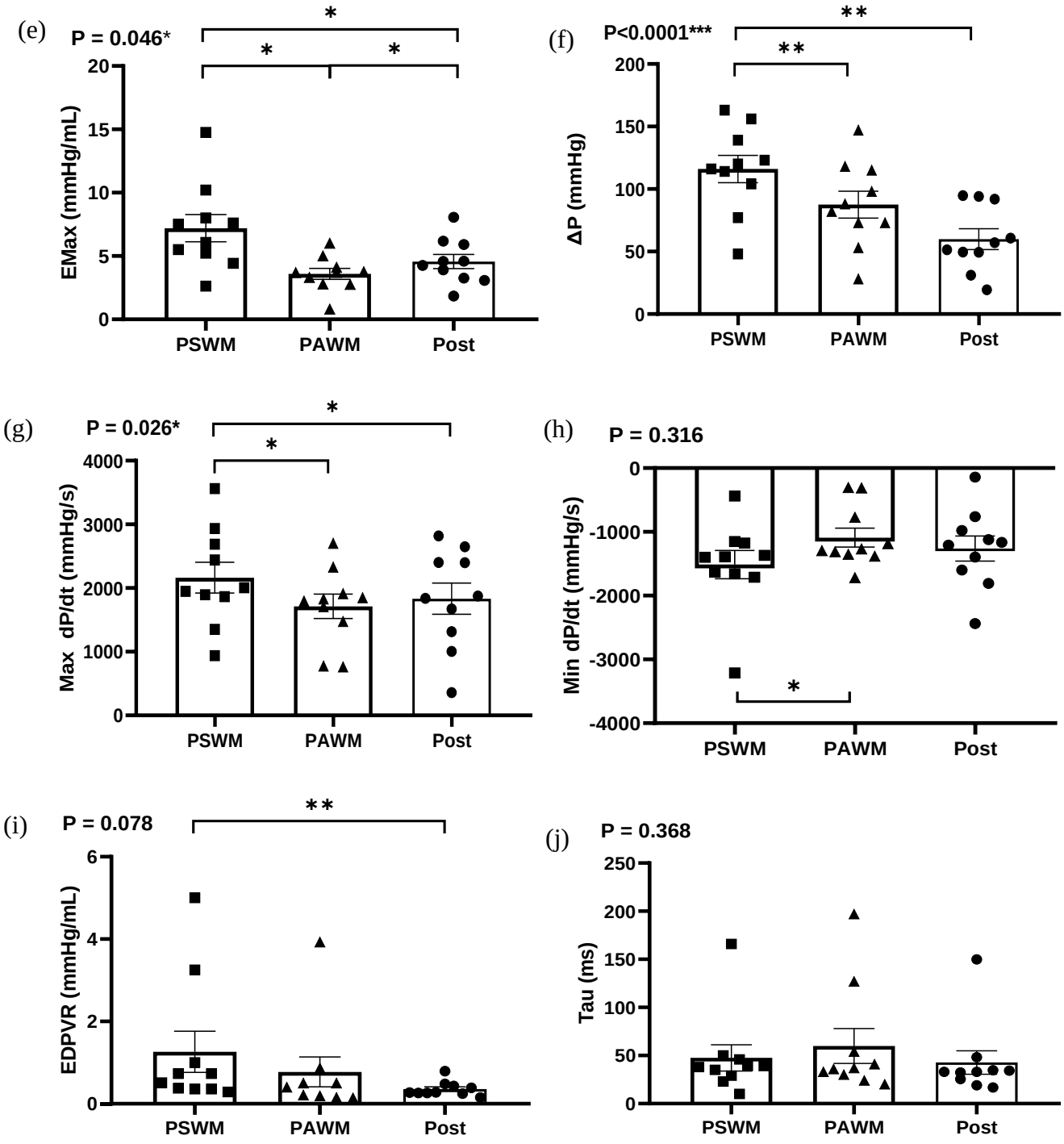

*Figure 6-2: Comparison of contractile parameters between PSW M, PAWM, and post-transplant for: a) PRSW b) SW c) ESPVR d) Max dP/dt/EDV e) EMax f) ΔP g)Max dP/dt h) Min dP/dt i) EDPVR and j) Tau. Displayed P values were calculated using Freidman tests. Comparisons between individual groups were done with Wilcoxon matched pairs signed rank tests. Data presented as mean ± SEM (N=10). * P<0.05; **P<0.01; ***P<0.001*

Correlations between measured parameters across the two working modes were calculated using Spearman correlation. Parameters were grouped according to whether they indicate global LV function, systolic function, or diastolic function. Statistically significant correlation was seen for both measured predictors of global function (PRSW and SW) as well as Tau (Table 6-1). All remaining parameters had correlation coefficients less than 0.575.

Table 6-1: Correlation of Contractile Parameters Between Modes during ESHP

Parameter	Spearman Rank Correlation	P Value
PRSW†	**0.78****	**0.007**
SW	**0.87***	**0.012**
ESPVR†	0.19	0.595
Max dP/dt/EDV†	0.15	0.669
EMax†	-0.38	0.281
ΔP	0.58	0.082
Max dP/dt	0.30	0.400
Min dP/dt	0.47	0.174
EDPVR†	0.16	0.653
Tau	**0.73***	**0.016**

** P<0.05; **P<0.01; ***P<0.001*

6.3.2 Correlation of Contractile Parameters During ESHP and Post - Transplantation

Correlations between *ex situ* parameters measured in both working modes and global post-transplant function, characterized by post-transplant cardiac index (Post-CI) were calculated using Spearman correlation. PRSW showed strong and statistically significant correlation with Post-CI whether measured in PSWM or PAWM, while Max dP/dt measured in PSWM and Max dP/dt/EDV and Min dP/dt measured in PAWM also showed statistically significant correlation with post-CI (Table 6-2).

Table 6-2: Correlation of ESHP contractile function to Post-Transplant CI

Parameter	PSWM		PAWM	
	Spearman Rank Coefficient	P Value	Spearman Rank Coefficient	P Value
PRSW†	**0.78***	**0.010**	**0.76***	**0.015**
SW	0.32	0.368	0.36	0.313
ESPVR†	0.22	0.537	0.50	0.144
Max dP/dt/EDV†	-0.04	0.918	**0.66***	**0.044**
EMax†	0.32	0.368	0.22	0.537
ΔP	0.38	0.279	0.40	0.250
Max dP/dt	**0.75***	**0.017**	0.53	0.123
Min dP/dt	-0.44	0.204	**-0.78***	**0.011**
EDPVR†	-0.55	0.105	-0.03	0.938
Tau	-0.54	0.110	-0.53	0.123

** P<0.05; **P<0.01; ***P<0.001*

As a means to understand predictive power for global LV post-transplant function, Spearman correlations between *ex situ* parameters measured in both working modes and post-transplant PRSW (Post-PRSW) were calculated. As was the case for Post-CI, PRSW measured *ex situ* in both modes showed strong correlation with post-PRSWTable 6-3). Unlike with post-CI, Tau measured in both modes also showed strong correlation with post-PRSW. Additional significant correlations with post-PRSW were seen for EDPVR and Max dP/dt measured in PSWM and Min dP/dt measured in PAWM. Max dP/dt/EDV measured in PAWM was close to significance with a P value of 0.0544.

Table 6-3: Correlation of ESHP contractile function to Post-Transplant PRSW

	PSWM		PAWM	
Parameter	**Spearman Rank Coefficient**	**P Value**	**Spearman Rank Coefficient**	**P Value**
PRSW†	**0.73***	**0.020**	**0.82****	**0.006**
SW	0.20	0.584	0.30	0.407
ESPVR†	0.31	0.387	0.53	0.123
Max dP/dt/EDV†	0.14	0.707	0.64	0.054
EMax†	0.16	0.657	0.07	0.865
ΔP	0.24	0.514	0.36	0.299
Max dP/dt	**0.77***	**0.013**	0.47	0.179
Min dP/dt	-0.53	0.123	**-0.75***	**0.017**
EDPVR†	**-0.66***	**0.044**	-0.22	0.542
Tau	**-0.74***	**0.018**	**-0.66***	**0.044**

***** *P<0.05;* ****** *P<0.01;* ******* *P<0.001*

Finally, Spearman correlation between contractile parameters measured *ex situ* in each mode and those same contractile parameters post-transplant in a so-called selfsame correlation was undertaken. In PSWM, only PRSW and Max dP/dt presented strong and statistically significant correlation (Table 6-4). On the other hand, in PAWM, PRSW ESPVR, Max dP/dt/EDV, EMax, Min dP/dt, and EDPVR all showed strong and statistically significant correlation with selfsame post-transplant parameters.

Table 6-4: Correlation of ESHP Contractile Function to Selfsame Post-Transplant Function

	PSWM		PAWM	
Parameter	**Spearman Rank Coefficient**	**P Value**	**Spearman Rank Coefficient**	**P Value**
PRSW†	**0.73***	**0.010**	**0.82****	**0.003**
SW	0.09	0.406	0.24	0.257
ESPVR†	-0.02	0.487	**0.82****	**0.003**
Max dP/dt/EDV†	-0.21	0.280	**0.64***	**0.027**
EMax†	-0.08	0.419	**0.60***	**0.037**
ΔP	0.35	0.165	0.35	0.158
Max dP/dt	**0.96*****	**<0.0001**	0.47	0.089
Min dP/dt	0.43	0.109	**0.85****	**0.001**
EDPVR†	0.41	0.121	**0.68***	**0.018**
Tau	0.46	0.093	0.54	0.057

** P<0.05; **P<0.01; ***P<0.001*

6.3.3 Non-Invasive Contractile Evaluation

In terms of non-invasive functional measurement, the first analysis undertaken was the direct correlation of parameters measured using the different methodologies (Table 6-5). The Invasive-Non-Invasive correlation refers to the correlations (Pearson's R) between contractile parameters measured using control volume analysis (combined in PSWM and PAWM) using the catheter and using the non-invasive technique. As is shown in the table, 6 of the 10 measured parameters presented statistically significant correlation. Of note, 4 of the 5 measured load independent parameters did not show statistically significant correlation between the two measurement methodologies. The results of the Invasive-Partially Invasive correlation show much stronger correlation for most load independent parameters with all parameters showing statistical

significance. The script used to calculate non-invasive parameter values is included as supplemental material (Appendix C)

Table 6-5: Correlation of Contractile Parameters Across Measurement Modalities

Parameter	Invasive – Non-Invasive		Invasive – Partially Invasive	
	Pearson's R	P Value	Pearson's R	P Value
PRSW†	**0.80*** **	**<0.0001**	**0.71*** **	**<0.001**
SW	**0.85*** **	**<0.00001**	**-**	-
ESPVR†	-0.21	0.374	**0.782*** **	**<0.0001**
Max dP/dt/EDV†	0.16	0.514	**0.69** **	**0.001**
EMax†	0.22	0.345	**0.48***	**0.032**
ΔP	**0.94*** **	**<0.00001**	-	**-**
Max dP/dt	**0.67** **	**0.001**	**-**	-
Min dP/dt	**0.67** **	**0.001**	**-**	-
EDPVR†	0.20	0.410	**0.80*** **	**<0.00001**
Tau	**0.68** **	**0.001**	-	**-**

** P<0.05; **P<0.01; ***P<0.001*

In addition to correlation *ex situ* between the catheter and non-invasive methods, the correlation of measurements taken *ex situ* with selfsame post-transplant parameters was undertaken (

Table 6-6). Using all 3 measurement techniques (including invasive measurements presented in Table 6-4), both PRSW and Max dP/dt showed statistically significant correlation with their post-transplant counterparts. Additionally, Min dP/dt measured using the non-invasive technique showed a marginally better correlation than using the invasive technique and reached statistical significance. For parameters measured in PAWM, load dependent parameters (SW, ΔP, Max dP/dt, and Min dP/dt) showed similar correlation across all measurement modes. Load independent

parameters (PRSW, ESPVR, Max dP/dt/EDV, EMax, and EDPCR) however, generally showed similar and significant correlation using the invasive and partially invasive methodologies with significantly worse correlation using the non-invasive technique.

Table 6-6: Correlation of ESHP Contractile Function Measured Across Different Modalities

Parameter	PSWM		PAWM	
	Non–Invasive	**Partially Invasive**	**Non-Invasive**	**Partially Invasive**
PRSW†	**0.71***	**0.90****	0.60*	**0.83****
SW	0.15	-	0.20	-
ESPVR†	0.42	0.13	0.10	**0.67***
Max dP/dt/EDV†	-0.13	0.18	-0.48	**0.58***
EMax†	-0.04	-0.09	0.02	0.53
ΔP	0.58	-	0.35	-
Max dP/dt	**0.65***	-	**0.63***	-
Min dP/dt	**0.60***	-	**0.82****	-
EDPVR†	0.33	0.50	-0.24	**0.69***
Tau	-0.03	-	0.21	-

** P<0.05; **P<0.01; ***P<0.001*

6.4 Discussion

In this study, we present the first direct comparison of the predictive power of PSWM and PAWM in a clinically relevant, large animal transplant model. Five DBD hearts and five DCD hearts were perfused *ex situ* for 4 hours and transplanted as a means to compare the effectiveness of PSWM and PAWM in predicting post-transplant outcomes. We report from our observations that while

the predictive power of the two modes is comparable for global contractile parameters, PAWM had a considerable advantage in predicting specific systolic and diastolic function post-transplant.

As demonstrated in Figure 6-2, owing to drastic differences in both preload and afterload, between *ex situ* and *in vivo* measurements, it is somewhat intuitive that a multitude of significant differences are observed between parameters measured during ESHP and post-transplant. Perhaps more importantly however, while our sample size was insufficient for the quantification of functional differences between DBD and DCD hearts (Appendix B), we observed substantial variation in most post-transplant parameters, allowing for a relevant study of post-transplant prediction. In terms of ESHP, measurements taken *ex situ* at the same timepoint in PAWM and PSWM show a statistically significant disparity in 7 of 10 measured parameters. Even further, only PRSW, Tau, and SW showed statistically significant correlation across the two modes (Table 6-1). As preload and inotropic support were constant across hearts during ESHP, this suggests that each of the remaining parameters exhibit some form of afterload dependence. Indeed, these dependencies have been previously described in the literature. [208, 209] This is noteworthy as while PAWM allows for the precise control of the resistance against which hearts eject during ESHP, resistance in PSWM is a function of an only partially controllable retrograde aortic support. The level of aortic support provided by the pump is set to control diastolic pressure (25 mmHg in our case), but the retrograde support necessary to produce this pressure is dependent on coronary tone, heart rate, heart size, and contractility. The consequence is that with a fixed diastolic pressure across hearts, variations in these uncontrollable parameters result in hearts being exposed to differing retrograde flows and as such differing resistances. For the multitude of parameters with afterload dependency, this introduces inherent variation in the data in PSWM that does not necessarily represent differing function.

To quantify our ability to predict post-transplant outcomes using ESHP, parameters measured *ex situ* in each mode were first correlated to post-transplant measurements of global myocardial function (CI) and isolated global LV function (PRSW) Observing Table 6-2 and Table 6-3, parameters measured *ex situ* show statistically significant correlation, suggesting that both PSWM and PAWM can be used to predict global post-transplant function. In both modes, PRSW shows strong and statistically significant correlation with post-CI and post-PRSW. Given its afterload independence and its definition as a marker of left ventricular work performance and reserve, both *ex situ* and *in vivo*, this is an intuitive result. [210] SW, our other marker of LV work, proved to

be a much less robust predictor, likely owing to its load dependence. In terms of systolic and diastolic markers, it is notable that Max dP/dt measured in PSWM and Min dP/dt measured in PAWM showed correlation with both post-CI and post-PRSW. In summary, while we can conclude that both post-CI and post-PRSW seem to be predictable with parameters measured during ESHP, we observe no discernable difference between PSWM and PAWM in terms of their comparative effectiveness in predicting global post-transplant function.

In order to quantify our ability to predict more specific aspects of post-transplant function, we next performed a selfsame correlation (Table 6-4). In this analysis, the difference between PSWM and PAWM is quite distinct, with 9 of the 10 measured parameters showing better correlation when measured in PAWM. Perhaps more importantly, this trend was seen in both systolic and diastolic parameters. In terms of systolic evaluation, only Max dP/dt shows significant selfsame correlation measured in PSWM while each of ESPVR, Max dP/dt/EDV and EMax show statistically significant correlation measured in PAWM. Interpreting this result, while it is possible to draw conclusions about pos-transplant systolic function from *ex situ* measurements in PSWM, PAWM allows for a more specific and nuanced prediction. In terms of diastolic function, this distinction is even more clear. None of the three diastolic parameters measured in PSWM presented statistically significant selfsame correlation, precluding the prediction of post-transplant diastolic function. In PAWM meanwhile, both Min dP/dt and EDPVR showed significant correlation with Tau falling just short (P=0.057).

The fact that PAWM performs substantially better in terms of selfsame correlation is important for numerous reasons. While markers of global function such as post-CI, post-SW and post-PRSW are often used in research and in clinical practice as predictors of post-transplant outcomes, they all suffer from a lack of predictive specificity.[211, 212] Regardless of global function, poor performance in any of our measured post-transplant systolic or diastolic parameters can be independently predictive of long-term systolic or diastolic dysfunction. [213, 214] Predicting post-transplant systolic and diastolic function during ESHP is therefore just as important as predicting global function. For diastolic function, this is particularly true in the ESHP setting. One of the biggest concerns with ESHP is the prevalence of myocardial edema. This edema manifests in many cases as a decrease in diastolic function, and increasing odds of primary graft failure following transplantation.[215] While edema itself can be measured at the end of the perfusion period as a

marker for myocardial injury, the ability to accurately determine diastolic function could be instrumental in understanding how and when edema occurs during ESHP.

In conjunction with these findings, we describe the use of a non-invasive control volume-based analysis of contractile parameters. This technique showed promising results for load dependent parameters but the use of stroke volume for the normalization of load independent relationships limited their accuracy. We sought to create a non-invasive measurement technique that would preclude the need for invasive measurement, while simultaneously allowing for the same breadth and accuracy of functional measurement. Our data suggests that for the load dependent parameters measured in this study, our non-invasive method achieves this aim. Observing Table 6-5, all load dependent parameters showed statistically significant correlation across measurement methodologies. It is somewhat intuitive therefore that, observing Table 6-6, all load dependent parameters that showed significant selfsame correlation measured invasively, also did so measured non-invasively. While the agreement between methodologies for load dependent parameters is encouraging, load independent parameters proved challenging to measure non-invasively. Due to the nature of control volume analysis, the calculation of volume change is feasible, but the calculation of instantaneous volumes impossible. Volume independent parameters were therefore normalized to changes in stroke volume in the non-invasive method rather than specific volumes as in the invasive method. Partially invasive parameters, using measured volumes from the catheter to normalize non-invasive results, were calculated to evaluate the impact of this discrepancy. For every load independent parameter, measurements taken using the non-invasive technique showed statistically significant correlation with those taken invasively and furthermore, showed selfsame correlation results that were very similar to their invasive counterparts. It would seem then that the limitation of the non-invasive technique is that end systolic and end diastolic volumes cannot be explicitly calculated, thus precluding the accurate calculation of load independent parameters. Nonetheless, this technique shows promise for future research, especially when considered in conjunction with other non-invasive techniques such as echocardiography that could be used to calculate these instantaneous volumes.

While we assert that the comparison between the predictive power of PSWM and PAWM is an important step in the advancement of ESHP, we present our work with a few important limitations. As with many large animal studies, follow up time was limited, leading to the inherent assumption that short term post-transplant cardiac performance was indicative of long-term outcomes.

Additionally, with some hearts weaning successfully after 60 minutes of reperfusion and others taking up to 180 minutes to wean, the recovery setting varied across hearts post-transplant. As planned however, we were able to achieve a wide range of functional recovery to perform the necessary correlations. Finally, we present our work in a limited sample, precluding the comparison of performance between DBD and DCD hearts, an important consideration in the field and an avenue of future work in our group. Coupled with additional future work in determining ideal measurement techniques and preservation strategies, this work could offer an avenue for improved primary graft function and an increase in the number of hearts available for transplantation.

In summary, we have successfully perfused and transplanted 10 porcine hearts and correlated *ex situ* functional parameters to post-transplant function. Owing to differing afterload characteristics *ex situ*, significant differences were seen between contractile parameters measured at the same timepoint and under the same loading conditions in PSWM and PAWM. While both modes offered a suitable means for predicting global post-transplant function, we observed a distinct advantage for PAWM in terms of predicting systolic and diastolic function post-transplant. As both systolic and diastolic function are independent predictors of post-transplant morbidity, and mortality, and theoretically treatable during ESHP, this distinction is an important step in the optimization of the *ex situ* technique.

Chapter 7

7 Conclusions and Recommendations

7.1 Summary of Results

Ex situ heart perfusion offers a promising avenue for expanding the donor pool through the augmentation of cardiac preservation and evaluation during the time between the excision of hearts from donors and their eventual transplantation. In contrast to traditional preservation methods, this technique could facilitate an increase in the efficiency with which currently acceptable donor hearts are used, and potentially even the use of marginal donor hearts. In this thesis the design and use of a multimodal ESHP system is described with a particular emphasis on the successful implementation of a fully adjustable Passive Afterload Working Mode. Perfusing hearts in this mode was shown not only to be eminently possible across even long term, 6-hour perfusion periods, but also proved to be a more physiologically relevant evaluation setting for the prediction of post-transplant outcomes using functional evaluation during ESHP. Combining these traits, it is concluded that PAWM offers a promising avenue for augmenting the applicability of ESHP, albeit one that requires a considerable amount of future research.

In Chapter 4, the development of the multimodal ESHP system is described in terms of the successful application of a modular design strategy in the creation of a system that is simultaneously flexible and controllable. To validate the system, 6 porcine hearts were excised and perfused in LM for 4 hours with LV contractile evaluation performed in PSWM at the 1 hour and 4-hour timepoints. After the 4-hour evaluation period, hearts were transitioned into biventricular PSWM or PAWM as a means to assess the effectiveness of the system in these additional settings. All told, system stability was demonstrated in each of LM, PSWM and PAWM with functional evaluation performed in both PSWM and PAWM using traditional pressure-volume catheterization as well as echocardiography. The modularity of the design of this system proved to be quite useful in that it enabled system operation in: LM, left or right sided 2-chamber working mode in either PSWM or PAWM, biventricular working mode in either PSWM or PAWM, and even the implementation of right atrial loading in LM. All told, it was shown that the proposed ESHP system is a safe, controllable and flexible platform for use in research into novel ESHP preservation and evaluation studies.

In Chapter 5, the augmentation of the passive afterload component of the ESHP system described in Chapter 4 is detailed in terms of the development and testing of a novel, adjustable afterload module. This module, based on a 4-element Windkessel, allows for adjustability of systemic and proximal resistors as well as a spring-loaded compliance element. The nature of this design solves many of the problems laid out in section 2.3.3. Namely, no portion of any of the afterload elements comes into direct contact with the perfusate, ensuring sterility, and afterload parameter settings can be adjusted throughout the perfusion period, ensuring that changes in LV contractility can be decoupled from aortic pressure variation. An important consideration for this work was the analytical modelling of each individual afterload element. Single element testing confirmed that using simple characteristic equations, both resistance and compliance could be accurately predicted and controlled throughout the entirety of their operating ranges. This allows for the prescription of specific afterload settings based on the desired preservative or evaluative setting for the heart. Assembling the components into the afterload module, 3 separate hearts were perfused for 6 hours in PAWM. Across the entire perfusion period, and for all 3 hearts, systolic and diastolic pressures were successfully maintained in their target ranges. Furthermore, after 6 hours of perfusion, with hearts evaluated using pressure-volume catheterization, contractile function was in line with what was seen in hearts described in Chapter 4. These results demonstrate that using this novel afterload module, extended PAWM perfusion is possible, and that it could offer a relevant setting for ESHP preservation and evaluation.

With system stability fully demonstrated in Chapters 4 and 5, attention turned to the analysis of evaluation strategies during ESHP, in particular, the comparative effectiveness of PSWM and PAWM as *ex situ* settings for the prediction of post-transplant cardiac function. Chapter 6 describes a porcine transplant study in which 5 DBD hearts and 5 DCD hearts were excised, perfused in LM for 4 hours, evaluated in both PSWM and PAWM at the 4-hour timepoint and then transplanted into size matched recipient pigs. By correlating measurements taken during ESHP with those taken post-transplant, the pertinence of each measured ESHP contractile parameter could be analyzed. In terms of global functional prediction, marked in our case by post-transplant cardiac index and preload recruitable stroke work, very little difference was observed between parameters measured in PSWM and PAWM. For prediction of specific parameters related to post transplant systolic and diastolic function however, the discrepancy was much larger. For almost all measured post-transplant contractile parameters, measurements taken in PAWM were more

predictive of post-transplant outcomes. While more research is required to confirm this finding, its cause can be attributed, at least in part, to an increase in parameter variability caused by uncontrollable variability in afterload in PSWM. Using the precise control demonstrated in Chapter 5, afterload settings can be fixed across different hearts in PAWM. In PSWM meanwhile, no such control exists. This afterload variability, coupled with the afterload dependence of many evaluated contractile parameters, results in measurement variation not attributable to contractile function changes. It is concluded that for post-transplant prediction, PAWM offers a more predictive setting during ESHP, a finding that could both augment the capability of the optimized ESHP technique and allow for more accurate analysis of the effectiveness of various perfusion strategies without the need for transplantation.

7.2 Recommendations for Future Work

While this thesis contributes progress towards an optimized ESHP system utilizing PAWM, substantial work remains in terms of optimizing the ESHP technique. Detailed in this section are specific areas within the field where future research could be focused in order to overcome the challenges facing the widespread implementation of ESHP

7.2.1 Development of Cutoff Points for Evaluative Parameters

Detailed in Chapter 6 is a hypothesis generating transplantation study meant to be the first step in the identification of physiologically relevant evaluation criteria as a means of post-transplant functional prediction. Within this study, it is shown that contractile parameters measured in PAWM were more indicative of post-transplant function. No conclusions, however, were drawn about what constitutes acceptable post-transplant performance, nor indeed about what values for these relevant ESHP parameters predict acceptable performance. Furthermore, the capability of evaluating RV function has not yet been demonstrated nor has its impact on post-transplant prediction. Goals in future work in the area of cardiac evaluation during ESHP are thus twofold: to augment the data set with additional experiments such that the sample is large enough to create an accurate predictive model of post-transplant performance based on LV and RV parameters measured during ESHP, and to define specific cutoff values for each of these ESHP parameters to enable simple identification of hearts that can be successfully used for transplant and those that cannot. This follows the work done using the Transmedics OCS where a lactate level below 2 mmol/L and a positive lactate extraction value are used to indicate that a heart is capable of

transplant.[99] Simple cutoff points such as these are eminently useful in clinical practice, and with contractile function showing a greater correlation to post transplant function, similar cutoff points for these ESHP values would be very useful.

Where creating the model for post-transplant prediction requires only an increase in sample size and statistical analysis, determining accurate cutoff values for ESHP parameters deemed to be meaningful is much more complex. A number of transplantation experiments need to be carried out in order to achieve a broad range of post-transplant outcomes. Using the data from these experiments, post-transplant parameter values for hearts that meet post-transplant acceptance criteria (i.e., weaned from cardiopulmonary bypass and remained stable for 1-hour) can be determined. Using these post-transplant values as inputs for the predictive model, cutoff values for parameters measured during ESHP can be determined and tested. This type of experimentation is very costly and time-consuming, perhaps explaining why it has not yet been completed. That being said, the implementation of a successful evaluation strategy that can provide surgeons reliable criteria for determining whether a heart should or should not be transplanted is of paramount importance and one of the key considerations with the field of ESHP.

7.2.2 Limiting Pulse Pressure in PAWM

As detailed in Chapter 5, one of the most important parameters in ESHP is aortic pressure. It is the characteristic that drives coronary perfusion and the single fundamental reason that ESHP is any different than CS. In Chapter 5 it is hypothesized that, as is the case in many aspects of biomedical engineering, the ability to match physiological pressure conditions could be beneficial for cardiac preservation during ESHP. With this in mind, physiological porcine pressures were prescribed to hearts tested in this chapter. In addition to pressure however, it has been postulated that the nature of the working heart itself could have an independent impact on cardiac preservation, activating biochemical pathways that are dormant in LM. [216] The study of the impact of this phenomenon is a very interesting field of study in itself. Unfortunately, due to the impact of the pulsatile nature of working mode aortic pressures, the study of the heart's biochemical response to working mode is coupled to the heart's response to aortic pressure pulsatility. In order to understand either of these phenomena independently, it is necessary to establish a working heart model with an aortic pressure similar to that seen in LM.

From an afterload perspective, this is theoretically possible though it would require the institution of compliance at values far greater than those contained within the physiological range and indeed, far greater than the afterload module in Chapter 5 has demonstrably instilled on *ex situ* hearts. Taking a pulse pressure below 5 mmHg to be a reasonable target for a LM-like pressure and considering that a cardiac output of 3 L/min with a heart rate of 72 bpm results in stroke volumes of 41 mL, compliance would need to be set in excess of 8 mL/mmHg to achieve a limited pulse pressure in PAWM. With this in mind, future work must include the adaptation of current afterload modules to allow for extremely high compliances if ever the independent impacts of pressure pulsatility and the biochemical response of the heart to working mode are to be studied independently and fully understood.

7.2.3 Optimization of Mode Specific Perfusion Parameters

In this thesis, the end goal was the facilitation of preservation and functional evaluation in all three primary perfusion modes. Emphasis was placed on the development of evaluative criteria such that future research into preservation strategies could be carried out without transplant studies. With the optimal evaluative setting not necessarily being the same as the optimal preservation setting, future work must include the optimization of ESHP preservation in each of the three primary modes. As it stands, within each of the three primary perfusion modes, perfusion parameter settings that optimize cardiac preservation remain unclear. Moreover, with hearts requiring varying levels of support depending on their contractile function or level of myocardial injury, a heart dependent control strategy for these parameters for fine adjustment around their optimal levels is necessary, and as yet undefined. Specific parameters include mean aortic pressure, aortic pulse pressure, perfusate temperature, cardiac rewarming time, perfusate oxygen concentration, and the perfusate composition itself. While each of these parameters could be, and in many cases have been, studied and optimized individually in terms of their preservative impact, this approach precludes the ability to optimize dependent characteristics in combination. This has the potential to result in the presumption that a parameter is set to its optimal level, when really the setting of a separate parameter changes the nature of what that optimal level is. As an example, coronary tone has a profound impact on what mean aortic pressure is necessary to provide adequate myocardial perfusion. This coronary tone, however, is itself very much dependent on perfusate temperature, another controllable perfusion characteristic.[217] As such, if a study were to be undertaken to determine the optimal mean aortic pressure in a hypothermic or sub-normothermic setting, it

cannot be assumed that this would also be the optimal pressure for normothermic perfusion. In order to understand these parameter relationships, a strategy that accounts for these dependencies must be used during the optimization period of this recommended future work.

Design of Experiments (DOE) is a tried and tested method for modelling and optimizing complex systems with numerous controllable parameters. By varying parameter settings across specific predefined levels over a multitude of experiments, specific and accurate conclusions about their independent and codependent impacts on experimental outcomes can be derived. In terms of ESHP, the utility of this approach is readily apparent, but its application has to this point been very difficult. The use of DOE requires an accurately measured marker of experimental outcome, which for ESHP would mean a reliable measurement of post-transplant outcome. With transplantation experiments being quite costly, and a DOE for even just 5 parameters requiring upwards of 25 experiments, excitement for the use of this technique for the optimization of ESHP has been understandably limited. With the augmentation of findings presented in Chapter 6 however, a very detailed prediction of post-transplant function is eminently possible without having to perform transplantation studies. For hearts of varying contractile quality (perhaps utilizing a DBD study group and a DCD study group as was done in Chapter 6), DOE should be used in conjunction with these ESHP functional measurements to optimize parameter settings in each of LM, PSWM and PAWM.

7.2.4 Comparison of the Preservative Impact of Different Perfusion Modes

With preservation optimized within each of the perfusion modes, studies into the relative impact of the utilization of the different perfusion modes could be undertaken. The goals of these particular studies would be twofold: to analyze the comparative preservative effectiveness of perfusing hearts in the three separate modes, and to deepen the understanding of the physiological phenomena associated with perfusing hearts in a working state as compared to a more traditional Langendorff Mode. The completion of first of these goals consists simply of perfusing different hearts in each of the three modes and comparing their respective preservative performance based on evaluation parameters outlined in Chapter 6. To account for the supposition that the optimal conditions for hearts could potentially vary with heart quality, for each mode a group of DCD hearts and a group of DBD hearts should be analyzed. Comparing function this way allows for not only the comparison of modes in terms of their preservative capabilities, but also in terms of their

robustness against hearts of differing quality. The analysis of the use of working mode on cardiac physiology compared to LM, while not as directly relevant to the organ shortage ESHP strives to solve, offers another very interesting line of future research. Using modifications to the afterload described in Chapter 5, laid out in section 7.2.2, it is eminently possible to match perfusion conditions in PAWM and LM. The only difference between the two modes would be ventricular loading, thus enabling the direct analysis of the effect of physiological diastolic filling and ventricular ejection on cardiac behavior. In terms of ESHP optimization, this information could feed back into the optimization of cardiac preservation strategies, but far more importantly, outside of ESHP this could offer a platform to study the metabolic effects of cardiac loading.

7.2.5 Moving PAWM to Clinical Studies

The final stage of proposed future work is the completion of the necessary steps to bring perfusion in PAWM from preclinical experimentation to clinical practice. Much of this work is related to the imperative task of demonstrating the safety of the technique, though with the relative cost of clinical studies in comparison to their preclinical counterparts, optimization tasks described in the preceding subsections should also be completed before clinical studies begin. In particular, the introduction of substantial automation to preclude the need of a surgeon to run the ESHP machine is of considerable importance. Within preclinical optimization studies should also be ample analysis on the safety of the PAWM technique. With safety demonstrated in the preclinical setting, pilot studies can be completed on discarded human hearts. This brings a multitude of additional considerations as not only will the optimized perfusion settings be slightly different than in the preclinical studies, so too will the cutoff points for evaluative parameters. For discarded human hearts in particular, these differences could be problematic as the quality of hearts could vary drastically. That being said, if clinically accepted lactate measurements used for the OCS meet, or are close to meeting acceptance criteria, that would provide a very compelling argument for moving towards clinical studies. The hope is that within the preclinical model, enough of the understanding in terms of how and why ESHP is successful or unsuccessful could be determined, but no matter how much foundational work is laid, more optimization will be necessary using human hearts. As the use of PAWM extends into these studies, with the additional controllable perfusion parameters its use entails, this is an important consideration that will require careful investigation.

7.3 Conclusion

In conclusion, this thesis demonstrates both the utility of PAWM and a system on which its application is possible. A multimodal ESHP system has been shown as an excellent platform for the comparative analysis of perfusion within these three modes with cardiac evaluation possible using a variety of invasive and noninvasive techniques. On this platform, a fully adjustable Windkessel based afterload module was shown to enable long term perfusion in PAWM, decoupling aortic pressure from left ventricular contractility. Additionally, in its demonstrably precise control, this afterload module also allowed for the instillation of very specific resistance and compliance values across different hearts. For the purposes of *ex situ* evaluation, this control manifested itself in an increase in physiological relevance of the evaluation setting as compared to a more traditional working mode. While considerable work remains in the optimization of perfusion parameters, PAWM offers an exciting avenue in the field of ESHP research. The results presented herein combined with future work in compliance chamber design, perfusion parameter optimization, the development of evaluative cutoff points and steps towards clinical translation, have the potential to greatly improve our ability to preserve and evaluate donor hearts and thus vastly expand the cardiac donor pool.

References

[1] E. J. Benjamin *et al.*, "Heart Disease and Stroke Statistics-2018 Update: A Report From the American Heart Association," *Circulation,* vol. 137, no. 12, pp. e67-e492, Mar 20 2018.

[2] D. K. C. Cooper, "Christiaan Barnard-The surgeon who dared: The story of the first human-to-human heart transplant," *Glob Cardiol Sci Pract,* vol. 2018, no. 2, p. 11, Jun 30 2018.

[3] T. Vogel, J. G. Brockmann, C. Coussios, and P. J. Friend, "The role of normothermic extracorporeal perfusion in minimizing ischemia reperfusion injury," *Transplantation Reviews,* vol. 26, no. 2, pp. 156-162, 2012/04/01/ 2012.

[4] K. K. Khush *et al.*, "The International Thoracic Organ Transplant Registry of the International Society for Heart and Lung Transplantation: Thirty-fifth Adult Heart Transplantation Report—2018; Focus Theme: Multiorgan Transplantation," *The Journal of Heart and Lung Transplantation,* vol. 37, no. 10, pp. 1155-1168, 2018/10/01/ 2018.

[5] E. M. Hsich, "Matching the Market for Heart Transplantation," (in eng), *Circulation. Heart failure,* vol. 9, no. 4, pp. e002679-e002679, 2016.

[6] B. A. Goldstein, L. Thomas, J. G. Zaroff, J. Nguyen, R. Menza, and K. K. Khush, "Assessment of Heart Transplant Waitlist Time and Pre- and Post-transplant Failure: A Mixed Methods Approach," (in eng), *Epidemiology (Cambridge, Mass.),* vol. 27, no. 4, pp. 469-476, 2016.

[7] M. S. Jahania, J. A. Sanchez, P. Narayan, R. D. Lasley, and R. M. Mentzer, Jr., "Heart preservation for transplantation: principles and strategies," (in eng), *Ann Thorac Surg,* vol. 68, no. 5, pp. 1983-7, Nov 1999.

[8] S. Sponga *et al.*, "Ex-vivo Perfusion on Marginal Donors in Heart Transplantation: Clinical Resuts and Pathological Findings," *The Journal of Heart and Lung Transplantation,* vol. 38, no. 4, pp. S42-S43, 2019.

[9] A. Page, S. Messer, and S. R. Large, "Heart transplantation from donation after circulatory determined death," *Ann Cardiothorac Surg,* vol. 7, no. 1, pp. 75-81, Jan 2018.

[10] C. W. White *et al.*, "Transplantation of Hearts Donated after Circulatory Death," (in eng), *Front Cardiovasc Med,* vol. 5, p. 8, 2018.

[11] P. S. Macdonald, "Heart Transplantation From DCD donors: From the Bedside to the Bench," *Transplantation,* vol. 101, no. 8, pp. 1753-1754, Aug 2017.

[12] S. Salehi, K. Tran, and W. L. Grayson, "Advances in Perfusion Systems for Solid Organ Preservation," (in eng), *The Yale journal of biology and medicine,* vol. 91, no. 3, pp. 301-312, 2018.

[13] M. Hsin and T. Au, "Ex vivo lung perfusion: a potential platform for molecular diagnosis and ex vivo organ repair," (in eng), *J Thorac Dis,* vol. 10, no. Suppl 16, pp. S1871-s1883, Jun 2018.

[14] D. Van Raemdonck, F. Rega, S. Rex, and A. Neyrinck, "Machine perfusion of thoracic organs," *J Thorac Dis,* vol. 10, no. Suppl 8, pp. S910-S923, Apr 2018.

[15] J. D. Hardy, W. R. Webb, M. L. Dalton, Jr., and G. R. Walker, Jr., "Lung Homotransplantation in Man," *JAMA,* vol. 186, pp. 1065-74, Dec 21 1963.

[16] F. Venuta and D. Van Raemdonck, "History of lung transplantation," *J Thorac Dis,* vol. 9, no. 12, pp. 5458-5471, Dec 2017.

[17] R. L. Hardesty and B. P. Griffith, "Autoperfusion of the heart and lungs for preservation during distant procurement," *J Thorac Cardiovasc Surg,* vol. 93, no. 1, pp. 11-8, Jan 1987.

[18] A. J. Fisher, J. H. Dark, and P. A. Corris, "Improving donor lung evaluation: a new approach to increase organ supply for lung transplantation," *Thorax,* vol. 53, no. 10, pp. 818-20, Oct 1998.

[19] S. Steen, T. Sjoberg, L. Pierre, Q. Liao, L. Eriksson, and L. Algotsson, "Transplantation of lungs from a non-heart-beating donor," *Lancet,* vol. 357, no. 9259, pp. 825-9, Mar 17 2001.

[20] M. Cypel *et al.*, "Normothermic ex vivo perfusion prevents lung injury compared to extended cold preservation for transplantation," *Am J Transplant,* vol. 9, no. 10, pp. 2262-9, Oct 2009.

[21] P. Wierup *et al.*, "Ex vivo evaluation of nonacceptable donor lungs," *Ann Thorac Surg,* vol. 81, no. 2, pp. 460-6, Feb 2006.

[22] T. M. Egan *et al.*, "Ex vivo evaluation of human lungs for transplant suitability," *Ann Thorac Surg,* vol. 81, no. 4, pp. 1205-13, Apr 2006.

[23] S. Steen *et al.*, "First human transplantation of a nonacceptable donor lung after reconditioning ex vivo," *Ann Thorac Surg,* vol. 83, no. 6, pp. 2191-4, Jun 2007.

[24] B. Khan *et al.*, "Successful Lung Transplantation From Hepatitis C Positive Donor to Seronegative Recipient," *Am J Transplant,* vol. 17, no. 4, pp. 1129-1131, Apr 2017.

[25] M. Galasso *et al.*, "Inactivating hepatitis C virus in donor lungs using light therapies during normothermic ex vivo lung perfusion," *Nat Commun,* vol. 10, no. 1, p. 481, Jan 29 2019.

[26] C. Akateh, E. W. Beal, B. A. Whitson, and S. M. Black, "Normothermic Ex-vivo Liver Perfusion and the Clinical Implications for Liver Transplantation," *J Clin Transl Hepatol,* vol. 6, no. 3, pp. 276-282, Sep 28 2018.

[27] F. O. Belzer, B. S. Ashby, P. F. Gulyassy, and M. Powell, "Successful seventeen-hour preservation and transplantation of human-cadaver kidney," *N Engl J Med,* vol. 278, no. 11, pp. 608-10, Mar 14 1968.

[28] R. M. Merion, N. P. Goodrich, and S. Feng, "How can we define expanded criteria for liver donors?," *J Hepatol,* vol. 45, no. 4, pp. 484-8, Oct 2006.

[29] C. Jay *et al.*, "A comprehensive risk assessment of mortality following donation after cardiac death liver transplant - an analysis of the national registry," *J Hepatol,* vol. 55, no. 4, pp. 808-13, Oct 2011.

[30] M. O. Hamed *et al.*, "Early graft loss after kidney transplantation: risk factors and consequences," *Am J Transplant,* vol. 15, no. 6, pp. 1632-43, Jun 2015.

[31] Y. W. Cho, P. I. Terasaki, J. M. Cecka, and D. W. Gjertson, "Transplantation of kidneys from donors whose hearts have stopped beating," *N Engl J Med,* vol. 338, no. 4, pp. 221-5, Jan 22 1998.

[32] M. Skrzypiec-Spring, B. Grotthus, A. Szelag, and R. Schulz, "Isolated heart perfusion according to Langendorff---still viable in the new millennium," *J Pharmacol Toxicol Methods,* vol. 55, no. 2, pp. 113-26, Mar-Apr 2007.

[33] O. J. A. f. d. g. P. d. M. u. d. T. Langendorff, "Untersuchungen am überlebenden Säugethierherzen," journal article vol. 61, no. 6, pp. 291-332, August 01 1895.

[34] H. G. Zimmer, "Who discovered the Frank-Starling mechanism?," *News Physiol Sci,* vol. 17, pp. 181-4, Oct 2002.

[35] S. W. Patterson and E. H. Starling, "On the mechanical factors which determine the output of the ventricles," (in eng), *The Journal of physiology,* vol. 48, no. 5, pp. 357-379, 1914.

[36] F. P. Knowlton and E. H. Starling, "The influence of variations in temperature and blood-pressure on the performance of the isolated mammalian heart," vol. 44, no. 3, pp. 206-219, 1912.

[37] J. R. Neely, H. Liebermeister, E. J. Battersby, and H. E. Morgan, "Effect of pressure development on oxygen consumption by isolated rat heart," *Am J Physiol,* vol. 212, no. 4, pp. 804-14, Apr 1967.

[38] R. Liao, B. K. Podesser, and C. C. Lim, "The continuing evolution of the Langendorff and ejecting murine heart: new advances in cardiac phenotyping," *Am J Physiol Heart Circ Physiol,* vol. 303, no. 2, pp. H156-67, Jul 15 2012.

[39] I. L. Grupp, A. Subramaniam, T. E. Hewett, J. Robbins, and G. Grupp, "Comparison of normal, hypodynamic, and hyperdynamic mouse hearts using isolated work-performing heart preparations," *Am J Physiol,* vol. 265, no. 4 Pt 2, pp. H1401-10, Oct 1993.

[40] L. J. De Windt, J. Willems, R. S. Reneman, G. J. Van der Vusse, T. Arts, and M. Van Bilsen, "An improved isolated, left ventricular ejecting, murine heart model. Functional and metabolic evaluation," *Pflugers Arch,* vol. 437, no. 2, pp. 182-90, Jan 1999.

[41] H. Bardenheuer and J. Schrader, "Supply-to-demand ratio for oxygen determines formation of adenosine by the heart," *Am J Physiol,* vol. 250, no. 2 Pt 2, pp. H173-80, Feb 1986.

[42] M. Monteagudo Vela, D. Garcia Saez, and A. R. Simon, "Current approaches in retrieval and heart preservation," *Ann Cardiothorac Surg,* vol. 7, no. 1, pp. 67-74, Jan 2018.

[43] J. L. Chan *et al.*, "Intermediate outcomes with ex-vivo allograft perfusion for heart transplantation," *J Heart Lung Transplant,* vol. 36, no. 3, pp. 258-263, Mar 2017.

[44] A. Ardehali *et al.*, "Ex-vivo perfusion of donor hearts for human heart transplantation (PROCEED II): a prospective, open-label, multicentre, randomised non-inferiority trial," *Lancet,* vol. 385, no. 9987, pp. 2577-84, Jun 27 2015.

[45] N. L. Stamp *et al.*, "Successful Heart Transplant after Ten Hours Out-of-body Time using the TransMedics Organ Care System," (in eng), *Heart Lung Circ,* vol. 24, no. 6, pp. 611-3, Jun 2015.

[46] D. Garcia Saez *et al.*, "Evaluation of the organ care system in heart transplantation with an adverse donor/recipient profile," *Ann Thorac Surg,* vol. 98, no. 6, pp. 2099-105; discussion 2105-6, Dec 2014.

[47] K. K. Dhital *et al.*, "Adult heart transplantation with distant procurement and ex-vivo preservation of donor hearts after circulatory death: a case series," *Lancet,* vol. 385, no. 9987, pp. 2585-91, Jun 27 2015.

[48] M. J. Wilhelm, "Long-term outcome following heart transplantation: current perspective," *J Thorac Dis,* vol. 7, no. 3, pp. 549-51, Mar 2015.

[49] A. A. Page, S. Messer, S. S. Tsui, and S. R. J. C. T. R. Large, "Early Results Using Donation After Circulatory Death (DCD) Donor Hearts," journal article vol. 3, no. 3, pp. 199-206, September 01 2016.

[50] C. W. White *et al.*, "Assessment of donor heart viability during ex vivo heart perfusion," *Can J Physiol Pharmacol,* vol. 93, no. 10, pp. 893-901, Oct 2015.

[51] A. Page *et al.*, "Does the Assessment of DCD Donor Hearts on the Organ Care System Using Lactate Need Redefining?," *The Journal of Heart and Lung Transplantation,* vol. 36, no. 4, pp. S16-S17, 2017.

[52] A. Hamed, S. Tsui, J. Huber, R. Lin, E. C. Poggio, and A. Ardehali, "19: Serum Lactate Is a Highly Sensitive and Specific Predictor of Post Cardiac Transplant Outcomes Using the Organ Care System," *The Journal of Heart and Lung Transplantation,* vol. 28, no. 2, p. S71, 2009.

[53] M. J. Collins, S. L. Moainie, B. P. Griffith, and R. S. Poston, "Preserving and evaluating hearts with ex vivo machine perfusion: an avenue to improve early graft performance and expand the donor pool," *Eur J Cardiothorac Surg,* vol. 34, no. 2, pp. 318-25, Aug 2008.

[54] F. O. Belzer and J. H. Southard, "Principles of solid-organ preservation by cold storage," *Transplantation,* vol. 45, no. 4, pp. 673-6, Apr 1988.

[55] E. Kevelaitis, N. C. Nyborg, and P. Menasche, "Coronary endothelial dysfunction of isolated hearts subjected to prolonged cold storage: patterns and contributing factors," *J Heart Lung Transplant,* vol. 18, no. 3, pp. 239-47, Mar 1999.

[56] E. E. Guibert, A. Y. Petrenko, C. L. Balaban, A. Y. Somov, J. V. Rodriguez, and B. J. Fuller, "Organ Preservation: Current Concepts and New Strategies for the Next Decade," *Transfus Med Hemother,* vol. 38, no. 2, pp. 125-142, 2011.

[57] S. G. Michel, G. M. LaMuraglia Ii, M. L. L. Madariaga, and L. M. Anderson, "Innovative cold storage of donor organs using the Paragonix Sherpa Pak ™ devices," (in eng), *Heart, lung and vessels,* vol. 7, no. 3, pp. 246-255, 2015.

[58] J. Suaudeau, M. Servoz-Gavin, and F. Morel, "[Preservation of isolated heart for 72 hours using hypothermic perfusion with a synthetic perfusion liquid]," *J Chir (Paris),* vol. 105, no. 5, pp. 573-98, May-Jun 1973. Conservation de coeur isole pendant 72 heures par perfusion hypothermique avec un liquide de perfusion synthetique.

[59] E. Proctor, R. Parker, and D. Turner, "Preservation of the isolated heart for 72 hours. A preliminary report on the development of a heart "bank"," *Guys Hosp Rep,* vol. 118, no. 1, pp. 75-84, 1969.

[60] E. Proctor and R. Parker, "Preservation of isolated heart for 72 hours," *Br Med J,* vol. 4, no. 5626, pp. 296-8, Nov 2 1968.

[61] W. N. Wicomb, D. Novitzky, D. K. Cooper, and A. G. Rose, "Forty-eight hours hypothermic perfusion storage of pig and baboon hearts," (in eng), *J Surg Res,* vol. 40, no. 3, pp. 276-84, Mar 1986.

[62] D. H. Rosenbaum, M. Peltz, M. E. Merritt, J. E. Thatcher, H. Sasaki, and M. E. Jessen, "Benefits of perfusion preservation in canine hearts stored for short intervals," *J Surg Res,* vol. 140, no. 2, pp. 243-9, Jun 15 2007.

[63] T. P. Fitton *et al.,* "Attenuation of DNA damage in canine hearts preserved by continuous hypothermic perfusion," *Ann Thorac Surg,* vol. 80, no. 5, pp. 1812-20, Nov 2005.

[64] S. G. Michel *et al.*, "Twelve-Hour Hypothermic Machine Perfusion for Donor Heart Preservation Leads to Improved Ultrastructural Characteristics Compared to Conventional Cold Storage," *Ann Transplant,* vol. 20, pp. 461-8, Aug 11 2015.

[65] S. G. Michel *et al.*, "Preservation of donor hearts using hypothermic oxygenated perfusion," (in eng), *Ann Transplant,* vol. 19, pp. 409-16, Aug 20 2014.

[66] K. Oshima *et al.*, "Long-term heart preservation using a new portable hypothermic perfusion apparatus," (in eng), *J Heart Lung Transplant,* vol. 18, no. 9, pp. 852-61, Sep 1999.

[67] O. Van Caenegem *et al.*, "Hypothermic continuous machine perfusion enables preservation of energy charge and functional recovery of heart grafts in an ex vivo model of donation following circulatory death," *Eur J Cardiothorac Surg,* vol. 49, no. 5, pp. 1348-53, May 2016.

[68] C. W. White *et al.*, "Avoidance of Profound Hypothermia During Initial Reperfusion Improves the Functional Recovery of Hearts Donated After Circulatory Death," *Am J Transplant,* vol. 16, no. 3, pp. 773-82, Mar 2016.

[69] A. Iyer *et al.*, "Normothermic ex vivo perfusion provides superior organ preservation and enables viability assessment of hearts from DCD donors," *Am J Transplant,* vol. 15, no. 2, pp. 371-80, Feb 2015.

[70] R. S. Poston *et al.*, "Optimizing donor heart outcome after prolonged storage with endothelial function analysis and continuous perfusion," *Ann Thorac Surg,* vol. 78, no. 4, pp. 1362-70;; discussion 1362-70, Oct 2004.

[71] M. Peltz *et al.*, "Perfusion preservation maintains myocardial ATP levels and reduces apoptosis in an ex vivo rat heart transplantation model," *Surgery,* vol. 138, no. 4, pp. 795-805, Oct 2005.

[72] T. Ozeki *et al.*, "Heart preservation using continuous ex vivo perfusion improves viability and functional recovery," (in eng), *Circ J,* vol. 71, no. 1, pp. 153-9, Jan 2007.

[73] W. H. Hassanein *et al.*, "Continuous perfusion of donor hearts in the beating state extends preservation time and improves recovery of function," *J Thorac Cardiovasc Surg,* vol. 116, no. 5, pp. 821-30, Nov 1998.

[74] J. M. Trahanas *et al.*, "Achieving 12 Hour Normothermic *Ex situ* Heart Perfusion: An Experience of 40 Porcine Hearts," (in eng), *Asaio j,* vol. 62, no. 4, pp. 470-6, Jul-Aug 2016.

[75] C. W. White *et al.*, "Right Ventricular Distension in Donor Hearts Following Cardiocirculatory Death: Implications for Post-Transplant Function," *The Journal of Heart and Lung Transplantation,* vol. 32, no. 4, p. S95, 2013.

[76] A. Iyer *et al.*, "Pathophysiological Trends During Withdrawal of Life Support: Implications for Organ Donation After Circulatory Death," *Transplantation,* vol. 100, no. 12, pp. 2621-2629, Dec 2016.

[77] A. Iyer *et al.*, "Increasing the tolerance of DCD hearts to warm ischemia by pharmacological postconditioning," *Am J Transplant,* vol. 14, no. 8, pp. 1744-52, Aug 2014.

[78] H. C. Chew, P. S. Macdonald, and K. K. J. J. o. T. D. Dhital, "The donor heart and organ perfusion technology," *2019*, pp. S938-S945, 2019.

[79] S. Messer and S. Large, "Resuscitating heart transplantation: the donation after circulatory determined death donor," *Eur J Cardiothorac Surg*, vol. 49, no. 1, pp. 1-4, Jan 2016.

[80] A. M. Scheule *et al.*, "A non-heart-beating donor model to evaluate functional and morphologic outcomes in resuscitated pig hearts," *J Invest Surg*, vol. 15, no. 3, pp. 125-35, May-Jun 2002.

[81] S. Osaki *et al.*, "Resuscitation of non-beating donor hearts using continuous myocardial perfusion: the importance of controlled initial reperfusion," (in eng), *Ann Thorac Surg*, vol. 81, no. 6, pp. 2167-71, Jun 2006.

[82] P. Niederberger *et al.*, "Heart Transplantation With Donation After Circulatory Death," *Circ Heart Fail*, vol. 12, no. 4, p. e005517, Apr 2019.

[83] D. Urcuyo *et al.*, "Development of a prolonged warm ex vivo perfusion model for kidneys donated after cardiac death," *Int J Artif Organs*, vol. 40, no. 6, pp. 265-271, Jun 9 2017.

[84] M. Selzner *et al.*, "Normothermic ex vivo liver perfusion using steen solution as perfusate for human liver transplantation: First North American results," *Liver Transpl*, vol. 22, no. 11, pp. 1501-1508, Nov 2016.

[85] M. Cypel *et al.*, "Normothermic ex vivo lung perfusion in clinical lung transplantation," *N Engl J Med*, vol. 364, no. 15, pp. 1431-40, Apr 14 2011.

[86] R. N. Bhattacharjee *et al.*, "Subnormothermic oxygenated perfusion optimally preserves donor kidneys ex vivo," *Kidney International Reports*.

[87] J. J. Nostedt, D. T. Skubleny, A. M. J. Shapiro, S. Campbell, D. H. Freed, and D. L. Bigam, "Normothermic Ex Vivo Machine Perfusion for Liver Grafts Recovered from Donors after Circulatory Death: A Systematic Review and Meta-Analysis," *HPB Surg*, vol. 2018, p. 6867986, 2018.

[88] G. Loor *et al.*, "Prolonged EVLP Using OCS Lung: Cellular and Acellular Perfusates," (in eng), *Transplantation*, vol. 101, no. 10, pp. 2303-2311, 2017.

[89] R. Slonim, C. Wang, and E. Garbarino, *The Market for Blood*. 2014.

[90] J. M. Kaths *et al.*, "Normothermic Ex Vivo Kidney Perfusion for the Preservation of Kidney Grafts prior to Transplantation," (in eng), *J Vis Exp*, no. 101, p. e52909, Jul 15 2015.

[91] J. M. Knaak, V. N. Spetzler, N. Goldaracena, K. S. Louis, N. Selzner, and M. Selzner, "Technique of subnormothermic ex vivo liver perfusion for the storage, assessment, and repair of marginal liver grafts," (in eng), *J Vis Exp*, no. 90, p. e51419, Aug 13 2014.

[92] T. N. Machuca and M. Cypel, "Ex vivo lung perfusion," (in eng), *Journal of thoracic disease,* vol. 6, no. 8, pp. 1054-1062, 2014.

[93] M. A. Schechter *et al.*, "An isolated working heart system for large animal models," *J Vis Exp,* no. 88, Jun 11 2014.

[94] C. W. White *et al.*, "A cardioprotective preservation strategy employing ex vivo heart perfusion facilitates successful transplant of donor hearts after cardiocirculatory death," *J Heart Lung Transplant,* vol. 32, no. 7, pp. 734-43, Jul 2013.

[95] C. W. White *et al.*, "A whole blood-based perfusate provides superior preservation of myocardial function during ex vivo heart perfusion," (in eng), *J Heart Lung Transplant,* vol. 34, no. 1, pp. 113-21, Jan 2015.

[96] R. M. Dongaonkar, R. H. Stewart, C. M. Quick, K. L. Uray, C. S. Cox, Jr., and G. A. Laine, "Award article: Microcirculatory Society Award for Excellence in Lymphatic Research: time course of myocardial interstitial edema resolution and associated left ventricular dysfunction," (in eng), *Microcirculation (New York, N.Y. : 1994),* vol. 19, no. 8, pp. 714-722, 2012.

[97] R. Vanin Pinto Ribeiro *et al.*, "Perfusate Composition Significantly Affects Endothelial Function and Myocardial Preservation During *Ex situ* Heart Perfusion," *Circ Heart Fail (Submitted),* 2019.

[98] J. K. Sandha *et al.*, "Steroids Limit Myocardial Edema During Ex Vivo Perfusion of Hearts Donated After Circulatory Death," *Ann Thorac Surg,* vol. 105, no. 6, pp. 1763-1770, Jun 2018.

[99] A.-F. Popov *et al.*, "Utilization of the organ care system - a game-changer in combating donor organ shortage," (in eng), *Medical science monitor basic research,* vol. 21, pp. 29-32, 2015.

[100] S. Dhein, F. W. Mohr, and M. Delmar, *Practical methods in cardiovascular research*. Berlin ; New York: Springer, 2005, pp. xx, 1010 p., 16 p. of plates.

[101] K. Suehiro *et al.*, "Posttransplant function of a nonbeating heart is predictable by an ex vivo perfusion method," (in eng), *Ann Thorac Surg,* vol. 71, no. 1, pp. 278-83, Jan 2001.

[102] J. de Hart *et al.*, "An ex vivo platform to simulate cardiac physiology: a new dimension for therapy development and assessment," *Int J Artif Organs,* vol. 34, no. 6, pp. 495-505, Jun 2011.

[103] J. M. Abicht *et al.*, "Large-Animal Biventricular Working Heart Perfusion System with Low Priming Volume-Comparison between *in vivo* and ex vivo Cardiac Function," (in eng), *Thorac Cardiovasc Surg,* vol. 66, no. 1, pp. 71-82, Jan 2018.

[104] J. Bermejo *et al.*, "Diastolic chamber properties of the left ventricle assessed by global fitting of pressure-volume data: improving the gold standard of diastolic function," (in eng), *J Appl Physiol (1985),* vol. 115, no. 4, pp. 556-68, Aug 15 2013.

[105] S. Colah *et al.*, "Ex vivo perfusion of the swine heart as a method for pre-transplant assessment," (in eng), *Perfusion,* vol. 27, no. 5, pp. 408-13, Sep 2012.

[106] A. E. Wei, M. Y. Maslov, M. J. Pezone, E. R. Edelman, and M. A. Lovich, "Use of pressure-volume conductance catheters in real-time cardiovascular experimentation," (in eng), *Heart, lung & circulation,* vol. 23, no. 11, pp. 1059-1069, 2014.

[107] F. Seemann *et al.*, "Noninvasive Quantification of Pressure-Volume Loops From Brachial Pressure and Cardiovascular Magnetic Resonance," *Circ Cardiovasc Imaging,* vol. 12, no. 1, p. e008493, Dec 2019.

[108] C. Yerebakan *et al.*, "Pressure-volume loops: feasible for the evaluation of right ventricular function in an experimental model of acute pulmonary regurgitation?," *Interactive CardioVascular and Thoracic Surgery,* vol. 9, no. 2, pp. 163-168, 2009.

[109] J. Mathew and A. I. Dipchand, "Right Ventricular Dysfunction Post-Heart Transplantation," in *Right Ventricular Physiology, Adaptation and Failure in Congenital and Acquired Heart Disease*, M. K. Friedberg and A. N. Redington, Eds. Cham: Springer International Publishing, 2018, pp. 193-216.

[110] P. Van Trigt, H. B. Bittner, S. W. Kendall, and C. A. Milano, "Mechanisms of transplant right ventricular dysfunction," (in eng), *Annals of surgery,* vol. 221, no. 6, pp. 666-676, 1995.

[111] H. B. Bittner, E. P. Chen, S. S. Biswas, P. Van Trigt, III, and R. D. Davis, "Right ventricular dysfunction after cardiac transplantation: primarily related to status of donor heart," *The Annals of Thoracic Surgery,* vol. 68, no. 5, pp. 1605-1611, 1999.

[112] E. Sage *et al.*, "Real-Time Computed Tomography Highlights Pulmonary Parenchymal Evolution During Ex Vivo Lung Reconditioning," *Ann Thorac Surg,* vol. 103, no. 6, pp. e535-e537, Jun 2017.

[113] G. J. Pelgrim *et al.*, "Validation of myocardial perfusion quantification by dynamic CT in an ex-vivo porcine heart model," *Int J Cardiovasc Imaging,* vol. 33, no. 11, pp. 1821-1830, Nov 2017.

[114] G. M. Ruggeri *et al.*, "Description of a Novel Set-up for Functional Echocardiographic Assessment of Left Ventricular Performance During Ex Vivo Heart Perfusion," *Anesth Analg,* vol. 127, no. 3, pp. e36-e39, Sep 2018.

[115] G. Ruggeri, R. V. Pinto Ribeiro, B. Gellner, J. Qua Hiansen, M. Badiwala, and M. Meineri, "Echocardiographic Evaluation of Right Ventricular Function during Ex Vivo Heart Perfusion," *The Journal of Heart and Lung Transplantation,* vol. 37, no. 4, pp. S383-S384, 2018.

[116] C.-M. Yu, "Challenges and opportunity in the era of quantitative echocardiography," (in eng), *Echo research and practice,* vol. 4, no. 4, pp. E3-E6, 2017.

[117] L. Xin *et al.*, "Ees Estimation Using Machine Learning Approach during Ex Vivo Heart Perfusion to Predict Early Graft Survival: A Preliminary Study in Porcine Model," *The Journal of Heart and Lung Transplantation*, vol. 38, no. 4, p. S242, 2019.

[118] J. Kobayashi *et al.*, "PRESSURE-TARGETED PERFUSION IS THE OPTIMAL STRATEGY OF THE PEDIATRIC EX-VIVO HEART PERFUSION FOR DONATION AFTER CARDIAC DEATH IN PORCINE MODEL," *Canadian Journal of Cardiology*, vol. 34, no. 10, p. S177, 2018.

[119] S. Osaki, M. R. Locher, E. B. Lushaj, S. A. Akhter, and T. Kohmoto, "Functional evaluation of human donation after cardiac death donor hearts using a continuous isolated myocardial perfusion technique: Potential for expansion of the cardiac donor population," *The Journal of Thoracic and Cardiovascular Surgery*, vol. 148, no. 3, pp. 1123-1130, 2014.

[120] R. M. Bell, M. M. Mocanu, and D. M. Yellon, "Retrograde heart perfusion: the Langendorff technique of isolated heart perfusion," (in eng), *J Mol Cell Cardiol*, vol. 50, no. 6, pp. 940-50, Jun 2011.

[121] G. Heusch, "Heart rate in the pathophysiology of coronary blood flow and myocardial ischaemia: benefit from selective bradycardic agents," (in eng), *British journal of pharmacology*, vol. 153, no. 8, pp. 1589-1601, 2008.

[122] H. F. Kuecherer, A. Just, and H. Kirchheim, "Evaluation of aortic compliance in humans," (in eng), *Am J Physiol Heart Circ Physiol*, vol. 278, no. 5, pp. H1411-3, May 2000.

[123] E. S. DeWitt, K. J. Black, and J. N. Kheir, "Rodent Working Heart Model for the Study of Myocardial Performance and Oxygen Consumption," (in eng), *Journal of visualized experiments : JoVE*, no. 114, p. 54149, 2016.

[124] N. Westerhof, J. W. Lankhaar, and B. E. Westerhof, "The arterial Windkessel," *Med Biol Eng Comput*, vol. 47, no. 2, pp. 131-41, Feb 2009.

[125] M. S. Olufsen and A. Nadim, "- On deriving lumped models for blood flow and pressure in the systemic arteries," in *Computational Fluid and Solid Mechanics 2003*, K. J. Bathe, Ed. Oxford: Elsevier Science Ltd, 2003, pp. 1786-1789.

[126] O. Frank, *Die Grundform des arteriellen pulses. Erste Abhandlung. Mathematische Analyze*. Z Biol, 1899.

[127] K. Sagawa, R. K. Lie, and J. Schaefer, "Translation of Otto Frank's paper "Die Grundform des Arteriellen Pulses" Zeitschrift fur Biologie 37: 483-526 (1899)," (in eng), *J Mol Cell Cardiol*, vol. 22, no. 3, pp. 253-4, Mar 1990.

[128] C. C. Mei, J. Zhang, and H. X. Jing, "Fluid mechanics of Windkessel effect," *Med Biol Eng Comput*, vol. 56, no. 8, pp. 1357-1366, Aug 2018.

[129] M. Capoccia, "Development and Characterization of the Arterial Windkessel and Its Role During Left Ventricular Assist Device Assistance," (in eng), *Artif Organs,* vol. 39, no. 8, pp. E138-53, Aug 2015.

[130] S. Madhavan and E. M. C. Kemmerling, "The effect of inlet and outlet boundary conditions in image-based CFD modeling of aortic flow," *Biomed Eng Online,* vol. 17, no. 1, p. 66, May 30 2018.

[131] E. Wetterer, "Flow and pressure in the arterial system, their hemodynamic relationship, and the principles of their measurement," (in eng), *Minn Med,* vol. 37, no. 2, pp. 77-86; passim, Feb 1954.

[132] E. Wetterer, *Quantitative Beziehungen zwischen Stromstärke und Druck im natürlichen Kreislauf bei zeitlich variabler Elastizität des arteriellen Windkessels*. 2019.

[133] N. Westerhof, G. Elzinga, and P. Sipkema, "An artificial arterial system for pumping hearts," *J Appl Physiol,* vol. 31, no. 5, pp. 776-81, Nov 1971.

[134] N. Westerhof, N. Stergiopulos, and M. Noble, *Snapshots of Hemodynamics: An Aid for Clinical Research and Graduate Education*. 2005.

[135] N. Westerhof, F. Bosman, C. J. De Vries, and A. Noordergraaf, "Analog studies of the human systemic arterial tree," (in eng), *J Biomech,* vol. 2, no. 2, pp. 121-43, May 1969.

[136] P. Segers *et al.*, "Pulmonary arterial compliance in dogs and pigs: the three-element windkessel model revisited," *Am J Physiol,* vol. 277, no. 2, pp. H725-31, Aug 1999.

[137] N. Stergiopulos, J. J. Meister, and N. Westerhof, "Simple and accurate way for estimating total and segmental arterial compliance: the pulse pressure method," *Ann Biomed Eng,* vol. 22, no. 4, pp. 392-7, Jul-Aug 1994.

[138] J. P. Murgo, N. Westerhof, J. P. Giolma, and S. A. Altobelli, "Aortic input impedance in normal man: relationship to pressure wave forms," *Circulation,* vol. 62, no. 1, pp. 105-16, Jul 1980.

[139] N. Stergiopulos, B. E. Westerhof, and N. Westerhof, "Total arterial inertance as the fourth element of the windkessel model," (in eng), *Am J Physiol,* vol. 276, no. 1, pp. H81-8, Jan 1999.

[140] R. Burattini, G. J. M. Gnudi, B. Engineering, and Computing, "Computer identification of models for the arterial tree input impedance: Comparison between two new simple models and first experimental results," journal article vol. 20, no. 2, pp. 134-144, March 01 1982.

[141] A. Noordergraaf, D. Verdouw, and H. B. Boom, "The use of an analog computer in a circulation model," (in eng), *Prog Cardiovasc Dis,* vol. 5, pp. 419-39, Mar 1963.

[142] P. Segers *et al.*, "Three- and four-element Windkessel models: assessment of their fitting performance in a large cohort of healthy middle-aged individuals," (in eng), *Proc Inst Mech Eng H,* vol. 222, no. 4, pp. 417-28, May 2008.

[143] B. Lambermont *et al.*, "Comparison between three- and four-element Windkessel models to characterize vascular properties of pulmonary circulation," (in eng), *Arch Physiol Biochem,* vol. 105, no. 7, pp. 625-32, Dec 1997.

[144] S. Zhou *et al.*, "A review on low-dimensional physics-based models of systemic arteries: application to estimation of central aortic pressure," *Biomed Eng Online,* vol. 18, no. 1, p. 41, Apr 2 2019.

[145] A. Quarteroni, S. Ragni, and A. Veneziani, *Coupling between lumped and distributed models for blood flow problems*. 2001, pp. 111-124.

[146] I. Kokalari, *Review on lumped parameter method for modeling the blood flow in systemic arteries*. 2013, pp. 92-99.

[147] V. Milisic and A. Quarteroni, *Analysis of lumped parameter models for blood flow simulations and their relation with 1D models*. 2004.

[148] G. Zhang, J.-O. Hahn, and R. Mukkamala, "Tube-load model parameter estimation for monitoring arterial hemodynamics," *Frontiers in physiology,* vol. 2, p. 72Accessed on: 2011. doi: 10.3389/fphys.2011.00072

[149] J.-O. Hahn, A. T. Reisner, and H. H. Asada, "Blind Identification of Two-Channel IIR Systems With Application to Central Cardiovascular Monitoring," *Journal of Dynamic Systems, Measurement, and Control,* vol. 131, no. 5, pp. 051009-051009-15, 2009.

[150] G. Zhang, M. Gao, and R. Mukkamala, "Robust, beat-to-beat estimation of the true pulse transit time from central and peripheral blood pressure or flow waveforms using an arterial tube-load model," (in eng), *Conf Proc IEEE Eng Med Biol Soc,* vol. 2011, pp. 4291-4, 2011.

[151] R. Burattini and K. B. Campbell, "Modified asymmetric T-tube model to infer arterial wave reflection at the aortic root," (in eng), *IEEE Trans Biomed Eng,* vol. 36, no. 8, pp. 805-14, Aug 1989.

[152] K. B. Campbell, R. Burattini, D. L. Bell, R. D. Kirkpatrick, and G. G. Knowlen, "Time-domain formulation of asymmetric T-tube model of arterial system," (in eng), *Am J Physiol,* vol. 258, no. 6 Pt 2, pp. H1761-74, Jun 1990.

[153] Y. Shi, P. Lawford, and R. Hose, "Review of Zero-D and 1-D Models of Blood Flow in the Cardiovascular System," *BioMedical Engineering OnLine,* vol. 10, no. 1, p. 33, 2011/04/26 2011.

[154] H. Liu *et al.*, "Multi-scale modeling of hemodynamics in the cardiovascular system," *Acta Mechanica Sinica,* vol. 31, no. 4, pp. 446-464, 2015/08/01 2015.

[155] M. Khalife, A. Decoene, F. Caetano, L. de Rochefort, E. Durand, and D. Rodriguez, "Estimating absolute aortic pressure using MRI and a one-dimensional model," (in eng), *J Biomech,* vol. 47, no. 13, pp. 3390-9, Oct 17 2014.

[156] A. R. Ghigo, J.-M. Fullana, and P.-Y. Lagrée, "A 2D nonlinear multiring model for blood flow in large elastic arteries," *Journal of Computational Physics,* vol. 350, pp. 136-165, 2017/12/01/ 2017.

[157] V. Casulli, M. Dumbser, and E. F. Toro, "Semi-implicit numerical modeling of axially symmetric flows in compliant arterial systems," (in eng), *Int J Numer Method Biomed Eng,* vol. 28, no. 2, pp. 257-72, Feb 2012.

[158] K. Perktold, R. O. Peter, M. Resch, and G. Langs, "Pulsatile non-newtonian blood flow in three-dimensional carotid bifurcation models: a numerical study of flow phenomena under different bifurcation angles," *Journal of Biomedical Engineering,* vol. 13, no. 6, pp. 507-515, 1991/11/01/ 1991.

[159] D. A. Steinman and C. A. Taylor, "Flow imaging and computing: large artery hemodynamics," (in eng), *Ann Biomed Eng,* vol. 33, no. 12, pp. 1704-9, Dec 2005.

[160] J. S. Milner, J. A. Moore, B. K. Rutt, and D. A. Steinman, "Hemodynamics of human carotid artery bifurcations: computational studies with models reconstructed from magnetic resonance imaging of normal subjects," (in eng), *J Vasc Surg,* vol. 28, no. 1, pp. 143-56, Jul 1998.

[161] G. Elzinga and N. Westerhof, "The pumping ability of the left heart and the effect of coronary occlusion," *Circ Res,* vol. 38, no. 4, pp. 297-302, Apr 1976.

[162] K. Sunagawa, W. L. Maughan, and K. Sagawa, "Optimal arterial resistance for the maximal stroke work studied in isolated canine left ventricle," (in eng), *Circ Res,* vol. 56, no. 4, pp. 586-95, Apr 1985.

[163] W. J Paulus, V. Claes, and D. Brutsaert, *Physiological pump loading of isolated cardiac muscle*. 1976, pp. 67-74.

[164] N. Ishide *et al.*, "Effects of changes in the aortic input impedance on systolic pressure-ejected volume relationships in the isolated supported canine left ventricle," (in eng), *Cardiovasc Res,* vol. 14, no. 4, pp. 229-43, Apr 1980.

[165] E. O. Kung, A. S. Les, F. Medina, R. B. Wicker, M. V. McConnell, and C. A. Taylor, "In vitro validation of finite-element model of AAA hemodynamics incorporating realistic outlet boundary conditions," (in eng), *J Biomech Eng,* vol. 133, no. 4, p. 041003, Apr 2011.

[166] E. O. Kung and C. A. Taylor, "Development of A Physical Windkessel Module to Re-Create In-Vivo Vascular Flow Impedance for In-Vitro Experiments," (in eng), *Cardiovascular engineering and technology,* vol. 2, no. 1, pp. 2-14, 2011.

[167] D. K. Hildebrand, Z. J. Wu, J. E. Mayer, Jr., and M. S. Sacks, "Design and hydrodynamic evaluation of a novel pulsatile bioreactor for biologically active heart valves," *Ann Biomed Eng,* vol. 32, no. 8, pp. 1039-49, Aug 2004.

[168] K. Dumont *et al.*, "Design of a new pulsatile bioreactor for tissue engineered aortic heart valve formation," *Artif Organs,* vol. 26, no. 8, pp. 710-4, Aug 2002.

[169] D. L. Timms, S. D. Gregory, M. C. Stevens, and J. F. Fraser, "Haemodynamic modeling of the cardiovascular system using mock circulation loops to test cardiovascular devices," (in eng), *Conf Proc IEEE Eng Med Biol Soc,* vol. 2011, pp. 4301-4, 2011.

[170] D. Timms, M. Hayne, K. McNeil, and A. Galbraith, "A complete mock circulation loop for the evaluation of left, right, and biventricular assist devices," (in eng), *Artif Organs,* vol. 29, no. 7, pp. 564-72, Jul 2005.

[171] M. C. Stevens *et al.*, "In vitro and *in vivo* characterization of three different modes of pump operation when using a left ventricular assist device as a right ventricular assist device," (in eng), *Artif Organs,* vol. 38, no. 11, pp. 931-9, Nov 2014.

[172] B. C. Ng, M. Kleinheyer, P. A. Smith, D. Timms, W. E. Cohn, and E. Lim, "Pulsatile operation of a continuous-flow right ventricular assist device (RVAD) to improve vascular pulsatility," (in eng), *PLoS One,* vol. 13, no. 4, p. e0195975, 2018.

[173] S. Konduri, Y. Xing, J. N. Warnock, Z. He, and A. P. Yoganathan, "Normal physiological conditions maintain the biological characteristics of porcine aortic heart valves: an ex vivo organ culture study," *Ann Biomed Eng,* vol. 33, no. 9, pp. 1158-66, Sep 2005.

[174] B. J. Tefft *et al.*, "Cardiac Valve Bioreactor for Physiological Conditioning and Hydrodynamic Performance Assessment," *Cardiovasc Eng Technol,* vol. 10, no. 1, pp. 80-94, Mar 2019.

[175] A. Kaasi, I. A. Cestari, N. A. Stolf, A. A. Leirner, O. Hassager, and I. N. Cestari, "A new approach to heart valve tissue engineering: mimicking the heart ventricle with a ventricular assist device in a novel bioreactor," *J Tissue Eng Regen Med,* vol. 5, no. 4, pp. 292-300, Apr 2011.

[176] J. R. Pohlmann, J. M. Toomasian, C. E. Hampton, K. E. Cook, G. M. Annich, and R. H. Bartlett, "The relationships between air exposure, negative pressure, and hemolysis," (in eng), *Asaio j,* vol. 55, no. 5, pp. 469-73, Sep-Oct 2009.

[177] A. M. Leopaldi *et al.*, "A novel passive left heart platform for device testing and research," *Med Eng Phys,* vol. 37, no. 4, pp. 361-6, Apr 2015.

[178] L. Xin *et al.*, "Primed Left Ventricle Heart Perfusion Creates Physiological Aortic Pressure in Porcine Hearts," vol. Online First, 2019

[179] V. L. Roger *et al.*, "Heart disease and stroke statistics—2012 update," *Circulation,* vol. 125, no. 1, pp. e2-e220, 2012.

[180] H.-G. Zimmer, "The isolated perfused heart and its pioneers," *Physiology,* vol. 13, no. 4, pp. 203-210, 1998.

[181] A. Iyer *et al.*, "Primary graft failure after heart transplantation," *Journal of transplantation,* vol. 2011, 2011.

[182] R. A. Jonas *et al.*, "The influence of hemodilution on outcome after hypothermic cardiopulmonary bypass: results of a randomized trial in infants," *The Journal of thoracic and cardiovascular surgery,* vol. 126, no. 6, pp. 1765-1774, 2003.

[183] J. W. Newburger *et al.*, "Randomized trial of hematocrit 25% versus 35% during hypothermic cardiopulmonary bypass in infant heart surgery," *The Journal of thoracic and cardiovascular surgery,* vol. 135, no. 2, pp. 347-354. e4, 2008.

[184] D. Abraham and L. Mao, "Cardiac pressure-volume loop analysis using conductance catheters in mice," *Journal of visualized experiments: JoVE,* no. 103, 2015.

[185] R. M. Lang *et al.*, "Recommendations for cardiac chamber quantification by echocardiography in adults: an update from the American Society of Echocardiography and the European Association of Cardiovascular Imaging," *European Heart Journal-Cardiovascular Imaging,* vol. 16, no. 3, pp. 233-271, 2015.

[186] H. T. Tevaearai Stahel, A. Zuckermann, T. P. Carrel, and S. L. Longnus, "Hearts Not Dead after Circulatory Death," (in eng), *Frontiers in surgery,* vol. 2, pp. 46-46, 2015.

[187] L. Xin *et al.*, "A New Multi-Mode Perfusion System for Ex Vivo Heart Perfusion Study," *J Med Syst,* vol. 42, no. 2, p. 25, Dec 23 2017.

[188] R. T. Dowell and A. A. Houdi, "Aortic peak flow velocity as an index of myocardial contractility in the conscious rat," (in eng), *Methods Find Exp Clin Pharmacol,* vol. 19, no. 8, pp. 533-9, Oct 1997.

[189] M. I. Bolton, *Advances in Swine in Biomedical Research. Edited by M. E. Tumbleson and L. B. Schook. Plenum Publishing Corporation, 1996. Volume 1* (Experimental Physiology, no. 4). 1997.

[190] G. N. Cattermole *et al.*, "The normal ranges of cardiovascular parameters measured using the ultrasonic cardiac output monitor," *Physiol Rep,* vol. 5, no. 6, Mar 2017.

[191] N. A. Mortensen, F. Okkels, and H. Bruus, "Reexamination of Hagen-Poiseuille flow: shape dependence of the hydraulic resistance in microchannels," (in eng), *Phys Rev E Stat Nonlin Soft Matter Phys,* vol. 71, no. 5 Pt 2, p. 057301, May 2005.

[192] S. A. Jones, "A relationship between reynolds stresses and viscous dissipation: Implications to red cell damage," *Annals of Biomedical Engineering,* vol. 23, no. 1, pp. 21-28, 1995/01/01 1995.

[193] B. R. Munson, T. H. Okiishi, and W. W. Huebsch, *Fundamentals of fluid mechanics*, 6th ed. Hoboken, NJ: J. Wiley & Sons, 2009.

[194] S. C. Koenig *et al.*, "Human, bovine and porcine systematic vascular input impedances are not equivalent: implications for device testing and xenotransplantation in heart failure," *J Heart Lung Transplant,* vol. 27, no. 12, pp. 1340-7, Dec 2008.

[195] D. K. Arnett *et al.*, "Blood pressure and arterial compliance in young adults: the Minnesota Children's Blood Pressure Study," *Am J Hypertens,* vol. 14, no. 3, pp. 200-5, Mar 2001.

[196] P. Tozzi, A. Corno, and D. Hayoz, "Definition of arterial compliance," *American Journal of Physiology-Heart and Circulatory Physiology,* vol. 278, no. 4, pp. H1407-H1407, 2000/04/01 2000.

[197] N. Stergiopulos, J. J. Meister, and N. Westerhof, "Scatter in input impedance spectrum may result from the elastic nonlinearity of the arterial wall," (in eng), *Am J Physiol,* vol. 269, no. 4 Pt 2, pp. H1490-5, Oct 1995.

[198] J. L. Hebert, Y. Lecarpentier, K. Zamani, C. Coirault, G. Daccache, and D. Chemla, "Relation between aortic dicrotic notch pressure and mean aortic pressure in adults," (in eng), *Am J Cardiol,* vol. 76, no. 4, pp. 301-6, Aug 1 1995.

[199] J. T. Church *et al.*, "Normothermic Ex Vivo Heart Perfusion: Effects of Live Animal Blood and Plasma Cross Circulation," *ASAIO J,* vol. 63, no. 6, pp. 766-773, Nov/Dec 2017.

[200] E. B. Friedrich and M. Bohm, "Management of end stage heart failure," *Heart,* vol. 93, no. 5, pp. 626-31, May 2007.

[201] L. H. Lund *et al.*, "The Registry of the International Society for Heart and Lung Transplantation: Thirty-second Official Adult Heart Transplantation Report--2015; Focus Theme: Early Graft Failure," (in eng), *J Heart Lung Transplant,* vol. 34, no. 10, pp. 1244-54, Oct 2015.

[202] M. R. Shah, R. C. Starling, L. Schwartz Longacre, M. R. Mehra, and P. Working Group, "Heart transplantation research in the next decade--a goal to achieving evidence-based outcomes: National Heart, Lung, And Blood Institute Working Group," *J Am Coll Cardiol,* vol. 59, no. 14, pp. 1263-9, Apr 3 2012.

[203] S. J. Messer *et al.*, "Functional assessment and transplantation of the donor heart after circulatory death," (in eng), *J Heart Lung Transplant,* vol. 35, no. 12, pp. 1443-1452, Dec 2016.

[204] D. H. Freed and C. W. White, "Donor heart preservation: straight up, or on the rocks?," *The Lancet,* vol. 385, no. 9987, pp. 2552-2554, 2015.

[205] R. Ribeiro *et al.*, "Contractility versus Metabolic Cardiac Assessment during *Ex situ* Heart Perfusion: A Pre-Clinical Transplant Study," *The Journal of Heart and Lung Transplantation,* vol. 38, no. 4, p. S240, 2019.

[206] M. V. Badiwala *et al.*, "Donor pretreatment with hypertonic saline attenuates primary allograft dysfunction: a pilot study in a porcine model," *Circulation,* vol. 120, no. 11 Suppl, pp. S206-14, Sep 15 2009.

[207] R. V. P. Ribeiro *et al.*, "A Pre-Clinical Porcine Model of Orthotopic Heart Transplantation," *J Vis Exp,* no. 146, Apr 27 2019.

[208] D. T. Mason, E. Braunwald, J. W. Covell, E. H. Sonnenblick, and J. Ross, Jr., "Assessment of cardiac contractility. The relation between the rate of pressure rise and ventricular pressure during isovolumic systole," (in eng), *Circulation,* vol. 44, no. 1, pp. 47-58, Jul 1971.

[209] R. M. Lang, K. M. Borow, A. Neumann, and D. Janzen, "Systemic vascular resistance: an unreliable index of left ventricular afterload," *Circulation,* vol. 74, no. 5, pp. 1114-23, Nov 1986.

[210] D. D. Glower *et al.*, "Linearity of the Frank-Starling relationship in the intact heart: the concept of preload recruitable stroke work," (in eng), *Circulation,* vol. 71, no. 5, pp. 994-1009, May 1985.

[211] H. Gasparovic *et al.*, "Pretransplant and perioperative predictors of early heart transplantation outcomes," *Croat Med J,* vol. 55, no. 6, pp. 553-61, Dec 2014.

[212] J. B. Ryan *et al.*, "The preload recruitable stroke work relationship as a measure of left ventricular contractile dysfunction in porcine cardiac allografts," (in eng), *Eur J Cardiothorac Surg,* vol. 22, no. 5, pp. 738-45, Nov 2002.

[213] J. A. Tallaj *et al.*, "Post-heart transplant diastolic dysfunction is a risk factor for mortality," (in eng), *J Am Coll Cardiol,* vol. 50, no. 11, pp. 1064-9, Sep 11 2007.

[214] D. R. Warriner *et al.*, "Closing the loop: modelling of heart failure progression from health to end-stage using a meta-analysis of left ventricular pressure-volume loops," (in eng), *PLoS One,* vol. 9, no. 12, p. e114153, 2014.

[215] J. Beuth, F. Falter, R. V. Pinto Ribeiro, M. Badiwala, and M. Meineri, "New Strategies to Expand and Optimize Heart Donor Pool: Ex Vivo Heart Perfusion and Donation After Circulatory Death: A Review of Current Research and Future Trends," *Anesth Analg,* vol. 128, no. 3, pp. 406-413, Mar 2019.

[216] S. Au - Hatami *et al.*, "Normothermic *Ex situ* Heart Perfusion in Working Mode: Assessment of Cardiac Function and Metabolism," *JoVE,* no. 143, p. e58430, 2019/01/12/ 2019.

[217] B. Herrera *et al.*, "Paradoxical effects of temperature on vascular tone," (in eng), *Cryobiology,* vol. 41, no. 1, pp. 43-50, Aug 2000.

Appendix A: Supplemental Data for Chapter 5

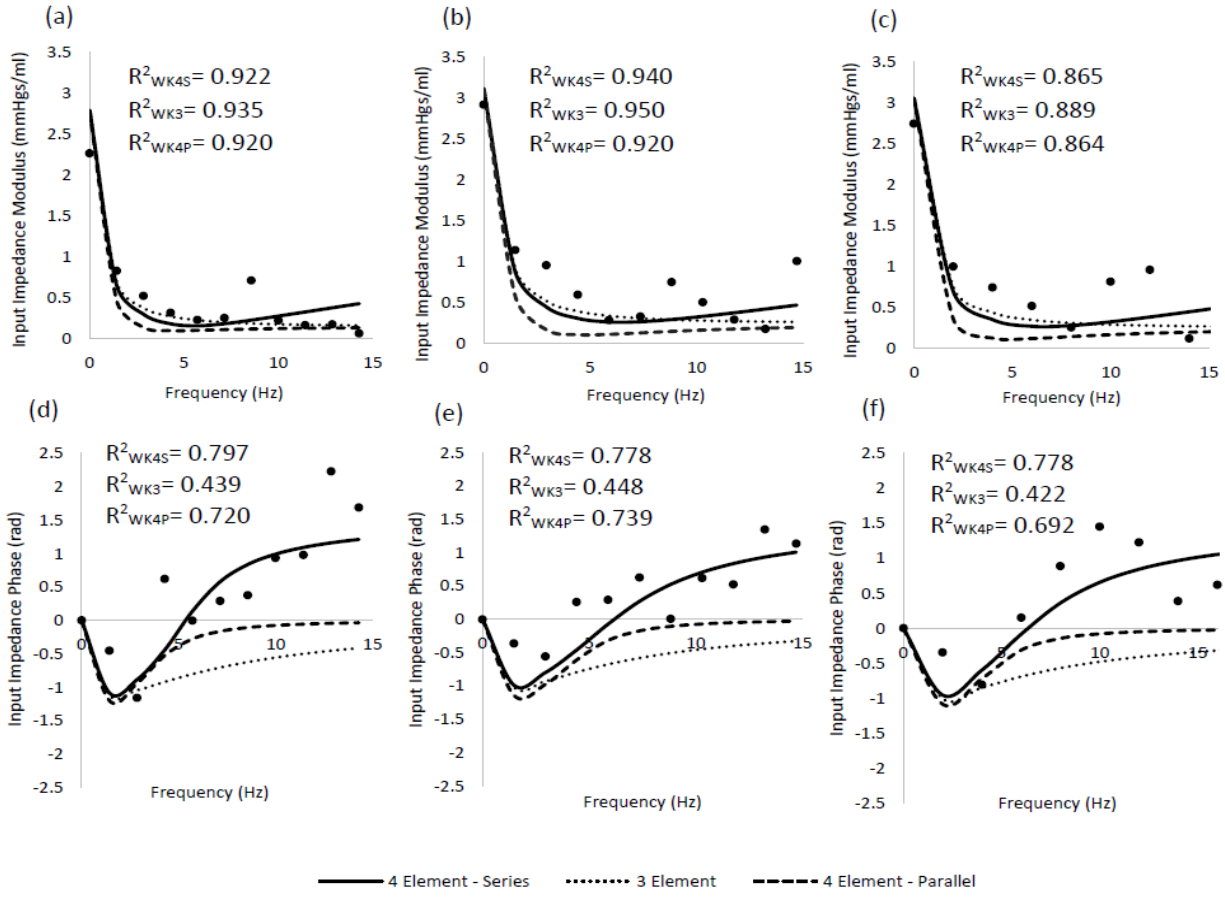

Figure A-7-1: a), b), c) The comparison, at the 6-hour time point, of measured and theoretical input impedance moduli for the three tested ex situ hearts. Theoretical curves are included for the 4 element Windkessel with the inductance in series with peripheral resistance (WK4S), the 3 element Windkessel (WK3) and the 4 element Windkessel with the inductance in parallel with peripheral resistance (WK4P). d), e), f) The comparison, at the 6-hour time point, of measured and theoretical input impedance phase for the three tested ex situ hearts. Theoretical curves are included for the 4 element Windkessel with the inductance in series with peripheral resistance (WK4S), the 3 element Windkessel (WK3) and the 4 element Windkessel with the inductance in parallel with peripheral resistance (WK4P)

Appendix B: Supplemental Data for Chapter 6

Shown in *Figure* are the contractile parameters measured post transplantation for the 5 DBD hearts and 5 DCD hearts. No statistically significant differences between groups are observed.

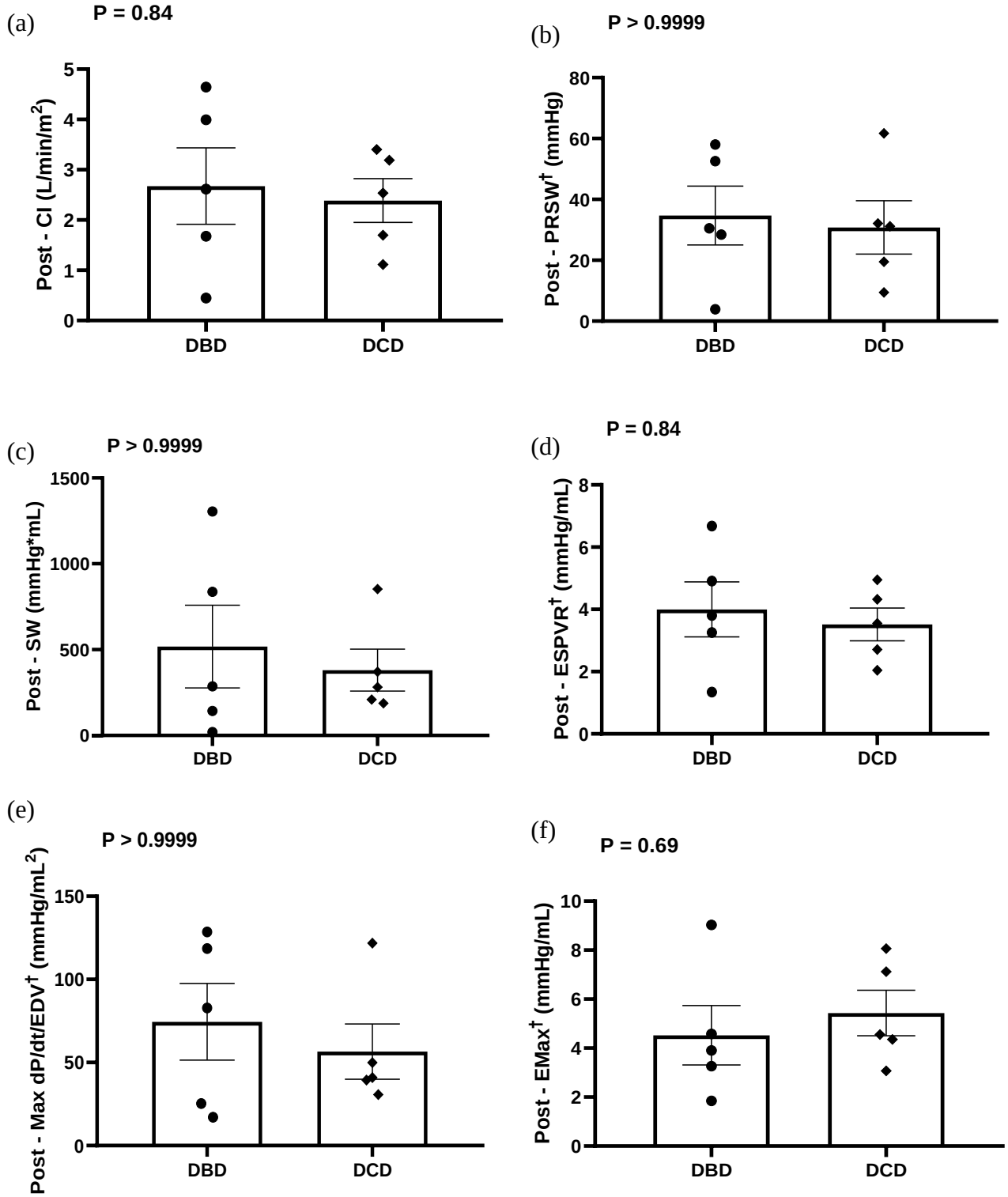

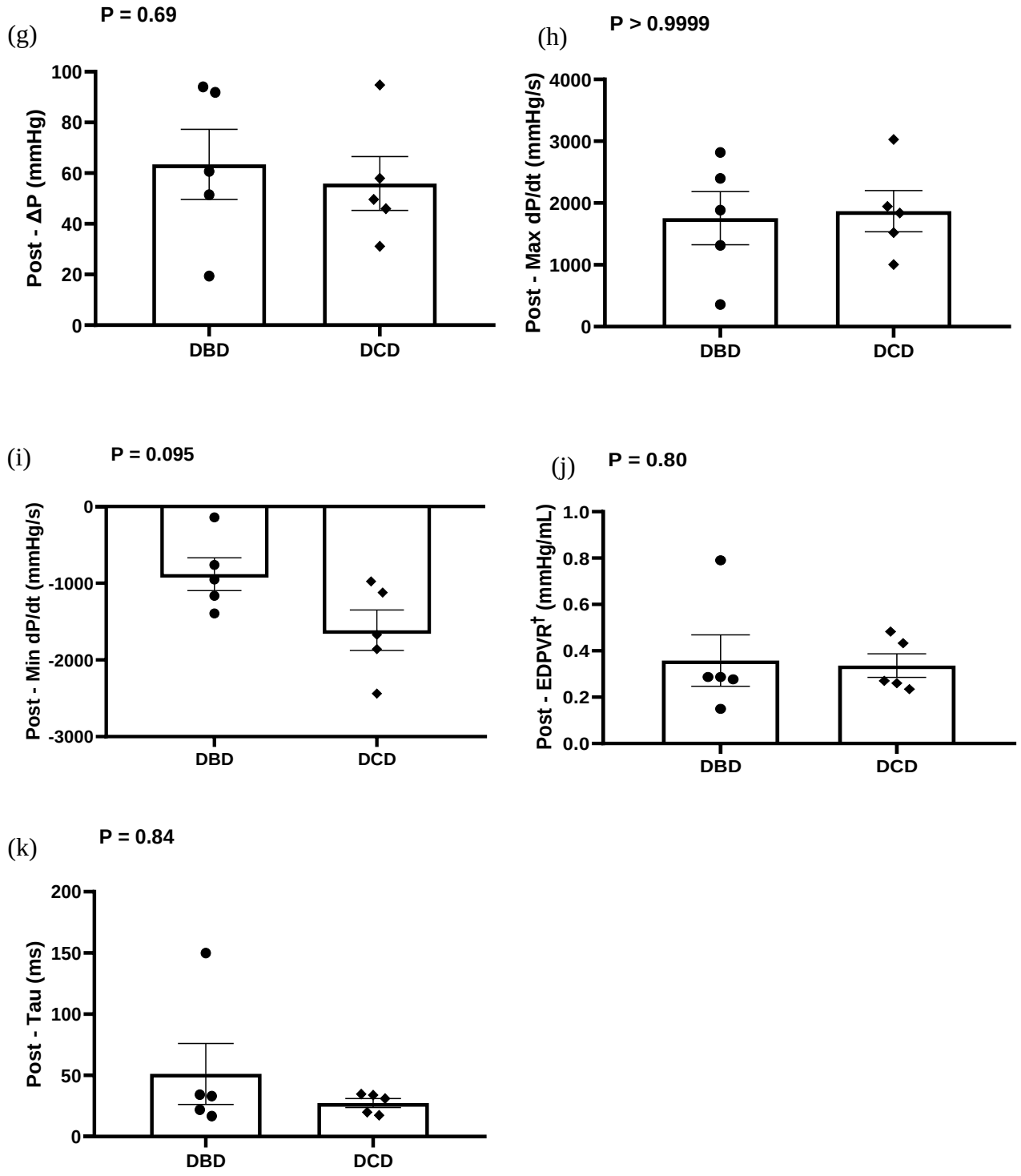

Figure B-1: Comparison of contractile parameters post transplantation between DBD and DCD hearts plotted with error bars representing the standard error of the mean for: a) Post - CI b) PRSW c) Post - SW d) Post - ESPVR e) Post - Max dP/dt/EDV f) Post - EMax g) Post - ΔP h) Post - Max dP/dt i) Post - Min dP/dt j) Post - EDPVR and k) Post - Tau

Appendix C: Matlab Code for Chapter 6

Contained herein is the Matlab script used in the control volume analysis described in Chapter 7 for non-invasive analysis of left ventricular contractile function. The script works by reading pressures and volumes supplied by the user, transforming them into aligned arrays and performing the necessary calculations for each individual parameter across each heartbeat. Parameter data are then averaged across all heartbeats with data stored in an output matrix.

```
clc;
close all;
clearvars;
colour=hsv;
warning('off','MATLAB:polyfit:RepeatedPointsOrRescale')

prompt = 'LV(enter 1) or RV(enter 2)or both(enter 3)?';
model = input(prompt);

prompt = 'RA Loaded? (enter 1 for no, 2 for yes)';
loadmodel = input(prompt);

if model ==1 || model == 3
    prompt = 'What is the initial Volume of the LV?';
    LVinitialvolume = input(prompt);
end

if model ==2 || model == 3
    prompt = 'What is the initial Volume of the RV?';
    RVinitialvolume = input(prompt);
end


%%get input data. Will measure them seperately with Different timescales and
store in file!%%
timeread = xlsread('Source_for_PV.xlsx', 'A:A');
LVpressure = xlsread('Source_for_PV.xlsx', 'B:B');
Aoflow = xlsread('Source_for_PV.xlsx', 'C:C');
PAflow = xlsread('Source_for_PV.xlsx', 'D:D');
LAflow = xlsread('Source_for_PV.xlsx', 'E:E');

if loadmodel ==2
    RAflowread = xlsread('Source_for_PV.xlsx', 'F:F');
else
    RAflow = zeros(1, max(size(Aoflow)));
end

if model == 2 || model ==3
    RVpressure = xlsread('Source_for_R_and_C_Solver.xlsx', 'G:G');
end

%make time the same size as the rest%

time = zeros(1, max(size(Aoflow)));
```

```
for i = 1: max(size(Aoflow))
    time(i) = timeread(i);
end

%make sure Ao and Coronary outflow equal LA inflow allowing for 5% error %
minaof = min(Aoflow);

if abs(mean(LAflow)+ mean(PAflow)-mean(RAflow)+
mean(Aoflow))>(0.05*mean(LAflow))

    %first try and rezero Aoflow%
    for i=1:max(size(Aoflow))
        Aoflow(i) = Aoflow(i)- minaof;
    end

    %check if it worked. If not, add the difference to Aoflow and force it
to%
    if abs(mean(LAflow)+ mean(PAflow)-mean(RAflow) +
mean(Aoflow))>(0.05*mean(LAflow))

        for i=1:max(size(Aoflow))
            Aoflow(i) = Aoflow(i) - (mean(LAflow)+ mean(PAflow)+
mean(Aoflow));
        end

    end
end

%Calculate LV Volume at every time point. Do the same for LA and RA input
volumes for later. No initial volumes yet%

LVVolume = zeros(1, max(size(Aoflow)));
LAVolume = zeros(1, max(size(Aoflow)));
RAVolume = zeros(1, max(size(Aoflow)));
timestep = 0.02;

for i=1:max(size(Aoflow))
    if i==1
        LVVolume(i)=((1000/60)*timestep*((-1)*LAflow(i) - Aoflow(i) -
PAflow(i)+ RAflow(i)));
        RVVolume(i) = ((1000/60)*timestep*((-1)*RAflow(i)-PAflow(i)+(-
1_)*LAflow(i)-Aoflow(i);
        LAVolume(i) = (1000/60)*timestep*((-1)*LAflow(i));
        RAVolume(i) = (1000/60)*timestep*((-1)*RAflow(i));
        %RAVolume(i) =
    else
        LVVolume(i) = LVVolume(i-1)+((1000/60)*timestep*((-1)*LAflow(i) -
Aoflow(i) - PAflow(i)+ RAflow(i)));
        RVVolume(i) = RVVolume(i-1)+ RVVolume(i) = ((1000/60)*timestep*((-
1)*RAflow(i)-PAflow(i)+(-1_)*LAflow(i)-Aoflow(i);
        LAVolume(i) = LAVolume(i-1)+(1000/60)*timestep*((-1)*LAflow(i));
        RAVolume(i) = LAVolume(i-1)+(1000/60)*timestep*((-1)*LAflow(i));
    end

end
```

```
%find index for first volume maximum. Align that with the start of systole
found in LVP%

for i=5:(max(size(Aoflow))-3)

    %find the first maximum LV volume. This will be what is used to seperate
loops%
    if LVVolume(i)>LVVolume(i-1)&& LVVolume(i)>LVVolume(i-2) &&
LVVolume(i)>LVVolume(i-3)&&LVVolume(i)>LVVolume(i+1)&&
LVVolume(i)>LVVolume(i+2) && LVVolume(i)>LVVolume(i+3)
        firsthighvol=i;
        break
    end

    if model ==2||model==3
        if RVVolume(i)>RVVolume(i-1)&& RVVolume(i)>RVVolume(i-2) &&
RVVolume(i)>RVVolume(i-3)&&RVVolume(i)>RVVolume(i+1)&&
RVVolume(i)>RVVolume(i+2) && RVVolume(i)>RVVolume(i+3)
            firsthighrvvol=i;
            break
        end
    end

end


for i=5:max(size(Aoflow))

    %find the first sharp pressure rise. This will be lined up with the first
minimum flow to align loops. marked by a 10 fold pressure increase over 0.04
seconds%
    if  LVpressure(i) > 10*abs(LVpressure(i-2))
        startsys=i-1;
        break
    end

    if model ==2||model==3

        if  RVpressure(i) > 10*abs(RVpressure(i-2))
            startrvsys=i-1;
            break
        end
    end

end

minvol = min(LVVolume);
minrvvol = min(RVVolume);

%Start loop 1 at the first volume minimum and the first pressure
minimum.%Line them up. change lowvolindex to match. shift so all volumes are
positive%
for i=1:max(size(LVVolume))-firsthighvol+1
```

```
    if minvol < 0
        LVVolume(i) = LVVolume(i+ firsthighvol-1)-minvol;
    else
    LVVolume(i) = LVVolume(i+ firsthighvol-1);
    end

    if model ==2||model==3
        if minvol < 0
            RVVolume(i) = RVVolume(i+ firsthighrvvol-1)-minrvvol;
        else
            RVVolume(i) = RVVolume(i+ firsthighrvvol-1);
        end
    end

end

for i=1:(max(size(LVpressure))-startsys+1)
    LVpressure(i) = LVpressure(i+ startsys-1);
    if model ==2||model==3
end

%Normalize Volumes to Cardiac output%

%find all the minimum volume indicies. This will be used to find stroke
volumes. Must be done after volume start is found%

highvolindex(1)=1;
j=2;
for i=6:(max(size(Aoflow))-5)

    if LVVolume(i)>LVVolume(i-1)&& LVVolume(i)>LVVolume(i-2) &&
LVVolume(i)>LVVolume(i-3)&& LVVolume(i)>LVVolume(i-4) &&
LVVolume(i)>LVVolume(i-5)&& LVVolume(i)>LVVolume(i+1)&&
LVVolume(i)>LVVolume(i+2) && LVVolume(i)>LVVolume(i+3)&&
LVVolume(i)>LVVolume(i+4) && LVVolume(i)>LVVolume(i+5)
        highvolindex(j)=i;
        j=j+1;
    end
end

k=1;
for i=6:(max(size(Aoflow))-5)

    if LVVolume(i)<LVVolume(i-1)&& LVVolume(i)<LVVolume(i-2) &&
LVVolume(i)<LVVolume(i-3)&& LVVolume(i)<LVVolume(i-4) &&
LVVolume(i)<LVVolume(i-5)&& LVVolume(i)<LVVolume(i+1)&&
LVVolume(i)<LVVolume(i+2) && LVVolume(i)<LVVolume(i+3)&&
LVVolume(i)<LVVolume(i+4) && LVVolume(i)<LVVolume(i+5)
        lowvolindex(k)=i;
        k=k+1;
    end
end

if size(lowvolindex)~= size(highvolindex)
    disp(size(lowvolindex))
```

```
    disp(size(highvolindex))
end

%calculate the number of beats%

beatnum = min(max(size(highvolindex)),max(size(lowvolindex)));


%Calculate the average measured stroke volume%
sumstrokevolume = 0;
for i=1:beatnum
    sumstrokevolume = sumstrokevolume + LVVolume(highvolindex(i))-
LVVolume(lowvolindex(i));
end

averagestrokevolume = sumstrokevolume/beatnum;

%calculate the true average stroke volume and the ratio between estimated and
true average%
trueaveragestrokevolume = max(LAVolume)/beatnum;

correctionratio = trueaveragestrokevolume/averagestrokevolume;

%Adjust to correct and add initial volume%
for i=1:max(size(LVVolume))
    LVVolume(i) = LVVolume(i)*correctionratio+LVinitialvolume;
end

%%Find Parameters for each loop. Start of systole is found at lowvolindex.
Need to find end systole and start and end of diastole%%

%%start systole is end diastole for our purposes. Indexed by highvolindex%

%start diastole is tracked by min pressure indicies%

%% end systole is when pressure levels off. Say 2 consecutive drops%%

counter = 1;
i=3;
endsys = zeros(1,beatnum);

while counter < max(size(highvolindex))-1
   if  LVpressure(i) < LVpressure(i-1) && LVpressure(i-1)<LVpressure(i-2) &&
LVpressure(i) > 20
       endsys(counter)=i-2;
       %%move to next beat at start of systole%%

       i = highvolindex(counter+1);
       counter = counter+1;
   else
       i=i+1;
   end
end

heartrate = 60*beatnum/time(max(highvolindex));
```

```
% Calculate LV Parameters%


%Pre-allocating space%%

enddiastolicpressure = zeros(1,beatnum-1);
enddiastolicvolume = zeros(1,beatnum-1);
endsysstolicvolume = zeros(1,beatnum-1);
endsysstolicpressure= zeros(1,beatnum-1);
begindiastolicpressure= zeros(1,beatnum-1);
begindiastolicvolume= zeros(1,beatnum-1);
MinVolume= zeros(1,beatnum-1);
MaxVolume = zeros(1,beatnum-1);
StrokeVolume= zeros(1,beatnum-1);
EjectionFraction = zeros(1,beatnum-1);
contractiontime = zeros(1,beatnum-1);
relaxationtime = zeros(1,beatnum-1);
systolicejectionperiod= zeros(1,beatnum-1);
diastollicfillingperiod = zeros(1,beatnum-1);
CardiacOutput = zeros(1,beatnum-1);
StrokeWork = zeros(1,beatnum-1);
MindPdt = zeros(1,beatnum-1);
MaxdPdt = zeros(1,beatnum-1);
MaxPressure = zeros(1,beatnum-1);
MinPressure = zeros(1,beatnum-1);
MeanSystolicPressure = zeros(1,beatnum-1);
MeanDiastolicPressure = zeros(1,beatnum-1);
DevelopedPressure = zeros(1, beatnum-1);
ContractilityIndex = zeros(1, beatnum-1);
Tau = zeros(1, beatnum-1);
MaximumVentricularPower= zeros(1, beatnum-1);
EffectiveArterialElastance= zeros(1, beatnum-1);
minsmoothed = zeros(1,beatnum-1);

for LoopCount = 1: beatnum-1

    enddiastolicpressure(LoopCount) = LVpressure(highvolindex(LoopCount));
    enddiastolicvolume(LoopCount) = LVVolume(highvolindex(LoopCount));
    endsysstolicvolume(LoopCount) = LVVolume(endsys(LoopCount));
    endsysstolicpressure(LoopCount) = LVpressure(endsys(LoopCount));
    begindiastolicpressure(LoopCount) = LVpressure(lowvolindex(LoopCount));
    begindiastolicvolume(LoopCount) = LVVolume(lowvolindex(LoopCount));
    MinVolume(LoopCount) = LVVolume(lowvolindex(LoopCount));
    MaxVolume(LoopCount) = LVVolume(highvolindex(LoopCount));
    StrokeVolume(LoopCount) = MaxVolume(LoopCount)-MinVolume(LoopCount);
    EjectionFraction(LoopCount) =
StrokeVolume(LoopCount)/MaxVolume(LoopCount);
    contractiontime(LoopCount) = time(endsys(LoopCount)) -
time(highvolindex(LoopCount));
    relaxationtime(LoopCount) = time(highvolindex(LoopCount+1))-
time(lowvolindex(LoopCount));
    systolicejectionperiod(LoopCount) = contractiontime(LoopCount)*heartrate;
    diastollicfillingperiod(LoopCount) = relaxationtime(LoopCount)*heartrate;
    CardiacOutput(LoopCount) = StrokeVolume(LoopCount)*heartrate;
    StrokeWork(LoopCount) = 0;
```

```
    %for things that need every data point in a loop to calculate
    for i = (highvolindex(LoopCount)):(highvolindex(LoopCount+1))

        %no stroke work if i=1%
        if i == 1
            dPdt = zeros(highvolindex(LoopCount+1)-
highvolindex(LoopCount),1);
            RawTau = zeros(highvolindex(LoopCount+1)-
highvolindex(LoopCount),1);
            smootheddPdt = zeros(highvolindex(LoopCount+1)-
highvolindex(LoopCount),1);
            dPdt(i) = LVpressure(i)/timestep;
            MindPdt(LoopCount)=dPdt(i);
            MaxdPdt(LoopCount)=dPdt(i);
            MinIndex= i;
            MaxPressure(LoopCount) = LVpressure(i);
            MinPressure(LoopCount) = LVpressure(i);
            RawTau(i) = 0;
            minsmoothed(LoopCount) = dPdt(i);

        elseif i == highvolindex(LoopCount) && i~=1
            clear dPdt;
            clear RawTau;
            dPdt = zeros(highvolindex(LoopCount+1)-
highvolindex(LoopCount),1);
            smootheddPdt = zeros(highvolindex(LoopCount+1)-
highvolindex(LoopCount),1);
            RawTau = zeros(highvolindex(LoopCount+1)-
highvolindex(LoopCount),1);
            MaxPressure(LoopCount) = LVpressure(i);
            MinPressure(LoopCount) = LVpressure(i);
            dPdt(i) = (LVpressure(i) - LVpressure(i-1))/timestep;
            smootheddPdt(i) = (((LVpressure(i+1)+LVpressure(i+2))/2) -
((LVpressure(i)+LVpressure(i-1))/2))/timestep;
            MindPdt(LoopCount)=dPdt(i);
            MaxdPdt(LoopCount)=dPdt(i);
            minsmoothed(LoopCount) = smootheddPdt(i);
            MinIndex =i;
            StrokeWork(LoopCount) = StrokeWork(LoopCount)+
(LVpressure(i))*(LVVolume(i-1)-LVVolume(i));
            RawTau(i) = abs((-1)*LVpressure(i)/smootheddPdt(i));

        elseif i > highvolindex(LoopCount)

            dPdt(i) = (LVpressure(i)-LVpressure(i-1))/timestep;
            StrokeWork(LoopCount) = StrokeWork(LoopCount)+
(LVpressure(i))*(LVVolume(i-1)-LVVolume(i));
            smootheddPdt(i) = (((LVpressure(i+1)+LVpressure(i+2))/2) -
((LVpressure(i)+LVpressure(i-1))/2))/timestep;

            if smootheddPdt(i) == 0
                RawTau(i) = abs((-1)*LVpressure(i)/smootheddPdt(i));

            else
                RawTau(i) = abs((-1)*LVpressure(i)/smootheddPdt(i));
            end
```

```
            if dPdt(i)>MaxdPdt(LoopCount)
               MaxdPdt(LoopCount) = dPdt(i);

            end

            if dPdt(i)< MindPdt(LoopCount)
               MindPdt(LoopCount) = dPdt(i);
            end

            if smootheddPdt(i)<minsmoothed(LoopCount)
                minsmoothed(LoopCount)=smootheddPdt(i);
                MinIndex = i;
            end

            if LVpressure(i)>MaxPressure(LoopCount)
               MaxPressure(LoopCount) = LVpressure(i);
            end

            if LVpressure(i)<MinPressure(LoopCount)
               MinPressure(LoopCount) = LVpressure(i);
            end

        end
    end

    DevelopedPressure(LoopCount) = MaxPressure(LoopCount)-
MinPressure(LoopCount);
    SystolicPressureSum = 0;
    DiastolicPressureSum = 0;

    %systole counter%
    for j=highvolindex(LoopCount):endsys(LoopCount)
        SystolicPressureSum = SystolicPressureSum+LVpressure(j);
    end

    MeanSystolicPressure(LoopCount) = SystolicPressureSum/(endsys(LoopCount)-
highvolindex(LoopCount));

    %diastole counter%
    for j=lowvolindex(LoopCount):highvolindex(LoopCount)
        DiastolicPressureSum = DiastolicPressureSum+LVpressure(j);
    end



    Tau(LoopCount) = 1000*nanmean(RawTau(MinIndex:lowvolindex(LoopCount)));

    MeanDiastolicPressure(LoopCount) =
DiastolicPressureSum/(endsys(LoopCount)-highvolindex(LoopCount));


end

%%Create Final Matrix%%
```

```
%Create Titles%
Titles(1) = cellstr(char('Maximum Pressure'));
Titles(2) = cellstr(char('Minimum Pressure'));
Titles(3) = cellstr(char('Begin Diastolic Pressure'));
Titles(4) = cellstr(char('End Diastolic Pressure'));
Titles(5) = cellstr(char('End Systolic Pressure'));
Titles(6) = cellstr(char('Developed Pressure'));
Titles(7) = cellstr(char('Systolic Ejection Period'));
Titles(8) = cellstr(char('Diastolic Filling Period'));
Titles(9) = cellstr(char('Mean Systolic Pressure'));
Titles(10) = cellstr(char('Mean Diastolic Pressure'));
Titles(11) = cellstr(char('Contraction Time'));
Titles(12) = cellstr(char('Relaxation Time'));
Titles(13) = cellstr(char('Max dPdt'));
Titles(14) = cellstr(char('Min dPdt'));
Titles(15) = cellstr(char('Contractility Index'));
Titles(16) = cellstr(char('Time Constant of Relaxation (Tau)'));
Titles(17) = cellstr(char('Maximum Volume'));
Titles(18) = cellstr(char('MinimumVolume'));
Titles(19) = cellstr(char('End Diastolic Volume'));
Titles(20) = cellstr(char('End Systolic Volume'));
Titles(21) = cellstr(char('Stroke Volume'));
Titles(22) = cellstr(char('Cardiac Output'));
Titles(23) = cellstr(char('Ejection Fraction'));
Titles(24) = cellstr(char('Stroke Work'));
Titles(25) = cellstr(char('Effective Arterial Elastance'));
Titles(26) = cellstr(char('Maximum Ventricular Power'));
Titles(27) = cellstr(char('Potential Energy(MEC)'));
Titles(28) = cellstr(char('Heart Rate'));

%define the number of Parameters... if you want to add one just add its title
and add to loop below%

numberofparameters = max(size(Titles));

ParameterValues = zeros(beatnum-1,numberofparameters);


%there are beatnum-1 points. last row is mean
for i = 1:beatnum-1

      for j=1:numberofparameters
            if j==1
            ParameterValues(i,j) = MaxPressure(i);
            end
            if j==2
            ParameterValues(i,j) = MinPressure(i);
            end
            if j==3
            ParameterValues(i,j) = begindiastolicpressure(i);
            end
            if j==4
            ParameterValues(i,j) = enddiastolicpressure(i);
            end
            if j==5
            ParameterValues(i,j) = endsysstolicpressure(i);
            end
```

```
if j==6
ParameterValues(i,j) = DevelopedPressure(i);
end
if j==7
ParameterValues(i,j) = systolicejectionperiod(i);
end
if j==8
ParameterValues(i,j) = diastollicfillingperiod(i);
end
if j==9
ParameterValues(i,j) = MeanSystolicPressure(i);
end
if j==10
ParameterValues(i,j) = MeanDiastolicPressure(i);
end
if j==11
ParameterValues(i,j) = contractiontime(i);
end
if j==12
ParameterValues(i,j) = relaxationtime(i);
end
if j==13
ParameterValues(i,j) = MaxdPdt(i);
end
if j==14
ParameterValues(i,j) = MindPdt(i);
end
if j==15
ParameterValues(i,j) = ContractilityIndex(i);
end
if j==16
ParameterValues(i,j) = Tau(i);
end
if j==17
ParameterValues(i,j) = MaxVolume(i);
end
if j==18
ParameterValues(i,j) = MinVolume(i);
end
if j==19
ParameterValues(i,j) = enddiastolicvolume(i);
end
if j==20
ParameterValues(i,j) = endsysstolicvolume(i);
end
if j==21
ParameterValues(i,j) = StrokeVolume(i);
end
if j==22
ParameterValues(i,j) = CardiacOutput(i);
end
if j==23
ParameterValues(i,j) = EjectionFraction(i);
end
if j==24
ParameterValues(i,j) = StrokeWork(i);
end
if j==25
```

```
            ParameterValues(i,j) = EffectiveArterialElastance(i);
            end
            if j==26
            ParameterValues(i,j) = MaximumVentricularPower(i);
            end
            if j==27
            %ParamterValues(i,j) = PotentialEnergy(i-1);
            end
            if j==28
            ParameterValues(i,j) = heartrate;
            end
       end

end

%find means
Means = mean(ParameterValues,1);


%create row labels%
rowlabel1=zeros(beatnum-1,1);

for i = 1:beatnum-1
    rowlabel1(i) = i;
end

rowlabels =
[cellstr(char('Beat'));num2cell(rowlabel1);cellstr(char('Mean'))];

%combine all labels and Matricies%

numbercomb = [Titles;num2cell(ParameterValues);num2cell(Means)];

FinalLVMatrix = [rowlabels,numbercomb];


%plot the PV loops%
plot(LVVolume,LVpressure);

return
```